ASTON UNIVERSITY

FAST RESPONSE STATIC VAR GENERATOR FOR IMPROVING THE POWER SYSTEM PERFORMANCE OF AN ELECTRIC ARC FURNACE

Zhengwen Zhang

Submitted for the Degree of Doctor of Philosophy

THE UNIVERSITY OF ASTON IN BIRMINGHAM

March 2002

ASTON UNIVERSITY

FAST RESPONSE STATIC VAR GENERATOR FOR IMPROVING THE POWER SYSTEM PERFORMANCE OF AN ELECTRIC ARC FURNACE (EAF)

Zhengwen Zhang

Doctor of Philosophy **April 2002**

Summary

Cascaded multilevel inverters-based Static Var Generators (SVGs) are FACTS equipment introduced for active and reactive power flow control. They eliminate the need for zigzag transformers and give a fast response. However, with regard to their application for flicker reduction in using Electric Arc Furnace (EAF), the existing multilevel inverter-based SVGs suffer from the following disadvantages:

- To control the reactive power, an off-line calculation of Modulation Index (MI) is required to adjust the SVG output voltage. This slows down the transient response to the changes of reactive power
- Random active power exchange may cause unbalance to the voltage of the d.c. link (HBI) capacitor when the reactive power control is done by adjusting the power angle δ alone.

To resolve these problems, a mathematical model of an 11-level cascaded SVG, was developed. A new control strategy involving both MI (modulation index) and power angle (δ) is proposed. A selected harmonics elimination method (SHEM) is taken for switching pattern calculations. To shorten the response time and simplify the control system, feed forward neural networks are used for on-line computation of the switching patterns instead of using look-up tables.

The proposed controller updates the MI and switching patterns once each line-cycle according to the sampled reactive power Q_s. Meanwhile, the remainder reactive power (compensated by the MI) and the reactive power variations during the line-cycle will be continuously compensated by adjusting the power angles, δ. The scheme senses both variables MI and δ, and takes action through the inverter switching angle, θ_i. As a result, the proposed SVG is expected to give a faster and more accurate response than present designs allow.

In support of the proposal there is a mathematical model for reactive power distribution and a sensitivity matrix for voltage regulation assessment, MATLAB simulation results are provided to validate the proposed schemes. The performance with non-linear time varying loads is analyzed and refers to a general review of flicker, of methods for measuring flickers due to arc furnace and means for mitigation.

ASTON UNIVERSITY

FAST RESPONSE STATIC VAR GENERATOR FOR IMPROVING THE POWER SYSTEM PERFORMANCE OF AN ELECTRIC ARC FURNACE (EAF)

Zhengwen Zhang

Supervisor:

Dr. N. R. Fahmi

School of Engineering and Applied Science

Aston University

Aston Triangle, Birmingham, B4 7ET

United Kingdom

Tel. +44(0) 121 359 3611-4293

Fax. +44(0) 121 333 5809

Email: zhangz@aston.ac.uk

March 2002

TO THE SOUL OF MY PARENTS – ZHANG PU-SHENG AND XIA HUA-XIU

ASTON UNIVERSITY

Acknowledgements

I wish to express my sincere thanks to Dr. N. R. Fahmi, my research supervisor, who is always at the helm of my research boat, and his help and guidance made my research in this area possible. Also, I would like to extend my thanks to Dr Q. M. Zhu, once the research co-supervisor for his encouragement and useful discussion during the first year of the research.

I am indebted to Professor W. T. Norris and Dr. T. N. Oliver for their kind help during the course of my research. Special thanks will give to Miss Oliver for her kindness to correct and polish my English writing of this paper.

Acknowledgement is also extended to all colleagues in the MEE department, especially, Mr. Ning Liu, B. Harrison, L. Radford and Dr. Zhang (electronics department) for their kind assistance.

Last but not least, I give my special thanks to my wife-Biqing and my son- Yidong, for their support, understanding and patience.

LIST OF CONTENTS

1. Z. Zhang, N. R. Fahmi, "Historical Review of the Power System Earthing Methods in China and Ferro-resonance Analysis", CIRED 2003, May 12-15, 2003, Barcelona (Accepted).
2. Z. Zhang, N. R. Fahmi, "Electric Arc Furnace (EAF) Features and its Compensation by Cascaded Multi-level SVG", CIRED 2003, May 12-15, 2003, Barcelona (Accepted).
3. Z. Zhang, N. R. Fahmi, "Modeling and Analysis of A Cascade Multilevel Inverters-based SVG with New Control Strategies for EAF Application", IEE Proceedings-C (Accepted).
4. Z. Zhang, N. R. Fahmi, W. T. Norris, "Flicker analysis and methods for EAF flicker mitigation", Conference IEEE Porto Power Tech'2001, Porto, Portugal, paper-276 (PST1-276 in the program), Sep. 10-13th, 2001.
5. Z. Zhang, N. R. Fahmi, "A sensitivity-matrix for assessing voltage regulation result", UPEC 2001, Swansea, Wales, paper-448 (2A-8 in the program), 12-14 Sep. 2001(accepted).
6. Z. Zhang, N. R. Fahmi, "A recurrent neural networks (RNN)-based control SVG for electric arc furnaces", UPEC 2001, Swansea, Wales, paper-450 (3D-4 in the program), 12-14 Sep. 2001(accepted).
7. Z. Zhang, N. R. Fahmi, Q. M. Zhu, "Special loads analysis" UPEC 2000, Belfast, Northern Ireland, 6-8 Sep. 2000, pp92 at Book of Abstracts.
8. Z. Zhang, N. R. Fahmi, "Reactive power optimal distribution" UPEC 2000, Belfast, Northern Ireland, 6-8 Sep. 2000, pp129 at Book of Abstracts.

LIST OF FIGURES

LIST OF TABLES

LIST OF RELATED EQUATIONS

LIST OF ABBREVIATIONS

Abbreviations	Full text
DOL	Direct-on-line start-up (motor)
SVC	Static VAr Compensator
STATCOM	Static Compensator
STATCON	Static Condenser
UPFC	Unified Power Flow Controller
FACTS	Flexible AC Transmission System
VSD	Variable Speed Drives
FC	Fixed Capacitors
EAF	Electric Arc Furnace
LF	Ladle Furnace
UHP	Ultra-High-Power (EAF)
SCVD	Short Circuit Voltage Depression
MRPV	Maximum Reactive Power Variation
TCR	Thyristor Controlled Reactors
TSC	Thyristor Switched Capacitors
SVG	Static VAr Generator
FFANN	Feed Forward Artificial Neural Networks
FFT	Fast Fourier Transform
MI	Modulation Index
SHEM	Selected Harmonics Elimination Method
THD	Total Harmonic Distortion
SDC	Separate DC source
HBI	H-Bridge Inverters
VSI/VSC	Voltage Source Inverters / Voltage Source Converters
ASVC	Advanced SVC
ASVG	Advanced SVG
GTO	Gate Turn Off Thyristor

PREFACE

The problems due to rapid variations of reactive power and harmonics generated by non-linear loads like electric arc furnaces (EAFs) are well known. The large and erratic reactive current swings in an EAF cause corresponding voltage drops across the (reactive) impedance of the ac system resulting in fluctuating terminal voltage. The fluctuating system voltage may cause variations in light output of electrical lamps flashing ("flicker") and disturbance in other electrical equipment. The earliest industrial flicker compensators were installed in the late 1950s and were based on the saturable reactor principle in which iron saturation characteristics were used to stabilize the voltage [64]. However power electronic switched compensators were introduced to replace the saturable reactor compensator, as they are much cheaper and more flexible in use. Static VAr Compensators (SVCs) were first developed in the late 1960s for the compensation of large, fluctuating industrial loads. In the early 1970s, two kinds of SVCs had been put in practical use for EAF flicker suppression. One is the Thyristor Controlled Reactor (TCR) type [65]. The other is the Thyristor Switched Capacitor (TSC) [66], [96]. The possibility of generating or absorbing controllable reactive power with various power electronic switching converters had been recognized at the end of 1980s, and several schemes were implemented in laboratory models [2].

The first Static VAr Generator (SVG) was made by the EPRI and Westinghouse in 1986. Now, the world's largest installation is the two +/- 160 MVA voltage sources GTO thyristor based converters, located at the Inez substation of American Electric Power (AEP) in eastern Kentucky [5]. In recent years, SVGs have been introduced to replace the conventional SVCs for arc furnace flicker compensation as they can overcome problems of the SVCs, such as large size and high cost. As reported [92], the largest SVG for EAF application is the SMI installation in Texas. Commissioned in 1998, it comprises a +/-80MVA STATCOM with a shunt-coupling transformer


Aston University
Illustration removed for copyright restrictions

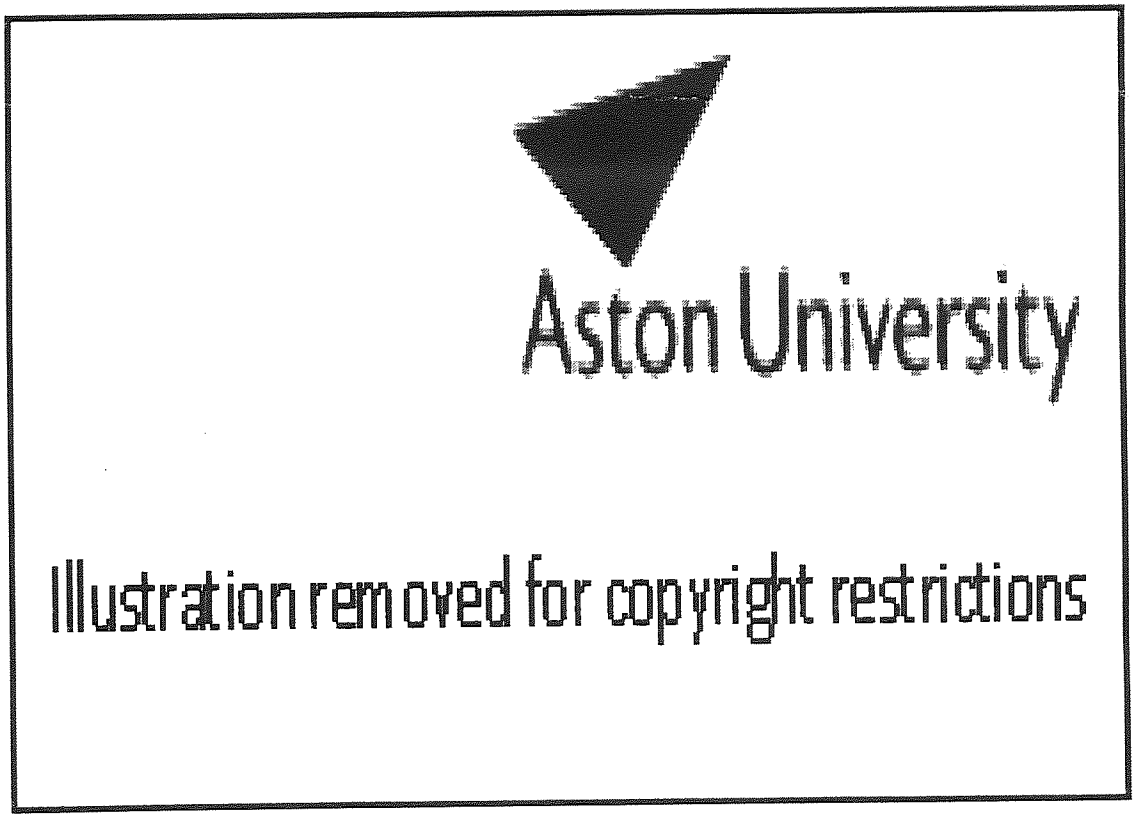
Aston University
Illustration removed for copyright restrictions

and operates in conjunction with a 60 MVA ac capacitor bank. However, the SVG (STATCOM) requires coupling components like a (zigzag) transformer to multiply converters and a high frequency switching PWM technique to reduce harmonics.

Nowadays, multilevel converter-based SVGs or STATCOM have been widely studied due to their capability of eliminating the zigzag transformers [72]-[77], [99], [103]. Referring to figures 4-1, 2, 3 & 4, the general structure of the multilevel converter is to synthesize a sinusoidal voltage from several levels of voltages, typically obtained from capacitor voltage sources. There are mainly three capacitor voltage synthesis-based multilevel converters. They are:

1) Diode-clamped converter (refer to Fig. 4-1)[72], [103],
2) Flying-capacitors converter (refer to Fig. 4-2)[99],
3) Cascaded-inverter with separated DC sources (refer to Fig. 4-3 & 4) [73]-[77].

The third configuration has the advantage of using small number of diodes & capacitors and fast response (within 1 ms), while the first and second configuration require a very large number of clamping diodes or flying capacitors respectively.

Naturally, the cascaded multilevel inverter configuration has drawn tremendous interest in the power industry. In 1996 [74], the authors developed a prototype of the cascade multilevel inverters-based SVG. Then, in [76], the authors designed a 50 MVA STATCOM based on cascading voltage source inverter. Recently, an improved cascade multilevel inverter configuration named "Binary multilevel voltage source inverter" was developed [77]. Unfortunately, with regard to their application for EAF compensation, the multilevel inverter-based SVG or STATCOM suffers the following disadvantages:

- To control the reactive power, an off-line calculation of Modulation Index (MI) is required to adjust the SVG output voltage. This slows down the transient response to the changes of reactive power
- Random active power exchange may cause unbalance to the voltage of the d.c. Link (HBI) capacitor when the reactive power control is done by adjusting the power angle δ alone.

These problems are addressed by the work of this research. In order to resolve the above stated problems, first of all, an accurate mathematical model for the system involved is essential. Many publications about SVG modeling are available to provide us useful analyzing methods like Vector Analysis [104]-[105], and Switching-Function [106]-[107]. Based on the methods of switching-function and vector analysis, this thesis gives a transient model for the eleven-level cascaded converters SVG.

Moreover, the control strategy is very important for the performance of an SVG. The researchers working in this area have made some improvement. In [108], the reactive power is controlled by adjusting phase angle δ, it has the disadvantage of creating unbalanced DC capacitor voltages, caused by the uncontrollable real power flow. Recently, the current hysteresis controller [109] also has limited application as the voltage source inverters to be forced to generate required reactive currents which may cause either unbalanced DC voltage or being the worst conditions of harmonics generated by SVG.

The control strategy proposed by this research work is based on adjusting both MI and phase angle δ. The controller renews the MI/switching patterns once each line-cycle according to the sampled reactive power Q_s. Meanwhile, the remainder reactive power (compensated by the MI) and the reactive power variations during the line-cycle will be continuously compensated by

adjusting the phase angle δ. In fact, it senses both variables MI and δ, but takes action only on one variable: the switching angle θ_i. Selected harmonics elimination method (SHEM) is taken for switching pattern calculations. In order to shorten the response time and simplify the control system, feed forward neural networks are employed for on-line computation of the switching patterns, instead of using off-line precalculated values look-up tables. So that, the proposed schemes have the following extra advantages:

- Faster response: Less calculation work/reading the look-up table means faster response (once each line cycle).
- Accurate, even if the MI control causes any delay to response of the load reactive power changes, the continuously working -δ compensation will make it up.
- There is no serious DC voltage unbalanced problem as the region of the δ can be controlled within a very small value, because majority VAr is compensated by adjusting MI.
- Neural networks can be a quick on-line computation method following proper training.

In *Chapter 1*, based on methods of variational calculus, the Lagrange Equations are developed to resolve the problem of reactive power optimal distribution. After given an overview about kinds of abnormal voltage conditions and methods for voltage regulation, a sensitivity matrix for voltage regulation assessment is included. Combined with the design experience of a 9.2MW synchronous motor using a direct on line (DOL) start up method, it also provides a p.u-impedance method for voltage-dip calculation.

Chapter 2 analyses electric characteristics of special loads such as Electric Arc Furnaces (EAFs), Converters and Railway traction in turn. Analyses were based on theoretical approaches and on results obtained from some on-the-spot experiments in the real metallurgic industry projects or railway routes in China. The statistical tables and empirical formulae shown, describing general

features of these loads, were concluded from the analysis. From the tables and equations that define operation, the performance of these dynamically changeable loads can be predicted and assessed.

Chapter 3 gives a general review about how to examine/assess voltage flicker and methods followed in measuring flickers due to arc furnace and means for mitigation. It also investigates fast response SVG for arc furnace flicker mitigation. It includes the discussion in the effects of utilities' conditions, compensator response-time and compensator capacity on arc furnace flicker reduction. A comparison between SVC and SVG on the applications of EAF compensation is carried out. Some discussions about the perspective of applying SVG for EAF compensation are also included in this chapter.

Chapter 4 investigates the application of cascade multilevel converters-based SVG for EAF compensation. Based on the methods of Vector-Analysis and Switching-Function and combined with the new control strategies by adjusting both MI and the phase angle (δ) between the system voltage and the SVG output voltage. The mathematical model for transient response of the proposed SVG is developed in this chapter. The details of the new control system are given *in chapter 5*.

Chapter 6 discusses the FFANN and its application in this research. Conclusions and further discussion are given in *Chapter 7*.

I. VOLTAGE VARIATIONS AND METHODS OF VOLTAGE REGULATIONS

ABSTRACT: This chapter introduces a mathematical model for assessing voltage regulation, which uses the basic principles of circuit analysis to derive the sensitivity-matrix (impedance-matrix). Based on methods of variational calculus, the Lagrange Equations are developed to resolve the problem of reactive power optimal distribution. An overview of abnormal voltage conditions and methods for voltage regulation is included, combined with the design experience of using a 9.2MW synchronous motor which employs a direct-on-line (DOL) start up method. The chapter also provides a p.u-impedance method for voltage-dip calculation.

1.1. INTRODUCTION

1.1.1. General

The quality of electricity supply is considerably influenced by the quality of the voltage provided to customers, which can be affected in various ways. There may be long periods of variation from the normal voltage, rapid voltage change, voltage deviation, voltage-dips (or voltage-sags), voltage fluctuation and flicker, or unbalance of 3-phase voltages. In addition, other irregularities such as variations in frequency, the presence of non-linear elements or load impedance will distort the voltage waveform, and transient spikes and surges may propagate along circuits in a supply system. In general, we can analyse existing voltage problems from two perspectives:

1. Looking at the disturbances generated at the utility side but affecting the customers
2. Looking at the customer caused disturbances that also affect the utility side.

The voltage problems generated at utility side include the interruptions, outages, external over-voltages transient internal over-voltages (switching of capacitors or inductors, unbalanced feeders, etc.), sustained internal over-voltage (neutral inversion, arcing ground phenomena, restrikes and resonance), temporary over-voltages, under-voltages and voltage unbalance. The other voltage problems caused by dynamic load variation and/or interaction between the load and the network characteristics also affect the voltage waveform supplied to utility customers. Harmonic interference and voltage flicker, dips, and unbalance are some of the most common problems encountered.

To most electric power engineers, the term voltage quality refers to a sufficient high grade of electric service. In an ideal ac power system, the voltage and frequency at every supply point

would be constant and free from harmonics, and the power factor would be unity. Consequently, the objectives of voltage control are mainly: power-factor correction, improvement of voltage regulation, and load balancing.

Many solutions have been offered to each of these problems over the years. However, voltage regulation takes a very important role in voltage quality control. Traditionally, voltage regulation involved the automatic generating control, transformers with off-line/on-line tap-changing, reactive power injection by shunt capacitors/ inductors, synchronous condenser. By the late 1970s, it became evident that dynamic compensation of electric power transmission systems was needed to achieve better utilization of existing generation and transmission facilities. The Static VAr Compensators (SVC) were successfully used for providing voltage support, increasing transient stability, and improving damping [1]. To be of large capacity, simple in structure, and economical, the converters-based compensators had been studied and developed at the end of 1980's [2]. The converters-based solutions to voltage quality appeared to be the way of the future [3]. Recently, more than 100 converter-based devices are used in Japan, and a 2x160MVA STATCON is installed in the USA [67], [5]. Nowadays, the converters-based compensators with more flexibility (multi-function) have been developed for a more economic solution. The UPFC (or FACTS) [6]-[7] is capable of achieving more than one kind of compensation by using ac-ac converters. Regardless of what devices are used for voltage regulation, we need a simple calculation method for assessing the voltage regulation results, or for selecting the compensation devices before the voltage regulator design.

The voltage control methods using: Generator Voltage Control [8], tap-changing transformers [9] and Reactive-Power Injection [10], or their combination including static compensation and harmonic filter, are highlighted first. Then, a sensitivity-matrix is derived for a system of two-generators with the combination of generator voltage control, tap-changing transformer and reactive power injection. On the top of that, in a real engineering project, we may face a problem like this: In a factory (typically, the Iron & Steel Industry) or the electrical utility, there may be two or more load nodes that need to be compensated because of reactive power shortage. If a fixed total compensating reactive power capacity is available to maintain the load bus voltage within a suitable range; and to minimise the total active power loss, then what criterion should we follow to distribute the reactive power to each load? This chapter addresses and analyses such a problem. On the basis of methods of variational calculus [18], we can create the

Lagrange Equations and work out some strategies to resolve this problem. A numerical example is also presented to validate this method.

1.1.2. Voltage Problems and Regulations

Voltage Problems

As stated earlier, we can present existing voltage problems from two perspectives:

1. Looking at the disturbances generated at the utility side but affecting the customers,
2. Looking at the customer caused disturbances that also affect the utility side and it is shown below:

Voltage variations resulted from power system faults	Voltage variations caused by special loads
• Interruptions • Outages • External Over-voltages(lightening) • Transient internal over-voltages(switching of capacitors or shunt inductors, unbalanced feeders, etc.) • Sustained internal over-voltages(neutral inversion, arcing ground phenomena, restrikes and resonance) • Temporary over-voltages • Under-voltages • Voltage unbalance	• Voltage Deviations • Voltage Sags and Swells • Voltage Fluctuations and Flickers • Voltage Notching/Harmonics • Voltage Unbalance

The voltage variations resulting from power system faults are excluded from consideration; as that might be the area of power system protections, high-voltage engineering.

Voltage Collapse Analysis :

With the development of electrical industry, there has been a continually increasing interest and investigation into voltage instability and collapse. After B. M. Weedy published the first paper

related to voltage instability [11], Venikov [12] proposed the first criteria for detecting the point of voltage collapse. Although voltage instability was known for a long time, the active work involving voltage instability started in 1980's. As described in [13], the voltage stability security assessment should indicate:

1. Where the voltage collapse occurs for any equipment outage or operation change.
2. All contingencies and operating changes that cause voltage collapse in that location.
3. The cause of the voltage collapse in terms of (1) lack of reactive supply on specific reactive source or (2) an inability to deliver reactive power to the specific region experiencing voltage collapse.
4. What operating changes could be made in anticipation to prevent the voltage instability from occurring, when a specific contingency and operating change combination predicted to cause voltage instability occurs.

According to [13], the voltage instability can be divided into two types. One is "loss of voltage control"; voltage instability which is caused by exhaustion of reactive supply with resultant loss of voltage control on a particular set of generators, synchronous condensers, or SVCs. The other is "clogging voltage instability", that occurs due to I^2X series reactive losses, tap changers reaching tap limits, switchable shunt capacitors reaching susceptance limits and such like. Since the "loss of voltage control" voltage instability and the "clogging voltage instability" are both due to a shortage of reactive power supply to a bus or coherent bus group, the structural stress test used must assess when and why a shortage of reactive power supply exists. Thus a $Q-V$ curve is used in the voltage stability security assessment methodology [14]. In [15], the main voltage stability and voltage collapse prediction methods are:

1. Voltage collapse index based on closely located power flow solution pairs.
2. Voltage collapse index based on $P-V$ or $Q-V$ curve.
3. Voltage collapse index based on normal load flow solution.
4. Minimum singular value of the power flow related Jacobian matrices.
5. Voltage collapse index based on the optimal impedance solution at maximum power transfer.

The possibility of an actual voltage collapse depends upon the nature of the load. If the load is stiff, e.g. induction motors, the collapse is aggravated. If the load is soft, e.g. heating, the power falls off rapidly with voltage and the situation is alleviated. It is evident that a critical factor is the power factor.

Methods of Voltage Regulations

- Automatic Generating Control

  Automatic Generating Control is a specialist field, it is intended here to discuss just two broad divisions of automatic regulators, both of which set out to control the output voltage of the synchronous generator by controlling the exciter. In general the deviation of the terminal voltage from a prescribed value is passed to control circuits and thus the field current is varied, and it is in the manner and speed in achieving this that the division occurs. The first type is Electromechanical; a well-known variety of this is the carbon-pile regulator. Another type depends upon the conversion of the deviated voltage into a torque by means of a "torque motor"; according to the angular position of the shaft of the motor, certain resistors in a resistor chain are cut out of the circuit and hence the exciter-field current changes. There are various other types, including the popular vibrating-reed regulator. Although the brushless exciter makes the regulators more efficient; all these types suffer from the disadvantages of being relatively slow acting and possessing dead bands, i.e. a certain deviation must occur before the mechanism operates.

- Transformers With Off-Line Tap-Changing

  Adjustment of the transformation ratio requires the introduction of tappings on one of the windings of the used transformer, (usually on the HV side) corresponding to the required steps in regulation. In the case of off-line regulation, the change from one tapping to another is carried out by means of a switch which is designed in such a way that the transformer must be disconnected from the system before the switch can be operated. The tappings are preferably placed on the winding corresponding to the voltage most likely to vary, usually the high voltage winding. As this winding has the higher number of turns and lower current, the design and the construction details are more easily resolved. The regulation is usually symmetrical above and below the rated voltage, $\pm 2.5\%, \pm 5\%$ ($or \pm 10\%$ in China), to suit the local conditions.

- Automatic Voltage Control

  Automatic voltage control can be done by automatic tap-changers on the transformers. It is based on the on-load tap-changer which avoids interruption to supply due to the transformer being switched out, and allows continuous adjustment of the transformer ratio to be made. The passage from one tap to another, without interrupting the principal circuit, requires the two tappings to be connected together for a very short period. To avoid a complete short circuit, this connection is made through a resistance, or less commonly an inductance. The transformer-mounted on-load tap changer, with rapid change-over using resistor, is commonly used. Results from about sixty years of constant progress in both performance and reliability have made it suitable for ever increasing voltages and currents.

- Injection of Reactive Power

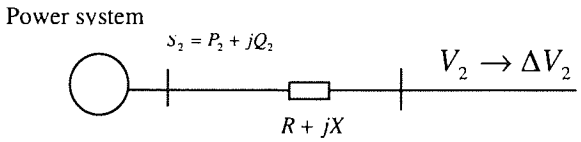

Fig.1- 1, A typical circuit for voltage deviation calculation

Refer to Fig. 1-1, consider a load $S_2 = P_2 + jQ_2$, fed to a bus-bar of rated voltage V_2 and though a transmission line with impedance $R + jX$. We can calculate the voltage deviation ΔV_2 as follows:

$$\Delta V_2 = (P_2 R + Q_2 X)/V_2 \qquad (1)$$

Neglecting the transmission-line resistance-R we obtain:

$$\Delta V_2 \approx (Q_2 X)/V_2 \qquad (2)$$

That is to say we can reduce the voltage deviation to a suitable range on the bus-bar by injecting reactive power Q_C to balance the load reactive power Q_2(let $Q_c - Q_2 \cong 0$). This is the principle of reactive power injection for voltage regulation

- Combined Use of Tap-Changing Transformers and Reactive-Power Injection

  The usual practical arrangement is shown in Fig.1-2, where the tertiary winding of a three-winding transformer is connected to a compensator. For given load conditions it is proposed to determine the necessary transformation ratios with certain outputs of the compensator.

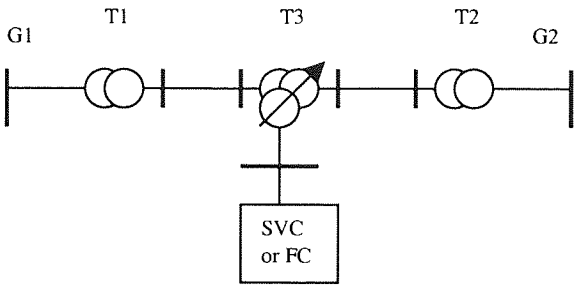

Fig. 1-2, A typical system with combined methods of voltage regulation

1.2. Voltage-dip Calculation and Methods for Motor Start-up [17]

There are three main problems which can arise from the connection of motors to electrical supply systems. The first is whether, under depressed voltage conditions at starting, the motor will successfully run up to speed. The second results from the effect on other customers of this voltage depression when starting the motor from standstill. The third arises from motors' energy feed back into the network when the supply voltage is suddenly reduced because of faults on the network.

1.2.1 Voltage-dip Calculation Due Motor Starting-up

Originally, the percentage voltage dip caused by motor starting-up can be calculated from the following equation:

$$V\% \cong \frac{\sqrt{3}kI}{V}(R\cos\phi + X\sin\phi)100\% \qquad (3)$$

Where:

k : Motor start-up current (pu)

I : Motor rated current

R, X : resistance and reactance of the system

ϕ : the power factor angle of the motor during starting-up

V : system phase –phase voltage.

In engineering calculations, it is difficult to use equation (3) to solve the multi-stage voltage levels system. In this case, we use a per-unit system. Fig. 1-3b shows the equivalent calculation circuit of Figure 1-3a, which neglects the resistance and considers the power factor angle-ϕ close to 90 degrees.

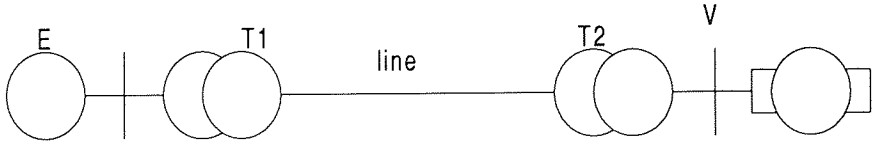

Fig. 1-3a, A typical motor connection

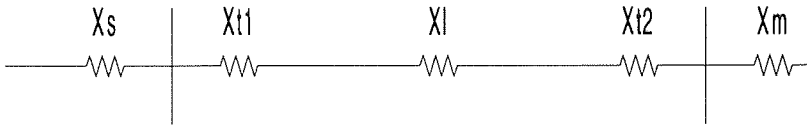

Fig. 1-3b, the equivalent circuit

Normally, set the base of a per-unit system as follows:

$S_B = 100MVA,\ V_B = V_{RATED},\ I_B = I_{RATED};\ X_S = 100/S_{sc},\ X_t = 100/S_t,\ X_m = 100/kS_m$

Where:

S_{sc}: short-circuit level of the power system

S_t: rated capacity of the transformer

k: motor starting MVA (pu)

S_m: motor rated capacity

X_L: impedance of the transmission line.

We obtain the calculation formula as follows:

$$V\% = \frac{X_s + X_l + X_t}{X_\Sigma} 100\% \quad \text{(Here: } X_\Sigma = X_s + X_l + X_t + X_m) \qquad (4)$$

We can derive an applicable equation (5) from equation (4) by taking capacity instead of impedance as below:

$$V\% = \frac{kS_m}{kS_m + S_{sc} + S_{Q\Sigma}} 100\% \qquad (5)$$

Here $S_{Q\Sigma}$ is the total capacity of all reactive power loads connected to the same bus-bar with the motor. We take these loads into consideration, because of their short-circuit current contribution during the motor starting.

1.2.2 Methods of Motor Start-up

Typically, there are three kinds of motor start-up, namely, Direct-On-Line (DOL), inductor / auto-transformer and VSD. From equation (5), we can derive the DISCRIMINANT of taking DOL start-up as below:

$$KS_m \le \frac{V\%}{100}\left(KS_m + S_{Q\Sigma} + S_{sc}\right) \qquad (6)$$

Where $V\%$ is the Permitted voltage-dip on the connected bus-bar (provided by customer).

1.3. MATHEMATICAL MODEL FOR VOLTAGE REGULATION

Refer to Figure 1-2, a two-generator system with the combination of generator voltage control (G_1, G_2), tap-changing transformer (T_3) and reactive power injection (SVC or FC), for such systems, we can define the general form of the Sensitivity Matrix as below:

$$\begin{bmatrix} \Delta V_i \\ \Delta Q \end{bmatrix} = \begin{bmatrix} \frac{\partial V_i}{\partial V_G} & \frac{\partial V_i}{\partial K} & \frac{\partial V_i}{\partial Q_C} \\ \frac{\partial Q}{\partial V_G} & \frac{\partial Q}{\partial K} & \frac{\partial Q}{\partial Q_C} \end{bmatrix} \begin{bmatrix} \Delta V_G \\ \Delta K \\ \Delta Q_C \end{bmatrix} + \begin{bmatrix} \frac{\partial V_i}{\partial P_L} & \frac{\partial V_i}{\partial Q_L} \\ \frac{\partial Q}{\partial P_L} & \frac{\partial Q}{\partial Q_L} \end{bmatrix} \begin{bmatrix} \Delta P_L \\ \Delta Q_L \end{bmatrix} \qquad (7)$$

Where:

ΔV_i: the voltage change in node-i after regulating

V_G : the terminal voltage of a generator or a power system(that can be equivalent to a generator) which is regulated by generator control means.

ΔK is the tap-changing ratio of a transformer (percentage)

Q_C: the capacity of reactive power compensation

P_L, Q_L are respectively active and reactive power of the load.

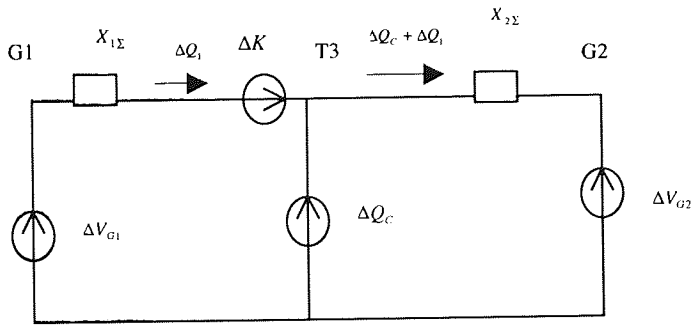

Figure 1-4. The equivalent circuit of Fig. 1-2

Figure 1-4 is the equivalent circuit of Figure 1-2;

Here:

$X_{1\Sigma}$ is the total impedance of the left side of node-3

$X_{2\Sigma}$ is the right-side total impedance of node-3.

Taking node-3 as the assessing point, the calculations are as follows (based on Superposition Principle, Thevenin and Norton Equivalent Circuits, and p.u system as well [16]):

1. $\dfrac{\partial V_i}{\partial V_G};\dfrac{\partial Q}{\partial V_G}$

Refer to equation (2) for the voltage deviation calculation, and let $\Delta K = \Delta Q_C = \Delta V_{G2} = 0$, then

$$\Delta V_{G1} \approx \frac{\Delta Q_1 (X_{1\Sigma} + X_{2\Sigma})}{V_{RATED}} \Rightarrow \Delta V_3 = \frac{\Delta V_{G1} X_{2\Sigma}}{X_{1\Sigma} + X_{2\Sigma}} \tag{8}$$

Since V_{RATED}=1(p.u)

$$\therefore \begin{cases} \dfrac{\partial Q_1}{\partial V_{G1}} = \dfrac{\Delta Q_1}{\Delta V_{G1}} = \dfrac{1}{X_{1\Sigma} + X_{2\Sigma}} \\ \dfrac{\partial V_3}{\partial V_{G1}} = \dfrac{X_{2\Sigma}}{X_{1\Sigma} + X_{2\Sigma}} \end{cases} \tag{9}$$

Similarly

$$\begin{cases} \dfrac{\partial Q_1}{\partial V_{G2}} = -\dfrac{1}{X_{1\Sigma} + X_{2\Sigma}} \\ \dfrac{\partial V_3}{\partial V_{G2}} = \dfrac{X_{1\Sigma}}{X_{1\Sigma} + X_{2\Sigma}} \end{cases} \tag{10}$$

2. $\dfrac{\partial V_i}{\partial Q_C};\dfrac{\partial Q}{\partial Q_C}$. We can consider the ΔQ_C feeds to all the nodes in this system. Calculating the voltage change in both sides of node-3 (corresponding to the change of Q_C) gives:

$$\Delta V_3 = -\frac{\Delta Q_1 X_{1\Sigma}}{V_{RATED}}; \Delta V_3 = \frac{(\Delta Q_1 + \Delta Q_C) X_{2\Sigma}}{V_{RATED}} \tag{11}$$

$$\therefore \frac{\partial V_3}{\partial Q_C} = \frac{X_{1\Sigma} X_{2\Sigma}}{X_{1\Sigma} + X_{2\Sigma}}; \frac{\partial Q_1}{\partial Q_C} = -\frac{X_{2\Sigma}}{X_{1\Sigma} + X_{2\Sigma}} \tag{12}$$

3. $\dfrac{\partial V_i}{\partial K};\dfrac{\partial Q}{\partial K}$

In this case, ΔK can be equivalent to a voltage-source $\Delta K V_T$: $\Delta K V_T = \Delta Q_1 (X_{1\Sigma} + X_{2\Sigma})$, Then:

$$\Delta Q_1 = \frac{\Delta K V_T}{X_{1\Sigma} + X_{2\Sigma}} \Rightarrow \Delta V_3 = \frac{\Delta K X_{2\Sigma}}{X_{1\Sigma} + X_{2\Sigma}} \tag{13}$$

$$\therefore \frac{\partial V_3}{\partial K} = \frac{X_{2\Sigma}}{X_{1\Sigma} + X_{2\Sigma}}; \frac{\partial Q_1}{\partial K} = \frac{1}{X_{1\Sigma} + X_{2\Sigma}} \tag{14}$$

Concluding above mathematical analysis, we obtain the Sensitivity Matrix as below:

$$M_S = \begin{bmatrix} \frac{\partial V_3}{\partial V_{G1}} & \frac{\partial V_3}{\partial V_{G2}} & \frac{\partial V_3}{\partial Q_C} & \frac{\partial V_3}{\partial K} \\ \frac{\partial Q_1}{\partial V_{G1}} & \frac{\partial Q_1}{\partial V_{G2}} & \frac{\partial Q_1}{\partial Q_C} & \frac{\partial Q_1}{\partial K} \end{bmatrix} \tag{15}$$

Substituting the above results into the equation (15), the sensitivity matrix in terms of system reactance is:

$$M_S = \frac{1}{X_{1\Sigma} + X_{2\Sigma}} \begin{bmatrix} X_{2\Sigma} & X_{1\Sigma} & X_{1\Sigma}X_{2\Sigma} & X_{2\Sigma} \\ & 1 & -1 & -X_{2\Sigma} & 1 \end{bmatrix} \tag{16}$$

In practice, if two or more points need to be assessed simultaneously, the calculation is similar to the above

1.4. REACTIVE POWER OPTIMAL DISTRIBUTION

1.4.1 LAGRANGE EQUATIONS

In a typical Iron & Steel company, a Main-substation feeds on several disturbing loads like Rolling Mills or Arc Furnaces, which need reactive power compensation. Or more popular, tie-linked two or three Substations in a metallurgic company feed several disturbing loads as shown as Fig. 1-5. Unfortunately, engineers usually compensate each load individually in engineering design. This paper is aimed to provide an approach to help electrical engineers in improving their reactive power compensation design. To be clear about the question, using the similar approach as used [19], we can mathematically outline it in a general form;

Let:

P_i = power output of i (MW)

Q_i = reactive power output of i (MVAr)

Q_{Gi}= reactive power supply of i (MVAr)

Q_{Li} =load reactive power output of i (MVAr)

λ = Lagrange multiplier (active power loss/MVAr)

$\sum \Delta P$ = total active power loss in the system

$\sum \Delta Q$ = total reactive power loss in the system

n = number of compensating nodes

Define:

$$K = \sum \Delta P = F_{(P_i, Q_i)} \tag{17}$$

with the constraint (because of reactive power balance) :

$$l = \sum_{i=1}^{n} Q_{Gi} - \sum_{i=1}^{n} Q_{Li} - \sum \Delta Q = 0 \tag{18}$$

A more straightforward approach to tackle this problem is to define a new function that is the linear combination of (17) and (18) as below:

$$L = K + \lambda l\,,\ L = \sum \Delta P + \lambda(\sum_{i=1}^{n} Q_{Gi} - \sum_{i=1}^{n} Q_{Li} - \sum \Delta Q) \tag{19}$$

Equation (19) is called Langrage function of n particle system. Such a system has n variables that we designated Q_{Gi} and independent variable λ [18].

To generalise, equation (19) should meet the following conditions:

$$\frac{\partial L}{\partial Q_{Gi}} = \frac{\partial \sum \Delta P}{\partial Q_{Gi}} + \lambda(1 - \frac{\partial \sum \Delta Q}{\partial Q_{Gi}}) = 0 \, (i = 1,2,\cdots n) \tag{20}$$

$$\frac{\partial L}{\partial \lambda} = \sum_{i=1}^{n} Q_{Gi} - \sum_{i=1}^{n} Q_{Li} - \sum \Delta Q = 0 \tag{21}$$

Rewriting equation (20) gives:

$$\frac{\frac{\partial \sum \Delta P}{\partial Q_{Gi}}}{1 - \frac{\partial \sum \Delta Q}{\partial Q_{Gi}}} = -\lambda \tag{22}$$

Neglecting ΔQ in practice without introducing much error, the simple form of (22) is:

$$\frac{\partial \sum \Delta P}{\partial Q_{G1}} = \frac{\partial \sum \Delta P}{\partial Q_{G2}} = \cdots = \frac{\partial \sum \Delta P}{\partial Q_{Gn}} \tag{23}$$

1.4.2 STRATEGIES FOR CALCULATING $\frac{\partial \sum \Delta P}{\partial Q_{Gi}}$ and $\frac{\partial \sum \Delta Q}{\partial Q_{Gi}}$ [20],[21],[22]

Now, the problems reduced to how to apply equation (23) to real project calculation. From the principle of Circuit Analysis, we can calculate the total active power and reactive power loss as equation (24) below:

$$\sum \Delta P + j \sum \Delta Q = \sum_{i=1}^{n} S_i = \sum_{i=1}^{n} \dot{V}_i I_i^* \tag{24}$$

The matrix form of (24) is:

$$\sum \Delta P + j \sum \Delta Q = V^T I^* \tag{25}$$

Since $V = ZI$, $V^T = I^T Z^T$ and $Z^T = Z$ (because of symmetry)

$$\therefore \sum \Delta P + j \sum \Delta Q = I^T Z I^* \tag{26}$$

Furthermore:

$$Z = R + jX = \begin{bmatrix} R_{11} & R_{12} & \cdots & R_{1n} \\ R_{21} & R_{22} & \cdots & R_{2n} \\ \vdots & \vdots & \vdots & \vdots \\ R_{n1} & R_{n2} & \cdots & R_{nn} \end{bmatrix} + j \begin{bmatrix} X_{11} & X_{12} & \cdots & X_{1n} \\ X_{21} & X_{22} & \cdots & X_{2n} \\ \vdots & \vdots & \vdots & \vdots \\ X_{n1} & X_{n2} & \cdots & X_{nn} \end{bmatrix}$$

$$I = I_a + jI_r = \begin{bmatrix} I_{a1} \\ I_{a2} \\ \vdots \\ I_{an} \end{bmatrix} + j \begin{bmatrix} I_{r1} \\ I_{r2} \\ \vdots \\ I_{rn} \end{bmatrix}$$

$$\therefore \sum \Delta P + \sum \Delta Q = (I_a + jI_r)(R + jX)(I_a - jI_r) \tag{26'}$$

$$\therefore \sum \Delta P = I_a^T R I_a + I_r^T R I_r + I_a^T X I_r - I_r^T X I_a$$

As $I_a^T X I_r = I_r^T X I_a$, Then:

$$\sum \Delta P = I_a^T R I_a + I_r^T R I_r =$$

$$[I_{a1} \quad \cdots \quad I_{an}] \begin{bmatrix} R_{11} & \cdots & R_{1n} \\ \vdots & \vdots & \vdots \\ R_{n1} & \cdots & R_{nn} \end{bmatrix} \begin{bmatrix} I_{a1} \\ \vdots \\ I_{an} \end{bmatrix} + [I_{r1} \quad \cdots \quad I_{rn}] \begin{bmatrix} R_{11} & \cdots & R_{1n} \\ \vdots & \vdots & \vdots \\ R_{n1} & \cdots & R_{nn} \end{bmatrix} \begin{bmatrix} I_{r1} \\ \vdots \\ I_{rn} \end{bmatrix}$$

$$= \sum_{j=1}^{n} \sum_{k=1}^{n} R_{jk} (I_{aj} I_{ak} + I_{rj} I_{rk}) \tag{27}$$

Similarly,

$$\sum \Delta Q = I_a^T X I_a + I_r^T X I_r = \sum_{j=1}^{n} \sum_{k=1}^{n} X_{jk} (I_{aj} I_{ak} + I_{rj} I_{rk}) \tag{28}$$

Where,

Z, V, I are respectively branch-impedance, node-voltage and branch-current Matrices;

Z^T, V^T, I^T are the transposing matrices of Z, V, I;

I^* is the conjugate complex of I;

I_a, I_r are respectively the active and reactive components of I.

Because the independent variable in equation (23) is the reactive power Q, we should transfer current variable I into reactive power Q. According to the principles of electric circuit analysis, with regard to i-node of a circuit, we have the equation:

$P_i + jQ_i = \dot{V}_i I_i^* = V_i(\cos\theta_i + j\sin\theta_i)(I_{ai} - jI_{ri})$, $(I_i I_{ai} + jI_{ri})$ Thus:

$$\begin{cases} I_{ai} = \dfrac{1}{V_i}(P_i\cos\theta_i + Q_i\sin\theta_i) \\ I_{ri} = \dfrac{1}{V_i}(P_i\sin\theta_i - Q_i\cos\theta_i) \end{cases} \tag{29}$$

Substitute the results of (29) into equations (27) and (28), leads to:

$$\sum\Delta P = \sum_{j=1}^{n}\sum_{k=1}^{n}\left[\alpha_{jk}(P_jP_k + Q_jQ_k) + \beta_{jk}(Q_jP_k - P_jQ_k)\right] \tag{30}$$

$$\sum\Delta Q = \sum_{j=1}^{n}\sum_{k=1}^{n}\left[\varepsilon_{jk}(P_jP_k + Q_jQ_k) + \eta_{jk}(Q_jP_k - P_jQ_k)\right] \tag{31}$$

Where:

$\theta_i, \theta_j, \theta_k$ are respectively the voltage phase angle of i, j,k -nodes; and

$$\alpha_{jk} = \frac{R_{jk}}{V_jV_k}\cos(\theta_j - \theta_k)$$

$$\beta_{jk} = \frac{R_{jk}}{V_jV_k}\sin(\theta_j - \theta_k)$$

$$\varepsilon_{jk} = \frac{X_{jk}}{V_jV_k}\cos(\theta_j - \theta_k)$$

$$\eta_{jk} = \frac{X_{jk}}{V_jV_k}\cos(\theta_j - \theta_k)$$

Now, we can evaluate the quantities of $\frac{\partial\sum\Delta P}{\partial Q_{Gi}}$ and $\frac{\partial\sum\Delta Q}{\partial Q_{Gi}}$ from equations (30) and (31) as follows:

$$\frac{\partial\sum\Delta P}{\partial Q_{Gi}} = \sum_{j=1}^{n}\sum_{k=1}^{n}\frac{\partial}{\partial Q_i}\left(\alpha_{jk}(P_jP_k + Q_jQ_k) + \beta_{jk}(Q_jP_k - P_jQ_k)\right) \tag{32}$$

$$\frac{\partial\sum\Delta Q}{\partial Q_{Gi}} = \sum_{j=1}^{n}\sum_{k=1}^{n}\frac{\partial}{\partial Q_i}\left(\varepsilon_{jk}(P_jP_k + Q_jQ_k) + \eta_{jk}(Q_jP_k - P_jQ_k)\right) \tag{33}$$

Operating equations (32) and (33), we obtain:

$$\frac{\partial\sum\Delta P}{\partial Q_{Gi}} = P_i^2\frac{\partial\alpha_{ii}}{\partial Q_i} + 2Q_i\alpha_{ii} + Q_i^2\frac{\partial\alpha_{ii}}{\partial Q_i};(j = i, k = i)$$

$$P_i P_k \frac{\partial \alpha_{ik}}{\partial Q_i} + Q_k(\alpha_{ik} + Q_i \frac{\partial \alpha_{ik}}{\partial Q_i}) + P_k(\beta_{ik} + Q_i \frac{\partial \beta_{ik}}{\partial Q_i}) - P_i Q_k \frac{\partial \beta_{ik}}{\partial Q_i}; (j = i, k \neq i)$$

$$P_j P_i \frac{\partial \alpha_{ji}}{\partial Q_i} + Q_j(\alpha_{ji} + Q_i \frac{\partial \alpha_{ji}}{\partial Q_i}) - P_j(\beta_{ji} + Q_i \frac{\partial \beta_{ji}}{\partial Q_i}) + P_i Q_j \frac{\partial \beta_{ji}}{\partial Q_i}; (j \neq i, k = i)$$

$$P_j P_k \frac{\partial \alpha_{jk}}{\partial Q_i} + Q_k Q_j \frac{\partial \alpha_{jk}}{\partial Q_i} + P_k Q_j \frac{\partial \beta_{jk}}{\partial Q_i}) - P_j Q_k \frac{\partial \beta_{jk}}{\partial Q_i}; (j \neq i, k \neq i) \quad (34)$$

We can simplify equation (34) to equation (35), considering $\alpha_{jk} = \alpha_{kj}$, $\beta_{jk} = -\beta_{kj}$, $\varepsilon_{jk} = \varepsilon_{kj}$, $\eta_{jk} = -\eta_{kj}$ and neglecting $\frac{\partial \alpha_{jk}}{\partial Q_i}$, $\frac{\partial \beta_{jk}}{\partial Q_i}$, $\frac{\partial \varepsilon_{jk}}{\partial Q_i}$, $\frac{\partial \eta_{jk}}{\partial Q_i}$ in practice without introducing noticeable error.

$$\frac{\partial \sum \Delta P}{\partial Q_{Gi}} = 2\sum_{k=1}^{n}(\alpha_{ik} Q_k + \beta_{ik} P_k) \quad (35)$$

Similarly,

$$\frac{\partial \sum \Delta Q}{\partial Q_{Gi}} = 2\sum_{k=1}^{n}(\varepsilon_{ik} Q_k + \eta_{ik} P_k) \quad (36)$$

1.4.3 NUMBERICAL EXAMPLE AND ITS APPLICATION

The principal formula for reactive power optimal distribution is equation (23), and equations (35), (36) are the original source for calculating equation (23).

Practice:

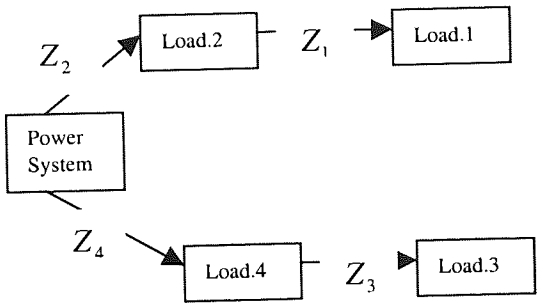

Figure 1- 5. A simplified power system connections

As an application, we assume a simplified power system as shown by Fig. 1- 5 above.

Refer to Fig. 1- 5, say: $Z_1 = 10 + j10$, $Z_2 = 20 + j20$, $Z_3 = 30 + j30$ and $Z_4 = 40 + j40$

Load 1=$5 + j10$, Load 2=$5 + j8$, Load 3=$5 + j6$, Load 4=$5 + j4$ (MVA)

If the total reactive power compensating capacity is 20 MVAr, then the exercise is how to distribute this reactive power to each load in order to minimise the total active power loss? To simplify the calculation, we assumed the voltage of all bus-bar is 20kV.

Three approaches can be considered.

Method 1, using equations (7), (19) step by step

Step 1.

$\theta = \tan^{-1}(\frac{Q}{P})$: $\theta_1 = 63.4^\circ, \theta_2 = 58.0^\circ, \theta_3 = 50.2^\circ, \theta_4 = 38.7^\circ, \theta_0 = 20^\circ$

Here θ_0 is the phase angle of the power system (assumed value).

Step 2.

$$\alpha_{ik} = \frac{R_{ik}}{V_i^2}\cos(\theta_i - \theta_k),\ \beta_{ik} = \frac{R_{ik}}{V_i^2}\sin(\theta_i - \theta_k)$$

Step 3.

$$\frac{\partial \sum \Delta P}{\partial Q_{Gi}} = 2\sum_{k=1}^{n}(\alpha_{ik}Q_k + \beta_{ik}P_k)$$

$$\frac{\partial \sum \Delta P}{\partial Q_{G1}} = 2\left(\frac{R_1}{V^2}\cos(\theta_1 - \theta_2)(Q_{C1} - 10) + \frac{R_2}{V^2}\cos(\theta_2 - \theta_0)(Q_{C1} + Q_{C2} - 18) + \right.$$

$$\left. \frac{R_1}{V^2}P_1\sin(\theta_1 - \theta_2) + \frac{R_2(P_1 + P_2)}{V^2}\sin(\theta_2 - \theta_0) \right)$$

$$\frac{\partial \sum \Delta P}{\partial Q_{G2}} = 2[\frac{R_2}{V^2}\cos(\theta_2 - \theta_0)(Q_{C1} + Q_{C2} - 18) + \frac{R_2(P_1 + P_2)}{V^2}\sin(\theta_2 - \theta_0)]$$

$$\frac{\partial \sum \Delta P}{\partial Q_{G3}} = 2\left(\frac{R_3}{V^2}\cos(\theta_3 - \theta_4)(Q_{C4} - 6) + \frac{R_4}{V^2}\cos(\theta_4 - \theta_0)(Q_{C3} + Q_{C4} - 10) + \right.$$

$$\left. \frac{R_3}{V^2}P_3\sin(\theta_3 - \theta_4) + \frac{R_4(P_3 + P_4)}{V^2}\sin(\theta_4 - \theta_0) \right)$$

$$\frac{\partial \sum \Delta P}{\partial Q_{G4}} = 2[\frac{R_4}{V^2}\cos(\theta_4 - \theta_0)(Q_{C3} + Q_{C4} - 10) + \frac{R_4(P_3 + P_4)}{V^2}\sin(\theta_4 - \theta_0)]$$

Where $Q_{C1}, Q_{C2}, Q_{C3}, Q_{C4}$ are namely the reactive power compensation for Load 1, 2, 3, 4.

Step 4.

Set up four calculating equations as below:

$$\frac{\partial \sum \Delta P}{\partial Q_{G1}} = \frac{\partial \sum \Delta P}{\partial Q_{G2}}$$

$$\frac{\partial \sum \Delta P}{\partial Q_{G3}} = \frac{\partial \sum \Delta P}{\partial Q_{G4}}$$

$$\frac{\partial \sum \Delta P}{\partial Q_{G2}} = \frac{\partial \sum \Delta P}{\partial Q_{G4}}$$

$$Q_{C1} + Q_{C2} + Q_{C3} + Q_{C4} = 20MVAr$$

Step 5.

Substituting the value of the ***known*** variables into the above equations and operating, we obtain the optimal reactive power distribution for each load as follows:

$$Q_{C1} = 9.5MVAr,\ Q_{C2} = 3.9MVAr,\ Q_{C3} = 5.0MVAr,\ Q_{C4} = 1.6MVAr \qquad (37)$$

Method 2, Engineering calculation:

The more straightforward way is, by considering the total active power loss equations via the variables P_i, Q_i, then take partial differential according to formula (23). Refer to Fig. 1-5:

$$\sum \Delta P = \sum_{i=1}^{4} \frac{S_i^2}{V_i^2} R_i = \sum_{i=1}^{4} \frac{P_i^2}{V_i^2} R_i + \sum_{i=1}^{4} \frac{Q_i^2}{V_i^2} R_i .$$

The term $\sum_{i=1}^{4} \frac{P_i^2}{V_i^2} R_i$ is a constant, and will be zero when differentiated, thus:

$$\sum_{i=1}^{4} \frac{Q_i^2}{V_i^2} R_i = \frac{1}{V^2} \left[10(Q_{C1} - 10)^2 + 20(Q_{C1} - 10 + Q_{C2} - 8)^2 + 30(Q_{C3} - 6)^2 + 40(Q_{C3} - 6 + Q_{C4} - 4)^2 \right]$$

Taking differentiation gives:

$$\frac{\partial \sum \Delta P}{\partial Q_{G1}} = \frac{1}{V^2} \left[20(Q_{C1} - 10) + 40(Q_{C1} + Q_{C2} - 18) \right]$$

$$\frac{\partial \sum \Delta P}{\partial Q_{G2}} = \frac{1}{V^2} \left[40(Q_{C1} + Q_{C2} - 18) \right]$$

$$\frac{\partial \sum \Delta P}{\partial Q_{G3}} = \frac{1}{V^2} \left[60(Q_{C3} - 6) + 80(Q_{C3} + Q_{C4} - 10) \right]$$

$$\frac{\partial \sum \Delta P}{\partial Q_{G4}} = \frac{1}{V^2} \left[80(Q_{C3} + Q_{C4} - 10) \right]$$

Taking similar procedures with step 4, and 5 as Method 1, we obtain:

$$Q_{C1} = 10.0MVAr,\ Q_{C2} = 8/3 = 2.7MVAr,\ Q_{C3} = 6.0MVAr,\ Q_{C4} = 4/3 = 1.3MVAr \quad (38)$$

Method 3, improved Method 1.

Based on the principle explained in Method 2, in practice, we can neglect the influence of the active power distribution in our calculations. Whereas, let the active power in all loads equal to zero. Then, we follow the steps as Method 1.,

$$1>\ \theta_i = 90^\circ$$

$$2>\alpha_{ik} = \frac{R_{ik}}{V_i^2}\ ,\ \beta_{ik} = 0$$

$$3>\frac{\partial \sum \Delta P}{\partial Q_{Gi}} = 2\sum_{k=1}^{4} \alpha_{ik} Q_k$$

$$\frac{\partial \sum \Delta P}{\partial Q_{G1}} = \frac{1}{20}[(Q_{C1} - 10) + 2(Q_{C1} + Q_{C2} - 18)]$$

$$\frac{\partial \sum \Delta P}{\partial Q_{G2}} = \frac{1}{20}[2(Q_{C1} + Q_{C2} - 18)]$$

$$\frac{\partial \sum \Delta P}{\partial Q_{G3}} = \frac{1}{20}[3(Q_{C3} + Q_{C4} - 10)]$$

$$\frac{\partial \sum \Delta P}{\partial Q_{G4}} = \frac{1}{20}[4(Q_{C3} - 6) + 3(Q_{C3} + Q_{C4} - 10)]$$

Repeating step 4, and step 5, as Method 1., we obtain:

$$Q_{C1} = 10.0MVAr\ ,\ Q_{C2} = 8/3 = 2.7MVAr\ ,\ Q_{C3} = 6.0MVAr\ ,\ Q_{C4} = 4/3 = 1.3MVAr \qquad (39)$$

The results are exactly the same as those obtained using Method 2.

To validate the results, assume that the total reactive power compensation is 28 MVAr, the compensating capacity of each load distributed by optimal mathematical model is equal to the reactive power shortage of each load. Substituting 28 MVAr into any equation of the above three methods instead of 20MVAr gives:

$$Q_{C1} = 10MVAr\ ,\ Q_{C2} = 8MVAr\ ,\ Q_{C3} = 6MVAr\ ,\ Q_{C4} = 4MVAr \qquad (40)$$

The results obtained in (40) validates this mathematical model.

II. SPECIAL LOAD ANALYSIS

ABSTRACT: This chapter analyses electric characteristics of special loads such as Electric Arc Furnaces (EAFs), Converters and Railway traction in turn. The analyses was based on theoretical approaches and on results obtained from some on-the-spot experiments in the real metallurgic industry projects or railway routes in China. The statistical tables and empirical formulae shown, which describe the general features of these loads, were concluded from the analysis. From the tables and equations that define operation, the performance of these dynamically changeable loads can be predicted and assessed.

2.1. General

It is impossible to take strategies for "Special Loads" reactive power compensation without first considering the load characteristics of dynamically changeable and unbalanced loads. Typical of such loads are: EAFs, Rolling Mills, Railway traction, Converters, Colliery winders and welding equipment; where rapid variations in load currents may result in fluctuations and non-linear components in the voltage at customers' intake points. Chart 2-1., shows the percentage content of the special loads in the following industries in Beijing, China, 1997 [23].

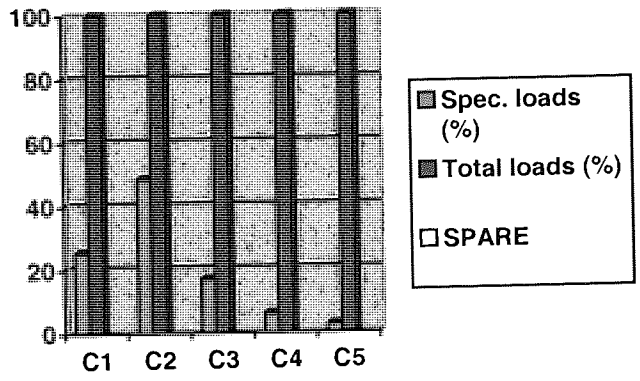

Chart 2-1.[1]

Where:

C1 (Customer 1) is the Metallurgic Industry

C2 (Customer 2) is Transportation

C3 (Customer 3) is the Chemical Industry

C4 (Customer 4) is the Machinery Industry

C5 (Customer 5) is the Telecommunications Industry

This chapter takes no account of Rolling Mills, Colliery winders and Welding equipment, since their load characteristics are relatively mild. There are also items of equipment mainly in use in domestic and commercial premises such as colour TVs, tape recorders, electric fans, air-conditioners, refrigerators and fluorescent lamps. Although individually not causing problems, they can collectively affect the quality of supply owing to the large number of items involved. Normally their influence is included in the contents of the background harmonics, and they are generally not considered as special loads.

In order to restrain the pollution of special loads to power system , we should be clear about such factors as the magnitude, contents of the non-linear components or un-balanced components, rate of change of the currents taken by the load, and whether the load changes occur at regular or random intervals of time.

To compensate effectively, it is important to dynamically model the highly varying, non-linear loads. Typically, the modelling of such loads has involved stochastic techniques. In recent studies with the modelling of EAFs, researchers have presented the use of chaotic dynamics to describe the operation of non-linear loads[24]. This chapter does not involve specific features of special loads, but includes the general description of their features for engineering calculations and as the basis of further research in this area.

[1] the statistical datum is provided by Electric Power Research Institute of China

2.2. CONVERTERS

Applications of power electronics converters continue to increase, especially because of their ability to help conserve energy and provide better control of traditional and new processes. However, the inherent non-linear nature of the solid-state equipment load places harmonic current demands and extraneous losses upon the electrical power systems[31]. Theoretically, the harmonics generated by an ideal rectifier are given by [32]:

$$h = kp \pm 1 \qquad (41)$$

Here:

h - harmonic number

p - pulse number

k - any integer from 1 to infinity.

In real engineering design, we use the following equation to predict the harmonic contents of rectifiers:

$$I_h = \frac{\beta S_{\max}}{\sqrt{3} V_0 h} \qquad (42)$$

Where:

$S_{\max}$ -total capacity of the rectifiers which have the same pulse number and be connected at the same bus-bar;

I_h - h order harmonic current;

β - is the correction coefficient and its values are given by Table 2-1 [30].

Table 2-1

Harmonics	5^{th}	7^{th}	11^{th}	13^{th}	17^{th}	19^{th}	23^{rd}	25^{th}
6-pulse	0.95	0.9	0.75	0.72	0.66	0.50	0.40	0.30
12-pulse	0.30	0.30	0.80	0.75	0.20	0.15	0.45	0.35

Theoretically, simple 3-pulse rectifiers produce all harmonics except the triplets where the harmonics are a multiple of 3. With the 6-pulse arrangement, the even harmonics are also eliminated. There are no 5^{th}, 7^{th}, 17^{th}, 19^{th} harmonic currents in ideal 12-pulse rectifiers [32]. In practice, the situation is not the same as stated above (refer to Table 2-2), possibly due to the contribution of system background harmonics and the influence of numerous system component

variations. It is important to measure the real harmonic currents in a system under various conditions before design.

With regard to the VSD harmonics, when the circuit is used in a cyclo-converter, the level of harmonics will vary with the firing delay angle. The harmonic content in the input current to a cycloconverter is particularly complicated because the currents and phase converters are continually varying at the motor frequency rate. It is possible, however, to come to some general conclusions which are given by[33], and practically useful.

1> The total input current is converted by the mains commutated thyristor switches before flowing into the motor and therefore the worst case supply harmonics will be on the basis of a constant firing angle where the harmonics from the three phases add together arithmetically. With full wave converters, the total input current will contain approximately: 20% of 5^{th}, 14% of 7^{th}, 9% of 11^{th}, and 8% of 13^{th} and etc (under the worst case).

2> The nearest condition to the worst case is at low speed and low voltage where the phase angles hardly move from 90 degrees delay.

3> Under the other conditions, the supply frequency related harmonics may be less than the above, but their values will be changing at a frequency related to the motor frequency. This means that there will be other harmonic frequencies present, which are related to the motor frequency or both motor and supply frequencies together. Table 2-2 strongly supports this conclusion.

Table 2-2.The real harmonic currents in a VSD used for a compressor in China [23]

Harmonics	3^{rd}	5^{th}	7^{th}	11^{th}	13^{th}	17^{th}
Contents %	5.57	**26.5**	**10.3**	**7.66**	**4.23**	4.06

2.3. RAILWAY TRACTION [34]

While some railway traction operates on DC using 3-phase trackside rectifiers, mainly in urban or suburban areas, the majority of traction supplies are now being provided at single-phase AC, typically 25kV, 50Hz / 60Hz. Since an almost total use of power electronics devices on traction power units in order to use DC motor, there has been a harmonic distortion in the supply network. Simultaneously, the single-phase supply of a railway traction from two or three phases of the main supply system results in voltage unbalance and thus leads to negative sequence currents.

Harmonics: Theoretical analysis method for railway traction is similar to that of converters discussed in section 2.2. Table 2-3 & 2-4 provide some results of on-the-spot experiments to support the following conclusions.

Table 2-3, Harmonic contents (%) in Shao-Shang-1(SS1)-Traction (made in China)[2]

Harmonics	3rd	5th	7th	9th	11th	13th	15th	17th	19th	21st	23rd	25th	27th	29th	31st
Contents %	**20.1**	**10.7**	**6.47**	**3.76**	**2.32**	1.55	1.17	0.95	0.80	0.71	0.61	0.57	0.41	0.21	0.20

Table 2-4, Content of harmonic currents varies with the total-load-current (TLC) (the number of the traction in a group, SS1-Traction made in China)[3]

Harmonics (orders)	3rd	5th	7th	9th	11th
TLC=0-100A, Harmonic contents %	23.0	12.3	6.9	3.9	2.7
TLC=100-200A	22.2	10.6	5.6	3.0	2.2
TLC=200-350A	21.5	10.0	5.2	2.5	1.5
TLC=350-500A	19.5	8.9	4.6	2.1	1.4
TLC>500A	17.3	7.5	3.6	1.3	1.1

[2] The datum of table 6 & 7 were provided by Beijing Huanxing Testing Center.

[3] Tests were done by Beijing Huanxing Testing Center at Zhou-Shi-Zhuang Substation, Feng-sha-da Traction line, China.

Although the individual harmonic contents are affected by many factors such as: the type of the traction, the rated capacity of the traction, the strategies used for traction harmonic mitigation and etc.; the following conclusions are applicable to all kinds of traction:

1> The harmonic contents caused by traction are mainly 3^{rd}, 5^{th}, 7^{th}, 9^{th}, and 11^{th}; and the magnitude of the harmonic current content (percentage) decreases with the number of harmonic order increases.

2> The individual harmonic current content (percentage)decreases with the total load current increases.

2.4. Electric Arc Furnaces (EAFs)

2.4.1 General

In recent years, there has been a substantial increase in the size and power input rating of EAFs. One consequence of this type of load is that an increasing number of utilities are being confronted by the problems of arc furnace loads. The main features of the operation of an EAF are [25]:

- Unfavourable power factor, Voltage drop.
- Violent current changes.
- Violent reactive power fluctuations.
- Harmonic currents.
- Unbalanced.

For convenience, it is necessary to find out the relationship between the following variables of an EAF: active power P, reactive power Q, complex power S and power factor $\cos\varphi$, via the current I. Assuming the 3-phase currents of an EAF are balanced, we can obtain the simplified EAF calculation circuit shown as Fig. 2-6.

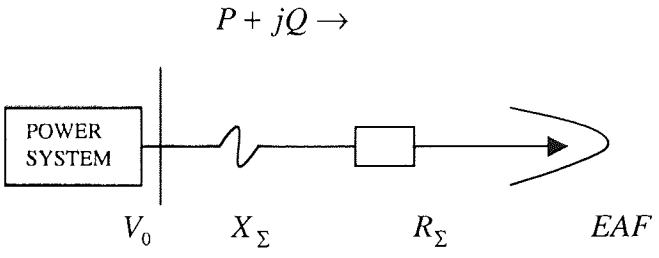

Fig. 2-6. The equivalent circuit of an EAF

From Fig. 2-6, and based on the principles of Circuit Analysis, we obtain:

$$P = \frac{V_0^2 R_\Sigma}{X_\Sigma^2 + R_\Sigma^2},$$

$$Q = \frac{V_0^2 X_\Sigma}{X_\Sigma^2 + R_\Sigma^2},$$

$$S = \frac{V_0^2}{\sqrt{X_\Sigma^2 + R_\Sigma^2}},$$

$$I = \frac{V_0}{\sqrt{X_\Sigma^2 + R_\Sigma^2}},$$

$$\cos\varphi = \frac{R_\Sigma}{\sqrt{X_\Sigma^2 + R_\Sigma^2}} \qquad (43)$$

Where X_Σ, R_Σ are respectively total reactance and resistance of the circuit (including that of the EAF). In a pu-system, say $V_B = V_0, S_B = S_{BE} = V_0^2 / X_\Sigma$ (S_{BE} is the maximum short-circuit capacity of the EAF), and provided $\Omega = X_\Sigma / \sqrt{X_\Sigma^2 + R_\Sigma^2}$; we obtain:

$$S = I = \Omega,$$
$$Q = \Omega^2,$$
$$P = \Omega\sqrt{1-\Omega^2},$$
$$\cos\varphi = \sqrt{1-\Omega^2} \qquad (44)$$

It is easy to describe the curves of equations (44) with the elemental mathematics. Refer to Fig. 2-7b for these curves.

From above, when $\Omega = 1/\sqrt{2}$ (or $X_\Sigma = R_\Sigma$);

$$P = P_{\max} = S_{BE}/2 \qquad (45)$$

From equations (43), considering $S_{BE} = V_0^2 / X_\Sigma$, we can derive a very useful equation as below:

$$P^2 + (Q - S_{BE}/2)^2 = \frac{4X_\Sigma^2 R_\Sigma^2 + (X_\Sigma^2 - R_\Sigma^2)^2}{4(X_\Sigma^2 + R_\Sigma^2)^2} S_{BE}^2, \text{ that is:}$$

$$P^2 + (Q - S_{BE}/2)^2 = (S_{BE}/2)^2 \qquad (46)$$

Naturally, this is the equation of a circle with a centre $(0, S_{BE}/2)$ and with radius $S_{BE}/2$, when V_0, X_Σ are kept constant (refer to Fig. 2-7a.). Fig. 2-7a shows the relationship between the real and reactive power of an EAF according to equation (46). Fig. 2-7b shows the electrical characteristics of an EAF following equation (44).

Refer to App.-Fig. 1~5 of Appendix I for some real engineering measurements of an EAF currents and reactive power curves which will support the above conclusions.

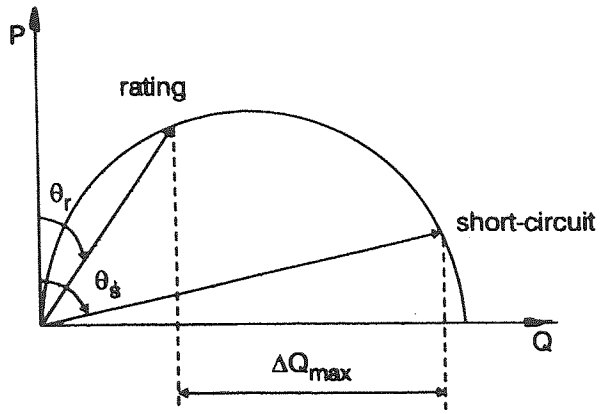

Fig. 2-7a, the relationship between the real and reactive power of an EAF according to equation (46).

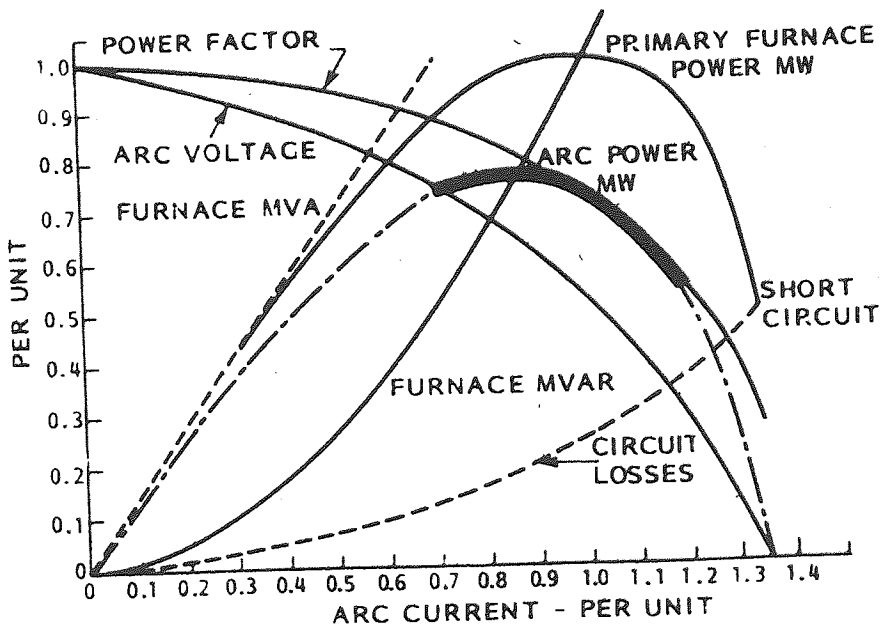

Fig. 2-7b, the electrical characteristics of an EAF following the equation (44).

2.4.2 Load Characteristics

1. Statistical Description of the EAF.

Table 2-5 shows the EAF load features in different stages of a heat of its smelting. The EAFs included in the table are the average arc furnaces used in China and ranged from 5t to 20t. For modern ultra-high-power (UHP) EAFs, the total time of a heat of smelting is only between 70 and 90 minutes. It is worth stating that the power consumption listed in the table does not include power consumed by the accessories of an EAF.

Table. 2-5

Periods	Time	P %	A %	Features
Charging	<2.5h	0	0	
Melting- down	0.5-2.5h	100	60-70	Violent change in power-factor, active/reactive power and currents. Unbalanced 20%; Flicker; and Voltage-fluctuation
Power off	<0.5h	0	0	
Oxidising	<0.5h	40-50	15-20	Vary relatively gentle
Removing slag		0	0	
Reducing	<2.0h	40-50	20-25	Same as above

2. Power factor and violent reactive power fluctuation [25], [26]

A particular feature of the operation of the EAF is the frequent recurrence of short circuits between the electrodes and the scrap-metal charge. Because of this feature, the power factor of the EAF varies from 0.1 to 0.2 while the short circuit occurs, and from 0.7 to 0.85 after obtaining the stable arcs [32].

Refer to Fig. 2-7a, the maximum reactive power variation can be calculated by the following formula:

$$\Delta Q_{max} = Q_{max} - Q_{min} = S_{BE}(\sin^2 \varphi_{max} - \sin^2 \varphi_{min}) \quad (47)$$

Since,

$\varphi_{max} \cong \cos^{-1} 0.1$, $\varphi_{min} \cong \cos^{-1} 0.85$

So that:

$$\Delta Q_{max} = S_{BE}(\sin^2 \varphi_{max} - \sin^2 \varphi_{min}) = 0.713\, S_{BE}$$

The active power must, of course, be transmitted from the generator to the EAF. The reactive power should not, as a matter of principle, be transferred over a long distance. This will result in increasing voltage drop and an increasing loss due to higher currents. This means extra transfer costs and excessive utilisation of the thermal capability of apparatus, particularly transformers and cables owing to higher currents.

3 Voltage drop

The reactive power causes a voltage drop on the primary side of the furnace transformers. The voltage dip is:

$$\Delta V = \frac{Q_{EAF} + 0.5 Q_{NET}}{S_{SC}} V_0 \qquad (48)$$

Where:

V_0 is no-load voltage,

Q_{EAF} is the reactive power of an EAF,

Q_{NET} is the network reactive power

S_{SC} is the fault level at the point of common coupling (pcc).

The voltage drop means lower active power to the EAF, longer melting-down time and lower production.

4 Voltage fluctuation

The current fluctuations due to the instability of the arcs will correspond to large fluctuations in the reactive power. Voltage fluctuations arise in the network owing to these reactive power fluctuations. In practice, the voltage fluctuation is given by:

$$\Delta V_f = \Delta V / V = \Delta Q / S_{SC} \qquad (49)$$

Here:

ΔQ is the reactive power fluctuation at pcc,

S_{SC} is the fault level at pcc.

From the above equation, limiting the voltage fluctuations without any special compensation facilities requires a high fault-level; so high that it is generally only available at the highest system voltage.

5 Harmonics

The current to the furnace is highly distorted particularly during the melting-down. An analysis of the current waveform shows a content of both harmonic and non-harmonic frequencies, as proved by theoretical analysis and real engineering measurements[27]:

- Normally the most predominant frequency is the 3rd harmonic
- Higher odd harmonics (5th, 7th) exist, and decrease in magnitude with increasing order number. The other higher odd harmonics exist too, but they have relatively small magnitudes, and as the order number increases the magnitude decreases.
- Also even harmonics (2nd, 4th, 6th) exist.

Tables 2-6 and 2-7 give us some information on the ratio expressed as a percentage between the harmonics and the amplitude of the fundamental current to the EAF, which support the above conclusions.

Table 2-6. statistics-average of harmonic current contents in EAFs used in China.

Harmonic order	2nd	3rd	5th	7th
Content %	5-12%	**9-15 %**	5-7 %	2-3 %

Table 2-7. real harmonic contents of a 150t EAF and a LF together.

	2^{nd}	3^{rd}	4^{th}	5^{th}	6^{th}	7^{th}	9^{th}	11^{th}	13^{th}	15^{th}	17^{th}	19^{th}	21^{st}
EAF	8.0	9.0	6.0	6.0	4.0	3.0	1.0	1.0	0.5	0.5	0.3	0.2	0.2
LF	4.0	9.0	4.0	4.0	2.0	2.0	1.0	1.0	0.3	0.3	0.2	0.1	0.1

6 Load Unbalanced

During the melting-down period there will be random current changes with two or three phases short-circuited, or one phase on open circuit. The swings from short-circuit to open circuit produce violent current fluctuations, often several times larger than the furnace nameplate rating, whether this be some kilowatts or tens of megawatts [27]. The result is that the reactive power in each phase seldom has the same value, even if the phase impedance are equal. During the melting of scrap-metals, the average value of the negative sequence current to an EAF is about 20 %. Due to the above, customers must install equipment for compensating reactive power, cancelling harmonics and balancing the EAF load.

2.4.3 Flicker and its Prediction [28],[29]

Operating EAFs produce flicker. There are two methods to predict the flicker caused by EAF, namely, short-circuit voltage depression (SCVD) and maximum reactive power variation (MRPV). The steps of calculations are as follows:

1> Calculating voltage fluctuation ΔV_f

SCVD:

$$\Delta V_f = \frac{S_{BE}}{S_{SC(\min)}} 100\% \qquad (50)$$

MRPV:

$$\Delta V_f = \frac{X_\Sigma \Delta Q_{\max}}{S_B} \qquad (51)$$

Here: S_B base- fault-level, normally 100MVA.

2> Short term flicker:

$$F_{st} = 0.5\Delta V_f \qquad (52)$$

3> Long term flicker:

$$F_{lt} = 0.36\Delta V_f \qquad (53)$$

4> For the same capacity EAFs in group;

$$F_{st\Sigma} = k_n F_{st} \quad (k_1 = 1, k_2 = 1.18, k_3 = 1.3) \qquad (54)$$

5> For the EAFs in group with different capacity;

$$F_{st\Sigma} = \left[\sum_{i=1}^{n} (F_{sti})^m \right]^{1/m} \qquad (55)$$

Here:

m=1 if EAFs' melting period overlaps each other [30];

m=2 if overlaps occasionally

m=3 if seldom overlaps

A full consideration of flicker produced by operating EAFs is given in chapter 3.

III. FLICKER ANALYSIS AND METHODS FOR ELECTRIC ARC FURNACE (EAF) MITIGATION

ABSTRACTS: This chapter gives a general review about how to examine/assess voltage flicker and methods followed in measuring flickers due to arc furnace and means for mitigation. It also investigates fast response SVG for arc furnace flicker mitigation. It includes discussions on the effects of utilities' conditions, compensator response-time and compensator capacity on arc furnace flicker reduction. A comparison between SVC and SVG on the applications of EAF compensation is carried out. Some discussions about the perspective of applying SVG for EAF compensation are also included in this chapter.

3.1 FLICKER ANALYSIS

3.1.1 Introduction

The problems due to rapid variations of reactive power and harmonics generated by non-linear loads like the EAFs are well known. The large and erratic reactive currents swings in an EAF which give rise to corresponding voltage drops across the (reactive) impedance of the ac system may result in fluctuating terminal voltage. The fluctuating system voltage may cause variations in light output of electrical lamps flashing ("flicker") and disturbance in other electrical equipment. About twenty years ago, the most important role of flicker measurement was to provide an objective answer to the question of whether flicker conditions are acceptable.

The first Flicker Meter was developed by UK Electrical Research Association (ERA, British) in 1972[35]. This meter was originally developed to measure uncompensated arc furnace caused flicker in the UK. Then, in 1974, Westinghouse Electric Corporation developed a light-weight flicker meter based on British ERA recommendations. In 1976, the Electricite' de France (EDF, French) also developed a flicker meter. In Japan the ΔV_{10} Japanese Meter was developed by CRIEPI (Central Research Institute of Electric Power Industry) in 1978[36]. In the early 1980s, UIE/IEC defined an internationally agreed method for flicker measurement and an agreed limit of tolerance[100]. Recently, many measuring techniques have been developed to evaluate the voltage flicker[37]. These measuring instruments can be divided into two categories, based on the demodulation methods of the modulated signal from the source voltage waveforms; analog algorithm[35]-[37] and digital algorithm[38]-[43], [78]-[81]. However, the calculation of fluctuation components at different frequencies (typically from 0.1 to 30 Hz) are implemented by fast Fourier transform (FFT) for most of these instruments.

In order to make improvement on flicker measurement today, special attention is focused on the following issues:

- Improving the calculating algorithm for a better accuracy like [44], [80], [81].
- Applying it in some specific industry loads flicker measurement: wave-power station[82], wind turbines [83] and EAFs [84], [85].
- Using Kalman filter estimation to predict the instantaneous flicker level[47], [43] & [48].

As the degrees of flicker severity depend on furnace operation types, mitigation devices and distribution network conditions, extensive studies by many organisations are given to solve the related problems. Various measures can be taken from the following aspects:

1. Stabilise the arcs of an EAF by improving:
   - the EAF electrode control or such[53]-[56], [87]-[91],
   - the composition of scrap[57],
   - the accuracy of arc furnace modelling for control[58]-[61],
   - the types of the furnace operation.
2. Take measures to increase the fault level at pcc [41], [43].
3. Select the well performance compensation devices to meet the flicker requirements for a given fault level[92]-[96], and carefully design the passive harmonic filter[54].

The practical solution of difficult problems associated with flicker will require using a variety of methods listed above in appropriate combination as reported by [41]. However, as a fitted EAF with a predictable fault level at the point of common coupling (pcc), the flicker compensator takes a very important role for the flicker mitigation.

The earliest industrial flicker compensators were installed in the late 1950s and were based on the saturable reactor principle, in which iron saturation characteristics were used to stabilise the voltage[64]. However the power electronic switched compensators were introduced to replace the saturable reactor compensator, as they are much cheaper and more flexible in use. The Static VAr Compensators (SVCs) were first developed in the late 1960s for the compensation of large, fluctuating industrial loads. In the early 1970s, two kinds of SVCs had been put in practical use for EAF flicker suppression. One is the Thyristor Controlled Reactor (TCR) type[65], and the other is the Thyristor Switched Capacitor (TSC)[66], [96]. The possibility of generating or

absorbing controllable reactive power with various power electronic switching converters had been recognised at the late 1980s and several schemes were implemented in laboratory models[2].

The first Static VAr Generator (SVG) was made by the EPRI and Westinghouse in 1986. Now, the world's largest installation is the two +/- 160 MVA voltage sources GTO thyristor based converters located at the Inez substation in eastern Kentucky [5]. In recent years, SVGs have been introduced to replace the conventional SVCs for arc furnace flicker compensation as they can overcome the problems of the SVCs such as large size and high cost. As reported[92], the largest SVG for EAF application is the SMI installation in Texas. Commissioned in 1998, it comprises a +/-80MVA STATCOM with a shunt coupling transformer and operates in conjunction with a 60 MVA ac capacitor bank. However, the SVG (STATCOM) requires coupling components like the (zigzag) transformer to multiply converters and a high frequency switching PWM technique to reduce harmonics.

Nowadays, multilevel converter-based SVGs or STATCOM have been widely studied due to its capacity of eliminating the zigzag transformers[70]-[77], [98]-[99]. Among the multilevel converter-based SVGs, the cascaded multilevel inverter configuration has drawn tremendous interest in the power industry because of its extremely fast response (within 1ms) and simple structure[70]. Following the development of the prototype cascaded multilevel inverter-based SVG in 1996[73], a 50 MVA STATCOM based on cascading voltage source inverters was introduced in 1999[75]. Although it performs better than the conventional SVG/STATCOM with regard to its application for EAF flicker compensation, it still leaves room for improvement. The next chapter will investigate the cascade multilevel converters-based SVG for EAF application and propose a new method for improvement.

3.1.2 Examining Flicker and its Mathematical Manipulations

Although various kinds of flicker meters were developed, they can be divided into five categories. Based on the definition given by UIE/IEC, we can define the input voltage signal $u_{(t)}$ in the form of $u_{(t)} = A(1 + m\cos\omega_{fl}t)\cos\omega t$, and the output signal $g_{(t)}$ in the form of $g_{(t)} = C\cos\omega_{fl}t$. Then we can derive mathematical models (or manipulations) of three typical flicker meters: UIE/IEC standard meter, Equivalent 10 Hz voltage flicker (ΔV_{10}) meter and Gauge-point voltage flicker meter as follows:

(1) UIE/IEC standard flicker meter

Taking square operation of both sides of $u_{(t)}$, we obtain equation (56) as follows:

$$u_{(t)}^2 = \frac{A^2}{2}(1+\frac{m^2}{2}) + mA^2\cos\omega_{fl}t + \frac{m^2A^2}{4}\cos 2\omega_{fl}t + \frac{A^2}{2}(1+\frac{m^2}{2})\cos 2\omega t + \frac{m^2A^2}{8}\cos 2(\omega+\omega_{fl})t + \frac{m^2A^2}{8}\cos 2(\omega-\omega_{fl})t + \frac{mA^2}{2}\cos(2\omega+\omega_{fl})t + \frac{mA^2}{2}\cos(2\omega-\omega_{fl})t \quad (56)$$

from equation (56), after filtering the DC component and fundamental frequency, it gives:

$$g_{(t)} \approx m\cos\omega_{fl}t \quad (57)$$

Where:

$\omega_{fl}, \omega, m, A$ are respectively, the frequency of the sinusoidal voltage fluctuations, fundamental frequency (50Hz/60Hz), peak value of the sinusoidal voltage fluctuation and peak value of the fundamental voltage.

(2) Equivalent 10 Hz voltage flicker (ΔV_{10}) and meter[38], [49]

ΔV_{10} is the measure of the voltage flicker. It is widely used in Japan, and a ΔV_{10} meter was built to estimate the voltage flicker according to the following equation:

$$\Delta V_{10} = \sqrt{\sum_{i=1}^{\infty}(a_n \Delta V_n)^2} \quad (58)$$

Where :

ΔV_n is the double amplitude of the voltage fluctuation component at frequency f_n, and it can be calculated from the spectrum analysis of the modulated signal.

a_n is the flicker sensitivity at frequency f_n, and the flicker-sensitivity curve corresponds to the frequency-characteristic curve of the ΔV_{10} weighting filter. In this case, the basic equation is:

$$K_{(\tau)} = \frac{1}{T}\int_{\tau}^{T+\tau} u_{(t)}^2 dt - \frac{1}{T}\int_{\tau}^{\tau+T}(A^2/2)dt \quad (59)$$

Neglecting the items having a frequency that is more than 2ω and considering $\omega T = 2\pi; \tau \to t$, then:

$$K_{(t)} = \frac{\omega m A^2}{2\omega_{fl}\pi}\sin(\omega_{fl}\pi/\omega)\cos(\omega_{fl}t + \omega_{fl}\pi/\omega) \qquad (60)$$

Finally, the output signal is:

$$g_{(t)} = m\cos(\omega_{fl}t + \omega_{fl}\pi/\omega) \qquad (61)$$

(3) Gauge-point voltage flicker and meter [35], [39]

UK Electricity Council Engineering Recommendation P7/2 defined the gauge-point voltage fluctuation V_{fg}, based on a statistical result of a voltage fluctuation test over a period of time of at least several days. The rms value of the fluctuation voltage is measured and recorded minute by minute, and then a cumulative probability curve is plotted. V_{fg} represents the voltage-fluctuation level that exceeds 1% of the readings. The V_{fg} limit is 0.25%, and the V_{fg} meter was developed by the ERA, UK. Theoretically, the calculation is equivalent to $u_{(t)}$ multiplied by a fundamental frequency unit (the peak value equals to one) rectangle wave function $p_{(t)}$ as (62):

$$p_{(t)} = \frac{4}{\pi}(\cos\omega t + \frac{1}{3}\cos 3\omega t + \frac{1}{5}\cos 5\omega t\cdots), (u_{(t)}p_{(t)} = \frac{2A}{\pi} + \frac{2mA}{\pi}\cos\omega_{fl}t + \frac{2A}{\pi}\cos 2\omega t + \cdots) \qquad (62)$$

After filtering and modulation, we obtain the output function as equation (63).

$$g_{(t)} = m\cos\omega_{fl}t \qquad (63)$$

(4) Maximum permissible voltage flickers (MPVF) and meter [38], [42], [78].

The MPVF in IEEE STD 519-1992 defines two curves given at the borderlines of irritation and visibility. Recently, a voltage-flicker measurement and evaluation system was developed to investigate the operation characteristics of multiple AC and DC EAFs [78]. The system voltage is sampled by an ADC for several seconds, and the magnitude V_n at frequency f_n in the modulation signal can be extracted from the rms voltage fluctuation over the sampling interval by using the FFT algorithm. Then the V_n - f_n curve can be displayed immediately along with the two MPVF curves. The V_n - f_n curve can be also averaged over a period of time, and we can

easily identify whether the voltage flicker is exceeded from the comparison between the MPVF curve and the measured V_n - f_n one.

(5) The others: The other definitions and meters for quantifying voltage flicker are the EDF meter and the FGH. They are used in France and Germany respectively. In France, the cumulative voltage flicker dose curve can not be exceeded at any time from the start of a measurement. In Germany, the acceptable voltage flicker is defined in terms of a short time (over 15 minutes) and long time (over seven days) 99% probability of a cumulative voltage flicker level.

3.1.3 Flicker Criteria

The Criteria used for measurement might be one (or more) of the following:

P_{st} / P_{lt} - short/long-term Flicker severity,

V_{fg} - Voltage flicker,

ΔV_f -Voltage depression,

ΔV_{10} - equivalent 10 Hz voltage flicker.

In engineering design, for EAF flicker, most countries use a similar criterion as that used by the CEGB criterion[100], which limit the short circuit voltage depression ΔV_f (SCVD) to 1.5%, 2.0 or 2.5 maximum. Table 3-8 shows the flicker criteria in some countries.
The empirical relationships among above variables used for measuring and design are as follows[86]:

$$V_{fg} \approx 0.12\Delta V_f \tag{64}$$

$$P_{st} \approx 0.5\Delta V_f \tag{65}$$

$$P_{lt} \approx 0.36\Delta V_f \tag{66}$$

$$P_{st} \approx 3\Delta V_{10} \tag{67}$$

Table 3-8. The flicker criteria used in some countries

Countries	Type of criteria	The criteria used
UK	P_{st} / P_{lt} V_{fg} ΔV_f	1.0/0.8 for 132 kV, 0.8/0.6 as above 132kV 0.25% for 132kV, 0.2% as above 2.0% for 132kV, 1.6% as above
China	ΔV_{10} ΔV_f	0.6% as max., 0.4% as mean 2.5% for 10kV, 2% for 15-110kV, 1.6% as above
Japan	ΔV_{10}, ΔV_f	0.45% as max., 0.32% as mean; 2.0% respectively
USA	ΔV_f, ΔV_{10} and V_{fg}	2.0% as maximum, 0.5% and 0.25% as max. respectively
French	ΔV_{10}	0.3%
Italy	ΔV_{10}	0.3%
Brazil	ΔV_f, ΔV_{10}	2.0%, 0.5% respectively
Iran	ΔV_f, ΔV_{10}	2.0%, 0.5% respectively
Argentina	ΔV_{10}	0.5%
Yugoslavia	ΔV_f	2.5%
Sweden	ΔV_f	2.5%
Holland	ΔV_f	1.75% single EAF, 2.0% two EAFs
Swiss	ΔV_f	1.2-1.6% for single EAF. 2-2.7% for two- EAF 2.8-3.7% for three or more EAFs

3.1.4 Digital Measurement of Voltage Flicker

The measurement of voltage flicker can be implemented with completely digital type meters or digital-analog hybrid ones. The demodulation can also be classified into two categories for the former. The first one directly analyses the sampled voltage waveform by using FFT to obtain different voltage-fluctuation components V_n at f_n (in the range 30-60 Hz for the 60 Hz system). The second indirectly extracts V_n from the rms voltage fluctuation. The frequency f_n of V_n varies from 0.1 Hz to 30 Hz in this case. The FFT was also used to acquire V_n for some hybrid-

type meters. Therefore it can be seen that the FFT was applied in most of the current voltage-flicker meters.

3.2 Brief Summary of Existing Flicker Meters

1. UK: The first Flicker Meter was developed by UK Electrical Research Association (ERA, British) in 1972[35]. This meter was originally developed to measure uncompensated arc furnace caused flicker in the UK. It measures the rms value of the fluctuation voltage waveform in the range of 0.5 to 27 Hz and utilises a time constant of approximately 100 seconds to obtain reasonably steady readings. The British engineering recommendations are based on the ERA meter.

2. USA: In 1974, Westinghouse Electric Corporation developed a light-weight flicker meter based on British ERA recommendations. The Meter described in [38] has been used for voltage flicker measurements at 500 kV, 161 kV, and 115, 34.5 13.8 kV voltage levels. The system designed to monitor and analyse voltage flicker requires an interface module to isolate and scale power system quantities such as voltages and currents. Analog signals are sampled using an A/D converter board in conjunction with an IBM-compatible personal computer (486 based minimum). The displayed data includes the perceptible, maximum and average curves for the entire duration of the case, and its visual screen displays in near real-time yield a powerful understanding of the system status.

3. France: In 1976, the Electricite' de France (EDF, French) also developed a flicker meter. This meter detects voltage fluctuations in a frequency range of approximately 0.5 to 25 Hz and forms a weighted squared average of such fluctuations. This weighted average provides an assessment of the flicker dose that a test subject would perceive as being produced by the fluctuation.

4. Japan: The ΔV_{10} Japanese Meter was developed by CRIEPI (Central Research Institute of Electric Power Industry) in 1978. This type of meter has been built to detect the fluctuating component of voltage. The instrument, called the ΔV_{10} meter, was accepted across Japan. It is similar to the EDF version, the most important difference is the use of a sensitivity curve that is based on a 100-V filament lamp.

5. Germany: The Forschungagemeinshoft fur Hochstrom Technix (FGH, Germany) Meter: This meter detects and filters the voltage modulation component of the supply voltage by means of an incandescent lamp. The set of 12 filters, having center frequencies in the range of 0.7 to 28 Hz, have different sensitivities corresponding to the perceptibility curve for sinusoidal flicker. The threshold of perceptibility for other periodical signals (e.g., meander and saw-tooth shaped) is accurately reproduced by this meter. The output of the meter is always given by the highest filter output. The signal is later smoothed. This meter gives an instantaneous measure of flicker and is also capable of registering flicker over a long period of time.

6. Canada: In [39], refer to Figure 3-8, the meter comprises five Blocks. The task of Block 1 is to transform the different input voltages into an output signal $U_{(t)}$ with always the same mean rms value. The voltage matching allows nominal input voltages in the range of 55-415 V at line frequency. The output of the demodulator is the fluctuation voltage. The human flicker sensation caused by voltage fluctuations via eye and brain is simulated by the combined non-linear behaviour of Blocks 2-4, including demodulation frequency weighting, squaring, and smoothing of the fluctuation voltage. The output of Block 4 is the instantaneous flicker sensation $P_{F(t)}$. For evaluation of stochastic flicker levels, especially of long-time recordings, the meter incorporates a device for statistical flicker-level analysis (Block 5).

7. Italy [80]: The meter is a digital flicker-meter based on the forward and inverse FFT., and on the filtering in the frequency domain for the implementation of the functional blocks of simulation of lamp-eye-brain response. The instrument, implemented with a NI acquisition board inserted on a PC and with a software developed with the Lab View tools, samples the voltage and furnishes the instantaneous flicker level, continuously sampled at 2 kHz.

8. The Others: Such as, Taiwan [44], Egypt [45], Slovenia [46], and etc.

9. The UIE Standard Flicker Meter

The various national flicker meters all provide some measure of the severity of flicker at a given installation. However, due to the different weightings given to the voltage fluctuation component as well as the different interpretations used to define the flicker dose, the meters do

not give consistent readings on common data. Consequently, UIE in cooperation with IEC, proposed and developed a standard meter for the measurement of flicker as early as the 1980's. The criteria used in developing the UIE meter include the following (refer to Fig. 3-8);

(1) Indication of instantaneous flicker value: the instrument should allow the instantaneously perceptible flicker to be evaluated.
(2) Voltage fluctuation waveform: the instrument should furnish, at least for its short-period indication, one and the same result for a given flicker impression regardless of the voltage fluctuation waveform. The flicker measuring method would thus be suitable for use with voltage fluctuation caused by EAF, welding machines, and combinations of individual thyristor-controlled apparatus.
(3) Long-time recording: the instrument should be capable of recording the short-time flicker value over a period of time.
(4) For a given fluctuation frequency, the indication on the instrument should be a simple function of the magnitude of the voltage fluctuation.
(5) Frequency range: the instrument should be able to handle regular and irregular voltage fluctuation, at least in the range of 1-25 Hz (2-50 voltage changes/s).
(6) Portability: it should be possible for one person to handle and connect the instrument.
(7) Checking: it should be equipped with a simple means for checking the correct operation.
(8) Record: the record (chart, magnetic tape, etc.) should be easy to evaluate, and it should be possible to make a fast preliminary investigation of the record on-site.
(9) Result: the result of the measurement should yield a simple (numerical) value which can be compared with an admissible value.
(10) Statistical assessment: when the flicker changes substantially over a period of time, a statistical evaluation is necessary and should be possible.

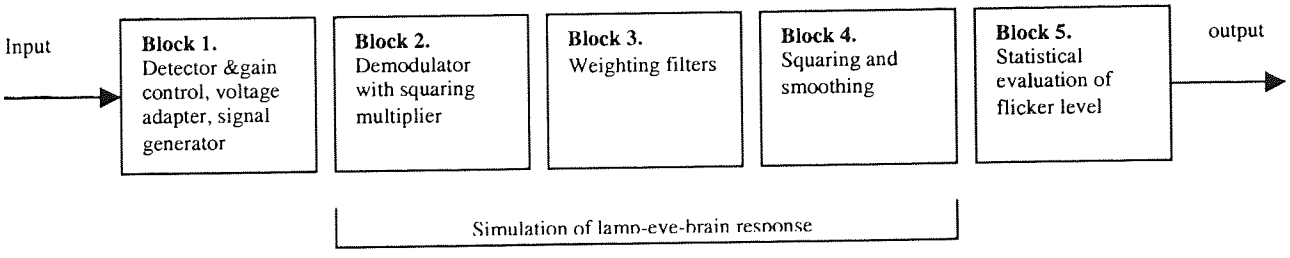

Fig. 3-8. Block diagram of UIE standard flicker meter

3.3 EAF Flicker Mitigation

As the degree of flicker severity depends on furnace operation types, mitigation devices and distribution network conditions, extensive studies were taken by many organisations (like EAF manufacturers, research institutes or steel makers) to solve the related problems. The root cause of the flicker is the unstable arc in each phase; and the EAF unbalanced load which is due to the dissimilar arcs of the three phases. Many factors affect the arc status of an EAF, such as electrode control strategies, furnace operation types (ac or dc furnace, long arc or short arc furnace), the compositions of scrap and the accuracy of arc furnace modelling for control. Therefore, various measures have been taken by EAF manufacturers. Mainly:

- Improving the control strategies[88],
- The replacement of the main transformer or adding a booster transformer/series inductor to the power source to stable the arc like [53]-[56] and [87]-[91],
- Identifying the melting behaviour of different types of scrap in specific numbers on a scale[57],
- Improving the strategies of EAF modelling for the accurate control e.g., [58]-[61],
- Selecting well performance compensation devices to meet the flicker requirements for a given fault level[92]-[96].

Nowadays, the flexible AC transmission system (FACTS) [62]can propose new techniques for balancing three phase arc furnace loads.

As the SCVD value is proportional to the furnace size, but inversely proportional to the fault level at pcc, a common argument between steel mills and utilities must be made in order to search for viable flicker solution. The solution is either that utilities should supply a sufficiently high minimum fault level or the steel mills should install compensation devices to meet the flicker requirements for the given fault level.

Limiting voltage flicker without any special compensation facilities requires a high fault level at pcc, so high that it is generally only available at the highest system voltages. To make sense, it can be calculated by the empirical formula [61] as below:

$$\Delta V_f = \frac{\Delta V}{V} = \frac{\Delta Q_{\max}}{S_{sc}} \approx \frac{0.8 S_{BE}}{S_{sc}} \leq 2\% \qquad (68)$$

considering $S_{BE} \approx (1.8-2.0)S_T$ (S_T is the capacity of the furnace transformer), then, $S_{sc} \geq 80S_T$ It is about eighty times of the furnace transformer capacity. In Chinese Design Recommendations, directly connecting an EAF to the system without any mitigation devices requires the fault level, $S_{sc} = (80-100)S_T$. Surely, it is necessary to suppress the flicker to a suitable range by using compensation devices.

Refer to App.-I-Fig. 6 ~7 of Appendix I, four curves of the flicker reduction (%) against the compensation ratio (%) with different SVC response time are published in [102]. The maximum flicker reduction with different SVC response time are respectively: 75% (at 100% compensation) while 5ms response SVC, 50% (at 100% compensation) with 10ms response SVC, 30% (at 70% compensation) with 15ms SVC, and 20% (at 60% compensation) with 20ms SVC. That is to say, the key point of flicker reduction is the response time of a SVC/SVG. A SVC (or SVG) is useless if its response time is more than 10ms.

3.4 Comparison of SVC and SVG for EAF flicker reduction

According to the design standards used in China, the compensation capacities using both SVG and SVC are listd in Table 3-9.

Where:

Q_{FC1} is the capacity of fixed capacitors (FC) for power factor correction,

Q_{FC2} is the extra FC capacity usde for balancing the inductive VAr of a SVC,

Q_{SVG} - capacity of the SVG

Q_{SVC} - the capacity of the SVC.

The unit for capacity in the Table is MW, and the unit for the cost is million US dollars.

Fig. 3-9 shows a typical system of an Iron & Steel Inc. in China.

Table 3-9, the copensation capacity and cost by using SVC/SVG for the system of Fig. 3-9

	Q_{SVG}/Q_{SVC}	Q_{FC1}/Q_{FC2}	Cost[1]	savings
SVG&FC	26.8	10.6/13.4	2.00	
SVC&FC	12.0	10.6/0.0	1.13	43.5%

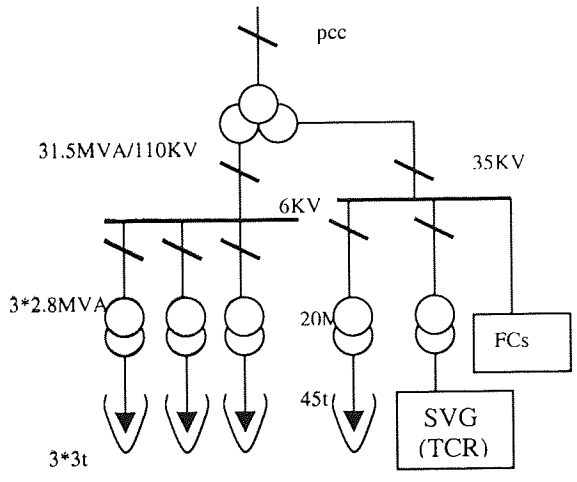

Figure 3-9. A typical supply system of an Iron & Steel Inc. in China

[4] The cost is calculated by the current average price $50 per KVAr for SVG and $40 per KVAr for SVC.

3.5 Conclusions

From the above discussion, with regard to their applications for arc furnace compensation, the SVG (or alternatively STATCOM) has several advantages over a conventional SVC. Based on the results in Table 3-9, and the simulation results obtained on the transient-network-analysis (TNA) devices (refer to Appendix I Fig. 5 & 6), the following conclusions can be made:

- Faster response: the response time of a SVG can be within 1 ms[70] while that of a SVC is more than 4-5 ms [97].
- Good performance for EAF flicker mitigation, the theoretical results show that the maximum flicker reduction by using SVG can be 90% at frequency of 10 Hz while the value by using SVC is about 75% at the same frequency[69].
- With the same capacity, harmonic generation of a SVG is less severe than that of a SVC
- A size reduction of 50% compared to a SVC is expected due to the reduction in the passive component of a SVG and the capacity (that is the size) reduction of the fixed capacitors (FC) which is in conjunction with the SVG.
- Capable to provide both active and reactive power compensation to the system, unlike SVC that is unable to provide active power compensation.
- A cost reduction of 40% compared to a SVC will be realized in production as GTO technology matures.

3.6 Future Work

In recent years, the capacity of arc furnace has abruptly risen. As a result, the problem of flicker has become quite severe. The modern high-power furnaces with a rated power of 100MVA or more are often coupled at the high voltage buses in order to limit their impacts on the system. However, the remaining impacts are widely spread in these cases, since they are dissipated, via the high voltage transmission and distribution system, to downstream middle-voltage and low-voltage networks supplied by the high voltage system which is meshed and extended. In conclusion, the advantages of applying SVG for EAF compensation mainly are:

(1) Currently, the optimised practical system configuration for EAF compensation is SVG in conjunction with fixed capacitors (FCs), although some theoretical studies about using solid-state devices to replace FCs have done so by employing white-noise theory, Kalman filter or simulation approach. There is still room for one to study the practical application of solid-state devices for EAF compensation (for both harmonic cancellation and flicker reduction).

(2) The key point of applying SVG for EAF compensation is "fast response". As reported, the multilevel inverters-based SVG, especially the cascaded multilevel inverters-based SVG, shows a bright future because of its fast response (within 1 ms) without the zigzag transformers. The small size inductors are used to instead of zigzag transformers as magnetic interface in the SVG. Additional to the SVG system configuration improvement, the other important factor is to take measures to reduce the delays from signal conditioning to generation of gating signals to the devices of SVG. Basically, the delays depend on three characteristics:

- The modulation method used.
- The design characteristics of the PWM modulator and.
- The method implemented to generate the reference template.

(3) As the definition of flicker by UIE/IEC is the modulation of the power system voltage, practical considerations for fluorescent flicker which can be caused by the frequencies in the range of 60 +/-20 Hz (40-80 Hz)[41], and for the dc furnace which can be caused by 187 Hz voltage distortion[52], must be taken into account in any further research.

IV. MODELLING AND ANALYSIS OF A CASCADE 11-LEVEL CONVERTERS-BASED SVG FOR EAF APPLICATION

ABSTRACT: This chapter aims to investigate the application of cascade multilevel converters-based SVG for EAF compensation. Based on the methods of Vector-Analysis and Switching-Function, combined with new control strategies based on adjusting both MI and the phase angle between the system voltage and the SVG output voltage, a mathematical model for transient response of the proposed SVG is developed and analysed in this chapter. The details of the new control system will be given in the next chapter.

4.1 INTRODUCTION

The problems due to rapid variations of reactive power and harmonics generated by non-linear loads like electric arc furnaces (EAFs) are well known and highlighted in the previous chapters. The large and erratic reactive current swings in an EAF will give rise to corresponding voltage drops across the (reactive) impedance of the ac system, and the voltage drops may result in fluctuating terminal voltage. The fluctuating system voltage may cause variations in light output of electrical lamps flashing ("flicker") and disturbance in other electrical equipment. The earliest industrial flicker compensators were installed in the late 1950s and were based on the saturable reactor principle in which iron saturation characteristics were used to stabilise the voltage[64]. The power electronic switched compensators were introduced to replace the saturable reactor compensator as they are much cheaper and more flexible in use. As reported [4], the largest SVG for EAF application is the SMI installation in Texas. Commissioned in 1998, it comprises a +/-80MVA STATCOM with a shunt coupling transformer and operates in conjunction with a 60 MVA a.c. capacitor bank. However, the SVG (STATCOM) requires coupling components like (zigzag) transformer to multiply converters and high frequency switching PWM technique to reduce harmonics.

Recently, multilevel converter-based SVGs or STATCOM have been widely studied due to their capability of eliminating the zigzag transformers [72]-[77], [99], [103]. Refering to Figures 4-1, 2, 3 & 4, the general operation of the multilevel converter is to synthesise a sinusoidal voltage from several levels of voltages, typically obtained from capacitor voltage sources. There are mainly three capacitor voltage synthesis-based multilevel converters:

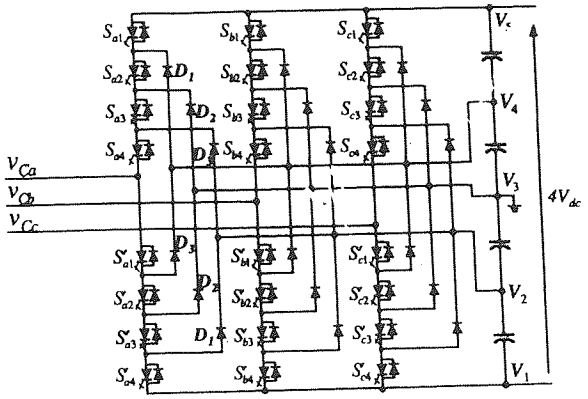

Fig. 4-1, Structure of the 5-level diode clamped inverter.

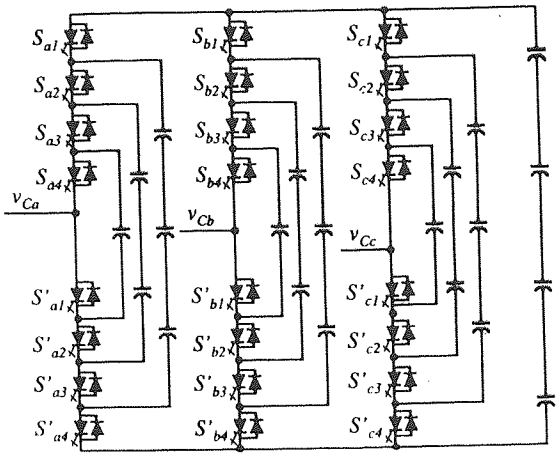

Fig. 4-2, Structure of the 5-level flying capacitor inverter.

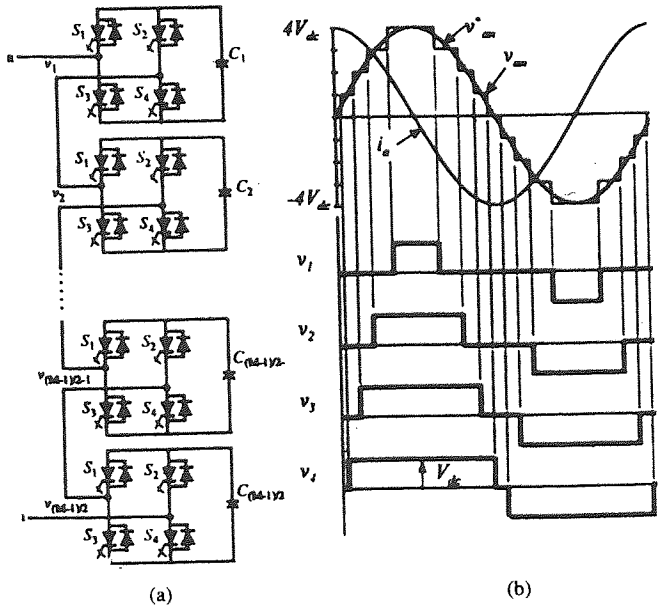

Fig. 4-3, Circuit diagram and the phase voltage waveform of a cascaded-inverters based converter with separate dc sources. (a) Circuit diagram. (b) Waveform showing a 9–level converter phase voltage.

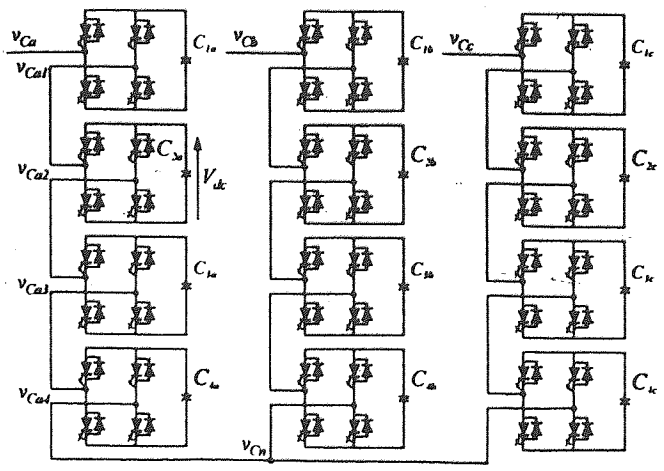

Fig. 4-4, A three-phase Y-configured cascaded-inverters based converter.

1) Diode-clamped converter (refer to Fig. 4-1)[72], [103].
2) Flying-capacitors converter (refer to Fig. 4-2)[99].
3) Cascaded-inverter with separated DC sources (refer to Fig. 4-3 & 4) [73]-[77].

The third configuration has the advantage of using a small number of diodes & capacitors and fast response (within 1 ms), whilst the first and second configurations require a very large number of clamping diodes or flying capacitors.
Naturally, the cascaded multilevel inverter configuration has drawn tremendous interest in the power industry. In 1996 [74], the authors developed a prototype of the cascade multilevel inverters-based SVG. Then, in [76], the authors designed a 50 MVA STATCOM based on cascading voltage source inverter. Recently, a improved cascade multilevel inverter configuration named "Binary multilevel voltage source inverter" was developed [77]. Unfortunately, with regard to their application for EAF compensation, the multilevel inverter-based SVG or STATCOM suffers the following disadvantages:

- To control the reactive power, an off-line calculation of Modulation Index (MI) is required to adjust the SVG output voltage. This slows down the transient response to the changes of reactive power
- Random active power exchange may cause unbalance to the voltage of the d.c. link (HBI) capacitor when the reactive power control is done by adjusting the power angle δ alone.

These problems are addressed by the work of this research. In order to resolve the above problems, firstly an accurate mathematical model for the system involved is essential. Many publications about SVG modelling are available to provide us useful analysing methods like Vector Analysis [104]-[105], and Switching-Function [106]-[107]. Based on the methods of switching-function and vector analysis, this thesis gives a transient model for the eleven-level cascaded converters SVG.

The control strategy is very important for the performance of a SVG. Some improvement has been made by the researchers working in this area. In [108], the reactive power is controlled by adjusting phase angle δ, as mentioned before it has the disadvantage of an unbalanced DC capacitor voltage caused by the uncontrollable real power flow. Recently, the current hysteresis controller [109] has also had limited application as the voltage source inverters to be forced to

generate required reactive currents which may cause either unbalanced DC voltage or being the worst conditions of harmonics generated by SVG.

The control strategy proposed by this research work is by adjusting both MI and phase angle δ. The controller renews the MI/switching patterns once each line-cycle, according to the sampled reactive power Q_s. Meanwhile, the remainder reactive power (compensated by the MI) and the reactive power variations during the line-cycle will be continuously compensated by adjusting the phase angle δ. In fact, it senses both variables MI and δ, but takes action only on one variable: the switching angle θ_i. Selected harmonics elimination method (SHEM) is taken for switching pattern calculations. In order to shorten the response time and simplify the control system, feed forward neural networks are employed for on-line computing of the switching patterns instead of look-up tables of off-line calculated ones. The proposed scheme has the following extra advantages:

- Faster response: compared with the other multilevel SVG controllers, it has less calculation work, and it read the look-up table only once each line cycle.
- Accurate, even if the MI control cause any delay to response of the load reactive power changes, the continuously working - δ compensation will make it up.
- No serious DC voltage unbalanced problem as the region of the δ can be controlled within a very small value, because majority VAr is compensated by adjusting MI.
- Neural networks can be a quick on-line computation method after proper training.

The mathematical model for transient modelling of a SVG system is given in this chapter, the control system will be discussed in the next chapter, and the neural schemes are investigated in chapter 6.

4.2 SYSTEM CONFIGURATION AND ENGINEERING CALCULATION

4.2.1 System calculations[86]

First of all, let us take the system in Fig. 3-9 as an example to explain how to take measures to reduce EAF voltage fluctuation at the point of common coupling (pcc), since many factors influence the EAF flicker level at pcc. The following measures are available and can be considered:

- Stabilise the arcs in an EAF by improving the EAF electrode control, the compositions of scrap, the accuracy of arc furnace modelling for control and the types of the furnace operation.
- Select the supply system with a high fault level or take measures to increase the fault level for a given supply system.
- Install effective compensation devices to meet the flicker requirements for the given fault level.

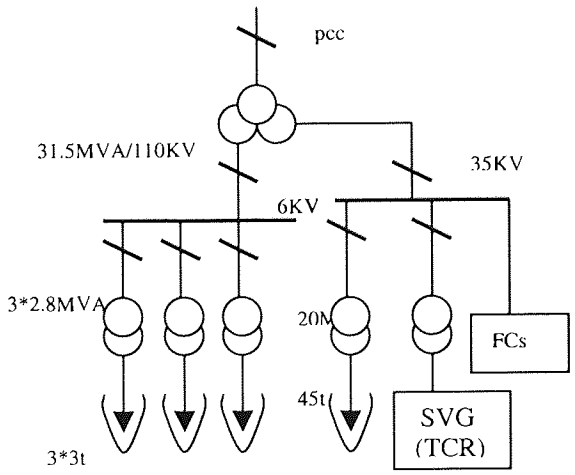

A typical supply system of an Iron & Steel Company in China (Figure 3-9.)

Real engineering experiences show that the compensation devices are indispensable for large capacity EAF. Sometimes, the practical solution of difficult problems in flicker will require using a variety of methods (increasing fault level, carefully designing passive harmonic filter and using well performance SVG/ STATCOM, etc.) in an appropriate combination. Fig. 3-9 shows the typical system connection of the compensation devices: SVC or SVG conjunction

with fixed capacitors (FCs). Here the FCs take the responsibility for both power factor correction and harmonic suppression. The total capacity of the FCs is split into three or four filter circuits which are tuned to different harmonic frequencies. The principle of passive filter calculation is relatively simple, but the real engineering calculation is somehow complicated as the system conditions are uncertain and filtering alternatives must be given for optimisation. Currently, it is neither possible, nor necessary, to replace the FC's with the solid state devices due to two main reasons:

- One is that the FC is the economic way to enable power factor correction,
- The other is that no electronics device does not produce harmonics itself.

For the SVC system, the total capacity of FCs includes an extra amount VAr (capacitive) to balance the inductive reactive power of the SVC. The typical calculation procedures are as follows.

Calculation conditions:

- Known parameters:

Fault level at pcc, S_{max}/S_{min} = 1500MVA/1050MVA, and nameplate parameters of the transformers and arc furnaces (omitted here)

- The voltage quality at pcc as dictated by utilities:

Max voltage fluctuation allowance $\leq 2\%$

ΔV_{10} Equivalent 10 Hz voltage flicker $\leq 0.5\%$

Total harmonic distortion (THD) $\leq 1.5\%$

Power factor ($\cos\varphi$) ≥ 0.92

(the above allowance values are from Chinese standards)

1. Impedance and voltage deviations (refer to Fig. 3-9)

Assumed the based capacity $S_B = 100MVA$ then:

The supply system equivalent impedance X_S (max/min) = 0.0952/0.0667

The total impedance from pcc to 3t arc furnaces $X_{\Sigma 3t} = 7.861$

The total impedance from pcc to 45t arc furnace $X_{\Sigma 45t} = 2.3487$

So the max voltage deviation at pcc caused by:

3t arc furnaces: $\Delta V_{\max 1} = X_S /(X_S + X_{\Sigma 3t}) = 1.2\%$

45t arc furnace: $\Delta V_{\max 2} = X_S /(X_S + X_{\Sigma 45t}) = 3.9\%$

Total max voltage deviation at pcc: $\Delta V_{\max} = \sqrt[4]{\Delta V_{\max 1}^4 + \Delta V_{\max 2}^4} = 3.91\%$

2. Max. reactive power variation

3t furnaces: $Q_{\max 1} = S_B /(X_S + X_{\Sigma 3t}) = 12.57MVA$

45t furnace: $Q_{\max 2} = S_B /(X_S + X_{\Sigma 45t}) = 40.92MVA$

Total max reactive power variation: $Q_{\max} = \sqrt[4]{Q_{\max 1}^4 + Q_{\max 2}^4} = 41.2MVA$

3. Arc furnace reactive power fluctuation and voltage flicker

As : $\Delta Q_{\max} = Q_{\max} \cos^2 \varphi_{EAF}$; $\Delta V_{10} = \Delta V_f / 4.6 = \Delta Q_{\max} /(4.6 S_{\min})$,

Then, the voltage flicker caused by 45t furnace is:

$\Delta V_{10} = 0.535\%$ (0.188% for the 3t furnaces)

4. Voltage flicker reduction ratio (%) $k_f = (0.535 - 0.5)/0.535 = 6.5\%$

5. Voltage deviation improvement ratio (%) $k_v = (3.91 - 2.0)/3.91 = 49\%$

6. Flicker improvement coefficient $\eta = Maximum[k_f, k_v] = 49\%$

7. Compensation ratio c_f (%): in engineering design, it is fixed from the $\eta - c_f$ curve, which can be found in each country's design recommendations. According to Chinese standards c_f =0.65/0.58 for SVC/ SVG respectively when $\eta = 49\% = 0.49$.

8. Capacity of SVG/ SVC

$Q_{SVC} = 0.65 Q_{\max} = 26.78MVA$

$Q_{SVG} = (0.58 Q_{\max})/2 \cong 12MVA$

Taking half the value of the total compensating capacity for SVG, as the SVG can generate both inductive and capacitive reactive power.

9. Capacity of FC for power factor correction (for the power factor 0.92)

$Q_{FC} = 10.61MVA$

10. Capacity of FC for balancing the inductive reactive power of the SVC (SVC system only)

$Q_{cb} = Q_{SVC} / 2 = 13.39MVA$

11. Passive filters

The total capacity of FC is 10.61 MVA for SVG, and 24.00MVA for SVC

12. Calculation results are shown on table 3-9.

Table 3-9, the compensation capacity (MVAr) for Fig. 3-9

	Q_{TCR} / Q_{SVG}	Q_{FC} / Q_{cb}	Total capacity
SVC(TCR&FC)	26.78	10.61/13.39	50.78
SVG & FC	12.00	10.61/0.00	22.61

4.2.2 Comparison of Different Inverter Configurations

(Refer to Figures 4-1~4 and the Figures in Appendix II for the diagrams of different inverter/converter configurations)

1. Conventional multi-pulse converters

Refer to Appendix II-fig.1, the structure of the conventional 48-pulse inverter, shows here the contrast with the multilevel inverter configurations with balk zigzag transformers.

2. Clamped-diode multilevel inverters

Fig. 4-1 is the 5-level clamped-diode inverter configuration. Advantages and disadvantages of a diode-clamp multilevel voltage source converter areas follows:

Advantages:

- When the number of levels is high enough, harmonic content will be low enough to avoid the need for filters.
- Efficiency is high because all devices are switched at fundamental frequency.
- Reactive power flow can be controlled.
- The control method is simple for back-to-back inter-tie system (UPFC system).

Disadvantages:

- Excessive clamping diodes are required when the number of levels is high.
- It is difficult to do real power flow control for the individual converter.

3. Flying capacitor inverters

Fig. 4-2 shows the structure of the 5-level flying capacitor inverter. Similarly, its advantages and disadvantages are as follows:

Advantages:

- Large amount of storage capacitors provide extra ride through capabilities during power outage..
- Provides switch combination redundancy for balancing different voltage levels.
- When the number of levels is high enough, harmonic content will be low enough to avoid the need for filters.
- Both real and reactive power flow can be controlled, making it a possible voltage source converter candidate for high voltage DC transmission.

Disadvantages:

- An excessive number of storage capacitors is required when the number of levels is high.
- The inverter control will be very complicated, and the switching frequency and switching losses will be high for real power transmission.

4. Cascade multilevel inverters / Chain circuit inverters

Appendix II-fig. 2 is the single-phase chain circuit. Actually, it is the same configuration with the cascade multilevel inverters shown as Fig. 4-3 ~ 4. This is a relatively new structure which can avoid extra clamping diodes or voltage balancing capacitors. Fig. 4-4 shows the basic structure of the cascaded-inverters with separate dc sources (SDC's). Fig. 4-3 shows the

synthesized phase voltage waveform of a 9-level cascade inverter with SDC's. Each single-phase full bridge inverter can generate three level outputs, $+V_{dc}$, 0, and $-V_{dc}$. This is made possible by connecting the DC sources sequentially to the AC side via the four gate-turn-off devices. Each level of full bridge inverter consists of four switches S_1, S_2, S_3, S_4. Turning on S_1, S_4 yields $v_1 = +V_{dc}$, turning on S_2, S_3 yields $v_1 = -V_{dc}$, turning off all the four switches yields $v_1 = 0$. Similarly, the AC output voltage at each level can be obtained in the same manner. Minimum harmonic distortion can be obtained by controlling the conducting angles at different inverter levels. The phase output voltage is the sum of four inverter outputs, $v_{an} = v_1 + v_2 + v_3 + v_4$. In summary, its advantages and disadvantages can be listed below:

Advantages:

- When the number of levels is high enough, harmonic content will be low enough to avoid the need for filters.
- Efficiency is high because all devices are switched at fundamental frequency.
- Reactive power flow can be controlled.
- The control method is simple for back-to-back inter-tie system (UPFC system).

Disadvantages:

- Excessive clamping diodes are required when the number of levels is high.
- It is difficult to do real power flow control for the individual converter.

5. Binary VSI

Appendix II-fig. 3 shows the 3-phase star connected 3-level binary VSI. The binary VSI, in fact, is the improved cascade multilevel inverter structure. Additional to the advantages and disadvantages of a cascade multilevel voltage source converter mentioned above, its own features are:

- Taking the 3-level inverter configuration for example, it requires the least power components and generates most AC output voltage steps (15 steps). This also benefits the capacitor DC voltage balancing control (only three capacitors).
- But, it suffers unequal device rating and unequal switching frequency which may cause more switching loss and the control complicated.

6. Comparison

Refer to Fig. 4-1~4 and the figures in Appendix, from above discussion, it seems that two schemes can be used for arc furnace application in order to improve SVG's performance, either the cascaded-inverters or the binary VSI. After being assessed from every aspect, we recognised that the cascaded inverter is the best answer.

Table 4-10 gives a list of power component requirements per phase leg among five multilevel converter configurations.

Table 4-10, Comparison of power component requirements per phase among five multilevel converters.

Converter type	Diode-clamp	Flying-capacitors	Cascaded-inverter	Chain circuit	Binary VSI
Main switching devices	(m-1)x2[5]	(m-1)x2	(m-1)x2	(m-1)x2	4m/5
Main diodes	(m-1)x2	(m-1)x2	(m-1)x2	(m-1)x2	4m/5
Clamping diodes	(m-1)(m-2)	0	0	0	0
DC capacitors	(m-1)	(m-1)	(m-1)/2	(m-1)/2	m/5[6]
Balancing capacitors	0	(m-1)(m-2)/2	0	0	0

[5]Where m is the number of levels (or steps) in the AC output voltage

[6] here m is the equivalent output voltage levels/steps (15 steps for 3-level converters)

4.3 PROPOSED SYSTEM CONFIGURATION

4.3.1 System configuration

Shown as Fig.4-5 (Fig. 4-6 is the equivalent calculation circuit), taking 11-level cascaded inverters for example (refer to [74] for the full description of the 11-level cascade converters configuration), according to Fourier Series analysis, the actual output voltage of a SVG is:

$$v_{an} = \sum_{k=0}^{\infty} B_k \sin[(2k+1)\omega t] \tag{69}$$

Here:

$k = 0,1,2,3\cdots$

$$B_k = \frac{4V_{dc}}{5(2k+1)\pi} \sum_{i=1}^{5} \cos[(2k+1)\theta_i])$$

As more general form as equation (70):

$$v_h = \sum_{k=1}^{\infty} V_h \sin[(2k+1)\omega t] \quad (k = 0,1,2,3\cdots) \tag{70}$$

Here:

$h = 2k+1,$

$$V_h = \frac{4V_{dc}}{5(2k+1)\pi} \sum_{i=1}^{5} \cos[(2k+1)\theta_i]$$

V_{dc} is the total capacitor voltage

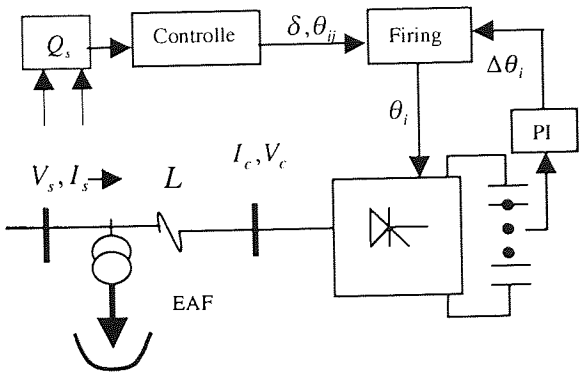

Fig. 4-5, the proposed SVG system configuration

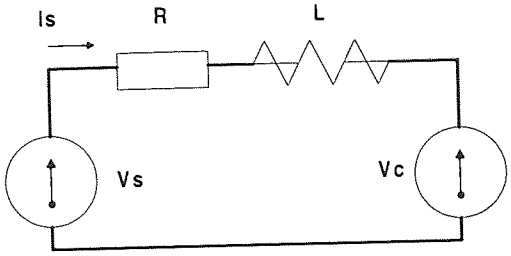

Fig. 4-6, the equivalent calculation circuit

If v_{dc} is the voltage of each H-bridge capacitor, for 11-level cascade inverters, the total capacitor voltage is given by: $V_{dc} = v_{dc1} + v_{dc2} + v_{dc3} + v_{dc4} + v_{dc5} = 5v_{dc}$

Taking the fundamental frequency as the output AC voltage of the SVG.

$$v_c = V_1 = [\frac{V_{dc}}{5\pi}\sum_{i=1}^{5}\cos\theta_i]\sin(\omega t) = \frac{4V_{dc}}{\pi}M_i\sin(\omega t) \qquad (71)$$

Here,

$$M_i = MI = \frac{1}{5}\sum_{i=1}^{5}\cos\theta_i$$

4.3.2 Three control methods and their mathematical equations

1. Reactive power control by MI[73], [75], [77]

It is well known that the amount and type (inductive or capacitive) of reactive power exchange between SVG and the system can be adjusted by controlling the magnitude of the SVG output voltage with respect to the system voltage. The reactive power supplied by SVG is given by:

$$Q = (V_c - V_s)V_s / X \qquad (72)$$

Where:

X is the equivalent impedance between SVG and the system,

V_c and V_s are the magnitudes of SVG AC output voltage and system voltage (V_c, V_s are in phase), respectively.

When Q is positive, the SVG supplies reactive power to the system. Otherwise, the SVG absorbs reactive power from the system. From equations (70) and (71), the SVG output voltage can be controlled by the MI. V_c is proportional to MI, as long as the individual H-bridge inverter is in the linear modulating region. Due to its ability to control the output voltage by the MI, the SVG has extremely fast dynamic response to the system reactive power demand.

2. **Reactive power control by the phase angle (δ) between the supply voltage and the inverter line voltage**[108]

It can be shown that (referring to the next section-mathematical modelling for detail), the reactive power Q and real power P drawn by the inverter are:

$$Q = \frac{V_s^2}{2r}\sin(2\delta) \tag{73}$$

$$P = \frac{V_s^2}{r}\sin^2(\delta) \tag{74}$$

Shown as equation (73) and (74) and in reference to Fig. 4-11, when the phase angle δ is in the region of a small value (say, within one degree), the amount of reactive power injected or absorbed is almost proportional to δ, and thus operating points that are in general confined to such a δ 's can be applied for linear control.

3. **Reactive power compensation by instantaneous current control**

In [109], the authors proposed the current hysteresis controller to the field of multilevel inverter SVG. This controller will force the inverter to directly generate the required reactive current. As the authors employ voltage source inverters to generate required current without improved MI control technique and SHEM scheme, this makes the control method has limited applications.

4.4 SELECTED HARMONIC ELIMILATION METHOD (SHEM)

Equations (70) tell us that the modulation angles θ_i can be varied to control the fundamental output voltage as well as to minimise the harmonic distortion. Then, the selected harmonic elimination method (SHEM) problem can be mathematically described as follows:

$$\sum_{i=1}^{5}\cos(\theta_i) = 5MI \tag{75}$$

$$\sum_{i=1}^{5}\cos[(2k+1)\theta_i] = 0^{7}, \text{ (for h=5, 7, 11, 13, 15)} \tag{76}$$

In this research, we select 5^{th}, 7^{th}, 11^{th}, 13^{th}, 15^{th} harmonics to be cancelled. These non-linear equations (75), (76) are resolved on-line by the feed forward neural networks after training (refer to chapter six for detail).

In the case of off-line calculated look-up table, the non-linear equations given by the above mathematics description are solved by using the Newton-Raphson numerical technique to control the fundamental output voltage magnitude and to eliminate or minimise harmonics.

4.5 CAPACITOR DC VOLTAGE BALANCING

Theoretically, as the phase current i_{sc} is leading or lagging the phase voltage V_c by 90 degrees, the average charge to each DC capacitor is equal to zero over every half line cycle. So the voltages on all the DC capacitors remain theoreticaly balanced. From Fig. 4-7, the average charge to each DC capacitor over one half cycle can be expressed as (77),

$$q_i = \int_{\theta_i}^{\pi-\theta_i} \sqrt{2} I \cos\theta d\theta = 0 \qquad i = 1,2,3,4,5 \qquad (77)$$

$[\theta_i, \pi - \theta_i]$ represents the time interval during which the DC capacitor connected to the AC side, and I is the rms value of the line current. In practice, the phase current i_{sc} is not accurately 90 degrees leading or lagging with the phase voltage, but a small displace a angle - $\Delta\alpha$ shown as $i_{sc}^{'}$ as Fig. 4-8, which might be caused by the uncontrolable real power flow (while using power angle δ to control the reactive power) and the real power losses in the inverters and capacitors. From equation (78) below, if $\Delta\alpha$ is positive ($i_{sc}^{'}$ is lagging to i_{sc}), the capacitor voltage V_{ci} increases. Otherwise, V_{ci} decreases.

$$\Delta V_{ci} = \frac{I_{sc}^{'}}{\omega C}\int_{\theta_i}^{\pi-\theta_i} \cos(\theta - \Delta\alpha) d\theta = \frac{2I_{sc}^{'}}{\omega C}\cos\theta_i \sin(\Delta\alpha) \approx \frac{2I_{sc}^{'}}{\omega C}\cos\theta_i \Delta\alpha \qquad (78)$$

Fig. 4-8 shows the principle of the DC capacitor voltage balancing. If V_{c2} (or V_{ci}), is shifted ahead by $\Delta\theta_2$ (or $\Delta\theta_i$), then the charge can be expressed as,

$$q_2 = \int_{\theta_2-\Delta\theta_2}^{\pi-\theta_2-\Delta\theta} \sqrt{2} I \cos\theta d\theta = 2\sqrt{2}\cos\theta_2 \sin\Delta\theta_2 \qquad (79)$$

which is proportional to $\Delta\theta_2$ (or $\Delta\theta_i$) when $\Delta\theta_2$ (or $\Delta\theta_i$) is small. Therefore, each H-bridge inverter unit's DC voltage can be controlled by slightly shifting the switching pattern.

---

[7] In real project calculation, these equations do not equal to zero but a very small value.

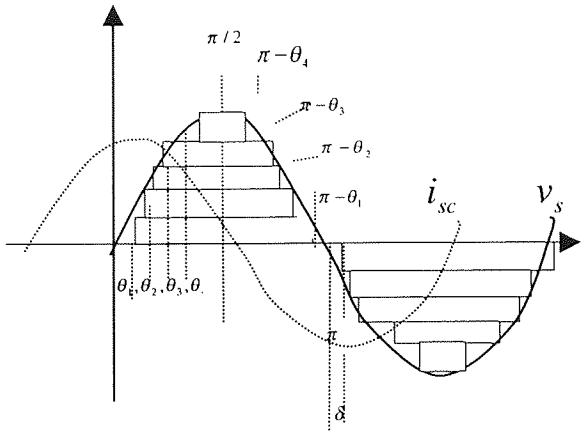

Fig. 4-7, the real waveform of 11-level cascade converters

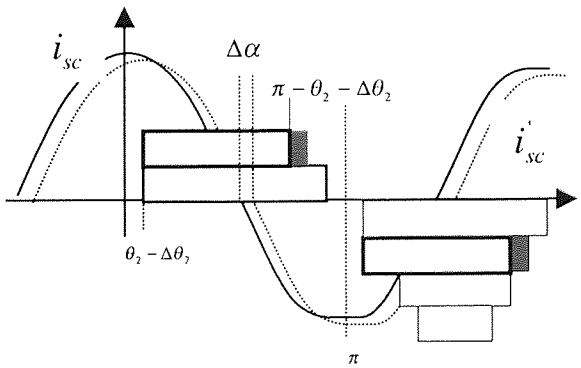

Fig. 4-8, $\Delta\theta_i$-replacement for DC voltage balancing

4.6 SYSTEM MODELLING

Fig. 4-5, shows the typical system connection of the proposed SVG, a full description of the 11-level cascaded inverters-based SVG circuit used for this study can be found in [74]. It is reasonable to make the following assumptions in this case:

- Neglect the harmonics of the SVG output voltage
- The system supply voltage is constant or changes are very small
- The phase angle δ is very small (within one degree limit)

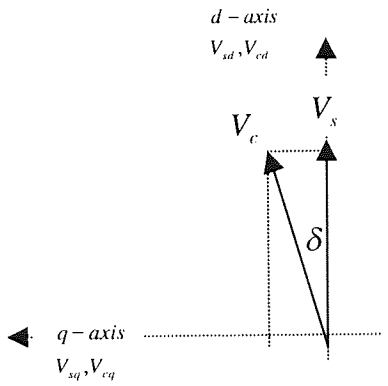

Fig. 4-9, SVG vectors in synchronous frame.

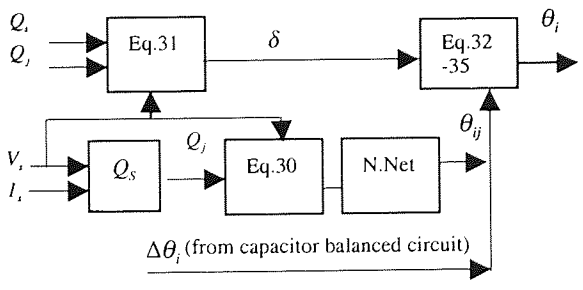

Fig. 4-10, Control system block diagram

In the diagrams Fig. 4-5~6 & 9~10:

V_s : The system supply voltage

V_c : The SVG output voltage

I_s : The current flow from system to SVG (I_s =- I_c)

R , L : A set of linked AC reactor and equivalent resistance including the SVG losses

Q_s : The system reactive power

Q_j : The value of j -th sampling of Q_s for MI renewing

δ : The phase angle between system voltage and the SVG output voltage.

θ_{ij} : The j -th calculated switching angle by Neural net

$\Delta\theta_i$: The switching angle displace for dc capacitor voltage balancing.

θ_i : The firing angle

Based on the assumptions, refer to Fig. 4-5 and Fig. 4-9~10, We can define:

$$[V_s]=\begin{bmatrix}V_{sa}\\V_{sb}\\V_{sc}\end{bmatrix}=V_s\begin{bmatrix}\sin(\omega t)\\\sin(\omega t-2\pi/3)\\\sin(\omega t+2\pi/3)\end{bmatrix} \tag{80}$$

$$[V_c]=[V_{ca}\quad V_{cb}\quad V_{cc}]^T=[S_w]V_{dc} \tag{81}$$

Here, the switching-function is in the form:

$$[S_w]=kM_i\begin{bmatrix}\sin(\omega t-\delta_a)\\\sin(\omega t-\delta_b-2\pi/3)\\\sin(\omega t-\delta_c+2\pi/3)\end{bmatrix} \text{ and}$$

V_{dc} is the DC voltage of the Capacitors, $k=4/\pi$

Then, refer to Fig. 4-6, we obtain equation (82) as below:

$$L\frac{d}{dt}[I_s]=[S_w]V_{dc}-[V_s]-R[I_s] \tag{82}$$

Taking d-q transformation, we obtain:

$$\begin{bmatrix} p \\ q \end{bmatrix} = \begin{bmatrix} u_d & u_q \\ u_q & -u_d \end{bmatrix} \begin{bmatrix} i_d \\ i_q \end{bmatrix} \tag{83}$$

$$\frac{d}{dt}\begin{bmatrix} i_d \\ i_q \end{bmatrix} = \begin{bmatrix} -R/L & \omega \\ -\omega & -R/L \end{bmatrix} \begin{bmatrix} i_d \\ i_q \end{bmatrix} + \begin{bmatrix} v_{sd} - v_{cd} \\ v_{sq} - v_{cq} \end{bmatrix} \tag{84}$$

$$\frac{dv_{dc}}{dt} = \frac{kM_i}{C}(i_d \cos\delta + i_q \sin\delta) \tag{85}$$

To simplify the calculations of equations (83), (84) & (85), and extract the variable δ from the above equations, refer to Fig. 4-9~10, the set vector of the system voltage V_s overlapped with d-axis and the SVG output voltage V_c having an angle δ ahead (or behind) of d-axis. Then [114]:

$$\begin{bmatrix} v_{cd} \\ v_{cq} \end{bmatrix} = kM_i V_{dc} \begin{bmatrix} \cos\delta \\ \sin\delta \end{bmatrix}, \quad \begin{bmatrix} v_{sd} \\ v_{sq} \end{bmatrix} = \sqrt{2}V_s \begin{bmatrix} 1 \\ 0 \end{bmatrix} \tag{86}$$

Substituting equation (86) into (83) (84) (85), and taking Laplace Transform gives:

$$\begin{bmatrix} sI_{d(s)} \\ sI_{q(s)} \\ sV_{dc(s)} - V_{dc0} \end{bmatrix} = \begin{bmatrix} -R/L & \omega & -\frac{kM_i \cos\delta}{L} \\ -\omega & -R/L & -\frac{kM_i \sin\delta}{L} \\ \frac{kM_i \cos\delta}{C} & \frac{kM_i \sin\delta}{C} & 0 \end{bmatrix} \begin{bmatrix} I_{d(s)} \\ I_{q(s)} \\ V_{dc(s)} \end{bmatrix} + \frac{\sqrt{2}V_s}{Ls} \begin{bmatrix} 1 \\ 0 \\ 0 \end{bmatrix} \tag{87}$$

Resolving equation (87), we obtain:

$$I_{d(s)} = \frac{n_{d1}s^2 + n_{d2}s + n_{d3}}{s^4 + (2R/L)s^3 + d_3 s^2 + d_4 s} \tag{88}$$

$$I_{q(s)} = -\frac{n_{q1}s^2 + n_{q2}s + n_{q3}}{s^4 + (2R/L)s^3 + d_3 s^2 + d_4 s} \tag{89}$$

$$V_{dc(s)} = \frac{V_{dc(0)}s^3 + (2RV_{dc(0)}/L)s^2 + n_{v3}s + n_{v4}}{s^4 + (2R/L)s^3 + d_3 s^2 + d_4 s} \tag{90}$$

Here:

$$d_3 = \frac{R^2}{L^2} + \omega^2 + \frac{k^2 M_i^2}{LC}, d_4 = \frac{k^2 M_i^2 R}{L^2 C}$$

$$n_{d1} = \frac{\sqrt{2}V_s - kM_i V_{dc(0)} \cos\delta}{L}, n_{d3} = \frac{k^2 M_i^2 V_s \sin^2\delta}{L^2 C}$$

$$n_{d2} = \frac{\sqrt{2}V_s R - kM_i R V_{dc(0)} \cos\delta}{L^2} - \frac{kM_i \omega V_{dc(0)} \sin\delta}{L}$$

$$n_{q1} = \frac{kM_i V_{dc(0)} \sin\delta}{L}, n_{q3} = \frac{\sqrt{2}k^2 M_i^2 V_s \cos\delta \sin\delta}{L^2 C}$$

$$n_{q2} = \frac{\sqrt{2}\omega V_s - kM_i \omega R V_{dc(0)} \cos\delta}{L} + \frac{kM_i R V_{dc(0)} \sin\delta}{L^2}$$

$$n_{v3} = \frac{R^2 V_{dc(0)}}{L^2} + \omega^2 V_{dc(0)} + \frac{\sqrt{2}kM_i V_s \cos\delta}{LC}$$

$$n_{v4} = \frac{\sqrt{2}kM_i V_s R \cos\delta}{L^2 C} - \frac{\sqrt{2}kM_i V_s \omega \sin\delta}{LC}$$

So that:

$$I_{d(\infty)} = \lim_{s\to 0} sI_{d(s)} = \sqrt{2}V_s \sin^2\delta / R \tag{91}$$

$$I_{q(\infty)} = \lim_{s\to 0} sI_{q(s)} = -\sqrt{2}V_s \sin 2\delta / (2R) \tag{92}$$

$$V_{dc(\infty)} = \lim_{s\to 0} sV_{dc(s)} = \frac{\sqrt{2}V_s (R\cos\delta - \omega L \sin\delta)}{kM_i R} \tag{93}$$

$$Q = V_s I_{q(\infty)} / \sqrt{2} = V_s^2 \sin 2\delta / (2R) \tag{94}$$

$$P = V_s I_{d(\infty)} / \sqrt{2} = V_s^2 \sin^2\delta / R \tag{95}$$

Fig. 4-11 shows the SVG output active/reactive power curves versus phase angle δ ($P-\delta, Q-\delta$ curves))

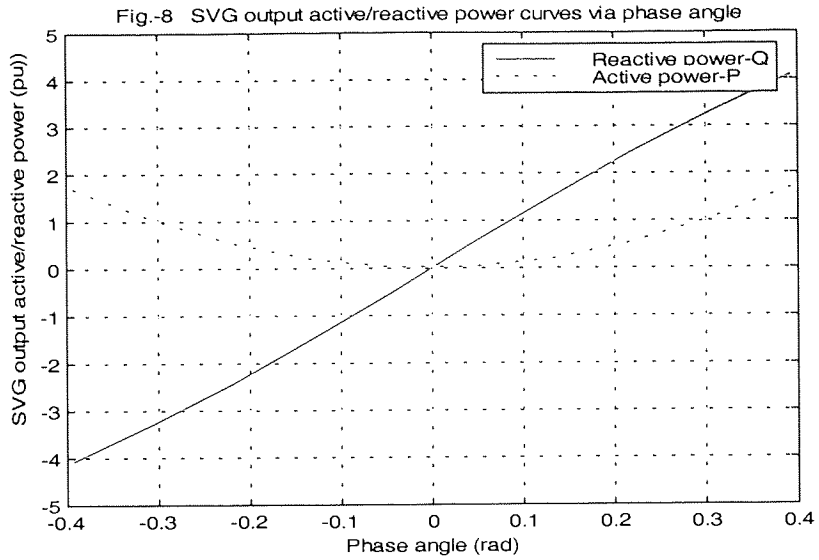

Fig. 4-11, SVG active/reactive power curves via phase angle ($P-\delta, Q-\delta$ curves)

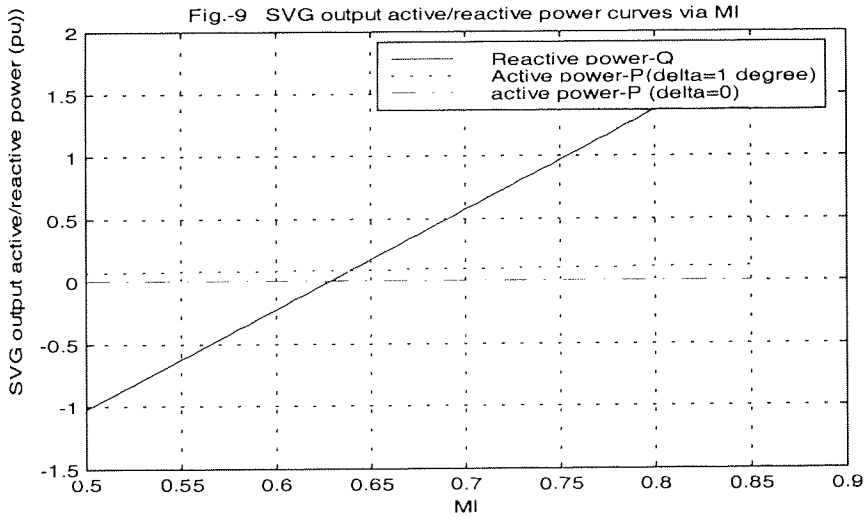

Fig. 4-12, SVG output active/reactive power curves via MI ($P-M_i$ $Q-M_i$ curves)

Transfer Function and Transient Response of Reactive Power:

To develop the transfer function and transient response, we apply the method of ASVC modelling given in [104] & [114] for this analysis. According to the assumptions stated above, we obtain:

$$\begin{aligned} &\Delta V_s = 0, \\ &\cos\delta \approx 1, \\ &\sin\delta \approx \delta, \\ &\left|\sqrt{2}V_s\right| = \left|V_{dc(0)}\right| \end{aligned} \tag{96}$$

Let:

$\Delta\delta = (\delta - 0)u_{(t)}$ (here $u_{(t)}$ is the step function), and,

$\Delta Q_{(s)} = Q_{(s)\delta=\delta} - Q_{(s)\delta=0}$

So,

$\Delta\delta_{(s)} = \delta / s$

From equations 91-96, we can derive the $Q-\delta$ transfer function as below:

$$\frac{\Delta Q_{(s)}}{\Delta\delta_{(s)}} = \frac{\frac{kM_i V_s^2}{L}(s^2 + \frac{R}{L}s + \frac{kM_i}{LC})}{s^3 + \frac{2R}{L}s^2 + (\frac{R^2}{L^2} + \omega^2 + \frac{k^2 M_i^2}{LC})s + \frac{k^2 M_i^2 R}{L^2 C}} \tag{97}$$

To validate this transfer function, we use the parameters of the prototype given in [74] for a simulation study. The MATLAB simulation results are shown in Fig. 4-13 & 14.

Fig. 4-13 shows the good performance of the system.

Fig. 4- 14 show that the system is stable without oscillation.

4.7. MATLAB simulation result

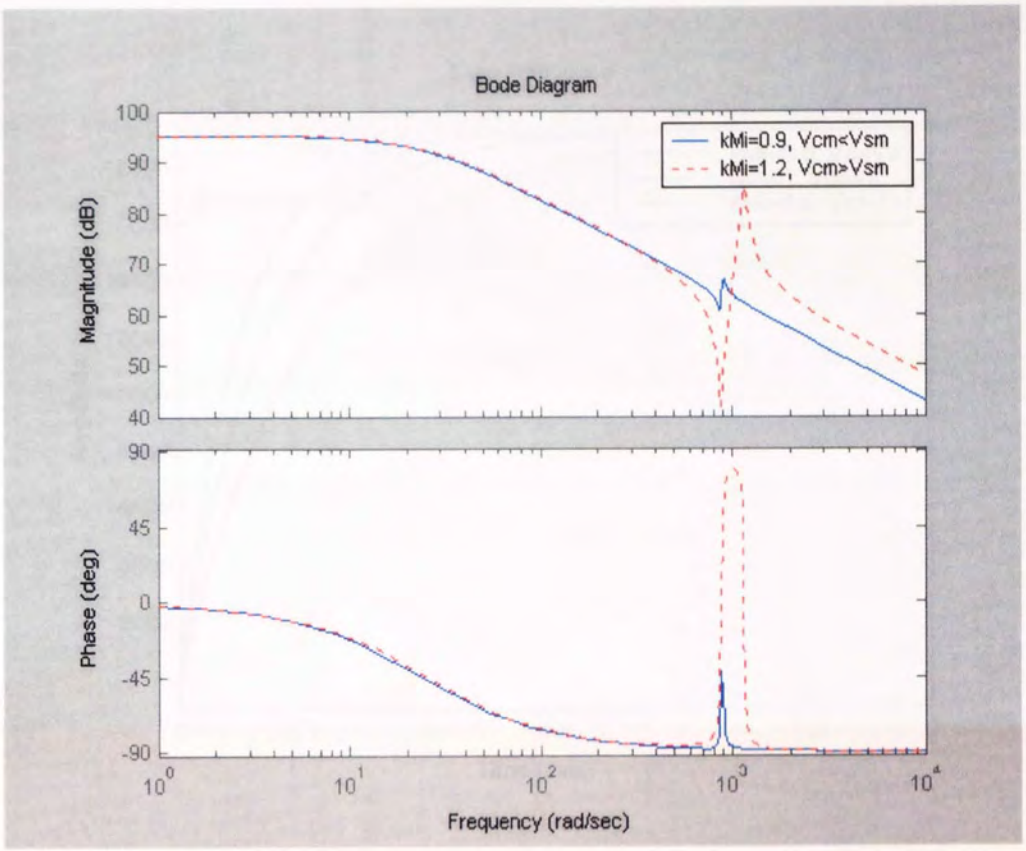

Fig. 4-13, the Bode Diagram

Fig. 4-14, Step response

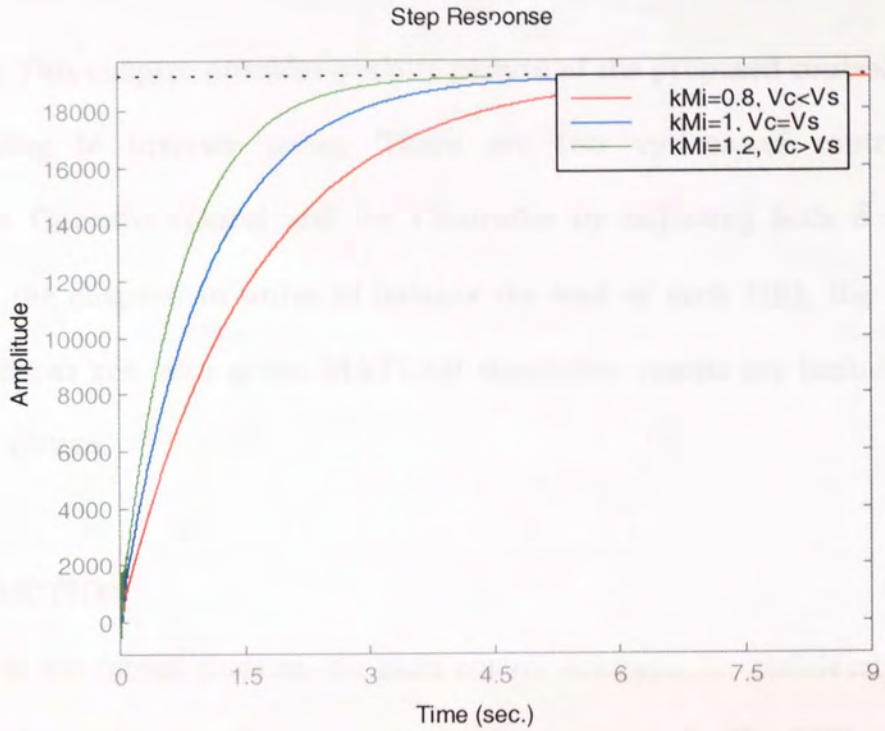

V. CONTROL STRATEGIES OF THE CASCADE MULTILEVEL CONVERTERS SVG

ABSTRACT: This chapter provides a whole picture of the proposed control system, from signal detecting to inverter firing. There are two options of control strategies: Instantaneous Currents control and the Controller by adjusting both δ and MI, are compared in the chapter. In order to balance the load of each HBI, the optimised full switching patterns are also given. MATLAB simulation results are included to validate the proposed system.

5.1 INTRODUCTION

As discussed in the former chapters, the main control strategies for multilevel inverter-based SVG/STATCOM are by adjusting either MI or the phase angle δ. The SVG with MI control suffers disadvantages as mentioned before. The reactive power control by adjusting phase angle δ also has its disadvantages, such as the capacity of SVG being restricted by the limited region of the phase angle δ (say, within ONE degree). If the phase angle δ is more than the stated limit (refer to equation (95)), the uncontrollable real power flow may cause serious unbalanced DC capacitor voltage. As stated in chapter 4, the current hysterics only has limited applications.

The proposed control strategy in this research is based upon adjusting both MI and phase angle δ. This system has two controllers: a main controller and a auxiliary controller. The main controller is to adjust MI, and the auxiliary controller is to adjust the phase angle δ. The following discussion will show that the proposed control strategy has the following features:

- The controller is mainly using proportional integral type which has an extremely fast response property.

- The reactive power changes during the line cycle will be compensated by adjusting the phase angle δ.
- No serious DC voltage unbalanced problem arises as the region of the δ can be controlled within a small value of one degree.

5.2 SIGNAL DETECTING METHODS

Many contributors who dealt with unbalanced three-phase systems having distorted currents and voltage, have attempted to redefine such quantities as active power, reactive power, active current, reactive current, power factor etc. Traditionally, Fortescue's symmetrical components were employed to detect the control signals from the arc furnace loads system. About twenty years ago, Akagi et al.[107] introduced a useful concept of instantaneous reactive power. This concept gives an effective method to compensate for the instantaneous components of reactive power for three-phase systems without energy storage. Recently, a generalised theory of instantaneous reactive power for three-phase power systems has been developed [108]. This theory is valid for sinusoidal or nonsinusoidal, balanced or unbalanced three-phase systems, with or without zero-sequence currents and/or voltages. In this research, we still use the conventional symmetrical components method for detecting instantaneous currents, and Akagi's theory for sensing instantaneous reactive power.

5.2.1 Instantaneous currents detecting mathematics procedures

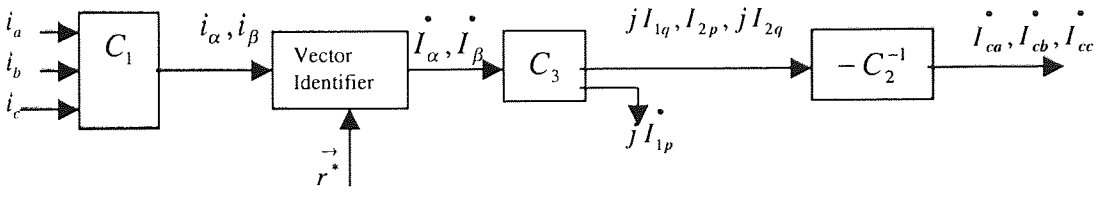

Fig. 5-1, Instantaneous currents detecting mathematics procedures

Refer to Fig. 5-1, the mathematical analysis are as followings:

Basic equations:

Define the 3-phase current as the form as equation (98)

$$\begin{bmatrix} i_a \\ i_b \\ i_c \end{bmatrix} = \begin{bmatrix} \sqrt{2} I_a \cos(\omega t + \varphi_a) \\ \sqrt{2} I_b \cos(\omega t + \varphi_b - 120^\circ) \\ \sqrt{2} I_c \cos(\omega t + \varphi_c - 240^\circ) \end{bmatrix} \tag{98}$$

Then:

$$\begin{bmatrix} i_\alpha \\ i_\beta \end{bmatrix} = C_1 \begin{bmatrix} i_a \\ i_b \\ i_c \end{bmatrix} \tag{99}$$

$$\begin{bmatrix} i_1 \\ i_2 \end{bmatrix} = C_2 \begin{bmatrix} i_a \\ i_b \\ i_c \end{bmatrix} \tag{100}$$

$$\begin{bmatrix} i_1 \\ i_2 \end{bmatrix} = C_3 \begin{bmatrix} i_\alpha \\ i_\beta \end{bmatrix} \tag{101}$$

Here:

$$C_1 = \sqrt{2/3} \begin{bmatrix} 1 & -1/2 & -1/2 \\ 0 & \sqrt{3}/2 & -\sqrt{3}/2 \end{bmatrix}$$

$$C_1^{-1} = \sqrt{2/3} \begin{bmatrix} 1 & -1/2 & -1/2 \\ 0 & \sqrt{3}/2 & -\sqrt{3}/2 \end{bmatrix}$$

$$C_2 = \frac{1}{\sqrt{2}} \begin{bmatrix} 1 & a & a^2 \\ 1 & a^2 & a \end{bmatrix}$$

$$C_2^{-1} = \frac{1}{\sqrt{3}} \begin{bmatrix} 1 & 1 \\ a^2 & a \\ a & a^2 \end{bmatrix}, a = e^{j120^\circ}$$

$$C_3 = \frac{1}{\sqrt{2}}\begin{bmatrix} 1 & j \\ 1 & -j \end{bmatrix}$$

$$C_3^{-1} = \frac{1}{\sqrt{2}}\begin{bmatrix} 1 & 1 \\ -j & j \end{bmatrix}$$

Where:

i_a, i_b, i_c are the 3-phase load currents;

i_α, i_β are the $\alpha - \beta$ transformation currents,

C_i, C_i^{-1} are respectively the transformation matrix and their reverse matrix;

i_1, i_2 are respectively the positive and negative sequence currents of the load.

90 degrees phase-shift

As $I^2 \sin^2 \omega t + I^2 \cos^2 \omega t = I^2$, we need to combine every $\cos \omega t$ with its 90 degrees phase-shift function ($\sin \omega t$) to form a rotating-vector. The phase-shift equation is:

$$\sin \omega t = \cot Y[\cos(\omega t - Y) - \cos \omega t \cos Y] \qquad (102)$$

Here:

$\cos \omega t$ is the input signal, $\sin \omega t$ is its output,

Y and its triangle functions are given by the phase-shift electronics circuit.

After phase-shift, the rotating-vector of i_α, i_β is as below:

$$\begin{aligned} \vec{I}_\alpha &= \sqrt{2} I_\alpha \cos(\omega t + \varphi_\alpha) + j\sqrt{2} I_\alpha \sin(\omega t + \varphi_\alpha) \\ \vec{I}_\beta &= \sqrt{2} I_\beta \cos(\omega t + \varphi_\beta) + j\sqrt{2} I_\beta \sin(\omega t + \varphi_\beta) \end{aligned} \qquad (103)$$

Vector identifier

Employing the reference unit vector $\vec{r} = \cos\omega t + j\sin\omega t$ from the pcc of the supply system,

Then:

$\vec{I}_\alpha * \vec{r}^*$ & $\vec{I}_\beta * \vec{r}^*$, thus:

$$\dot{I}_\alpha = \sqrt{2}I_\alpha \cos\varphi_\alpha + j\sqrt{2}I_\alpha \sin\varphi_\alpha,\ \ \dot{I}_\beta = \sqrt{2}I_\beta \cos\varphi_\beta + j\sqrt{2}I_\beta \sin\varphi_\beta \qquad (104)$$

For currents compensation

$$\begin{bmatrix} \dot{I}_1 \\ \dot{I}_2 \end{bmatrix} = C_3 \begin{bmatrix} \dot{I}_\alpha \\ \dot{I}_\beta \end{bmatrix} = \begin{bmatrix} (I_\alpha \cos\varphi_\alpha - I_\beta \sin\varphi_\beta) + j(I_\alpha \sin\varphi_\alpha + I_\beta \cos\varphi_\beta) \\ (I_\alpha \cos\varphi_\alpha + I_\beta \sin\varphi_\beta) + j(I_\alpha \sin\varphi_\alpha - I_\beta \cos\varphi_\beta) \end{bmatrix} \qquad (105)$$

Removing the real part of $\dot{I}_1$ from equation (105) and taking negative of the other parts in the equation, the currents to be compensated are:

$$\begin{bmatrix} \dot{I}_{ca} \\ \dot{I}_{cb} \\ \dot{I}_{cc} \end{bmatrix} = -C_2^{-1} \begin{bmatrix} j(I_\alpha \sin\varphi_\alpha + I_\beta \cos\varphi_\beta) \\ (I_\alpha \cos\varphi_\alpha + I_\beta \sin\varphi_\beta) + j(I_\alpha \sin\varphi_\alpha - I_\beta \cos\varphi_\beta) \end{bmatrix} \qquad (106)$$

5.2.2 Instantaneous reactive power detecting

Reactive power sensing equation is:

$$Q_s = \begin{bmatrix} Q_a \\ Q_b \\ Q_c \end{bmatrix} = \begin{bmatrix} \begin{vmatrix} v_b & v_c \\ i_b & i_c \end{vmatrix} \\ \begin{vmatrix} v_c & v_a \\ i_c & i_a \end{vmatrix} \\ \begin{vmatrix} v_a & v_b \\ i_a & i_b \end{vmatrix} \end{bmatrix} \qquad (107)$$

5.3 TWO OPTIONS FOR THE PROPOSED SVG CONTROL

At the beginning, there are two options for the proposed schemes. One is Instantaneous Currents control, the other is the Controller by adjusting both δ, MI.

5.3.1 Option 1. Instantaneous Currents control

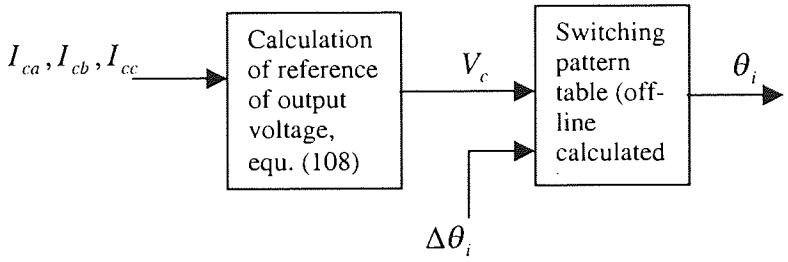

Fig. 5-2, Instantaneous Currents Controller.

Refer to Fig. 5-2, the detected currents to be compensated I_{ca}, I_{cb}, I_{cc} are obtained by the detecting circuit and are given mathematically by the equation (106). The corresponding compensation (SVG output) voltage is calculated from:

$$V_{ca} = I_{ca}(R + jX) + V_s \qquad (108)$$

Where:

X, R are the total reactance and resistor between SVG and supply system, respectively.

V_s is the supply system voltage. The switching displaced angle $\Delta\theta_i$ for dc capacitor voltage balancing is from the DC voltage balancing circuit; and θ_i is the firing angle of the SVG inverters. The disadvantages of applying this method for EAF compensation are:

- This method is under the condition of the load voltage constant while the EAF has voltage deviation and fluctuation.
- The currents of an EAF changes too fast to be dynamically traced

5.3.2 Option 2. Controller by adjusting both δ, MI

1. The basic equations for control based on the above strategies

From the results obtained in chapter-4, we can derive the following equations for the proposed SVG control.

MI renewing each line-cycle equation is given by (109)

$$(MI)_j = \frac{2XQ_j + V_s^2}{kV_s^2} \tag{109}$$

The power angle can be calculated using the follow equation

$$\delta \approx \frac{RQ_\Sigma}{V_s^2} = \frac{R(Q_s - Q_j)}{V_s^2} \tag{110}$$

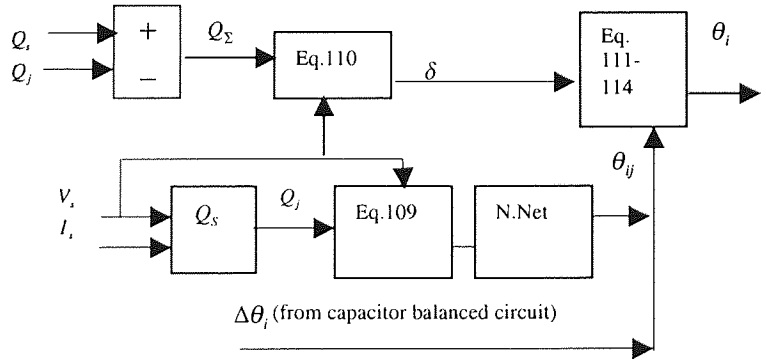

Fig. 5-3, Control system block diagram

Refer to Fig. 5-3, the exact firing angles after δ -shift and $\Delta\theta_i$ -replacement for DC capacitor voltage balances are as follows:

Positive DC voltage firing angles begin at:

$$\theta_i = \theta_{ij} - \delta - \Delta\theta_i \tag{111}$$

Positive DC voltage firing angles end at:

$$\pi - \theta_{ij} - \delta - \Delta\theta_i \qquad (112)$$

Negative DC voltage firing angles begin at:

$$\pi + \theta_{ij} - \delta - \Delta\theta_i \qquad (113)$$

Negative DC voltage firing angles end at:

$$2\pi - \theta_{ij} - \delta - \Delta\theta_i \qquad (114)$$

Where:

V_s : The system supply voltage

V_c : The SVG output voltage

I_s : The current flow from system to SVG (I_s =- I_c)

R , L : A set of linked AC reactor and equivalent resistance including the SVG losses

Q_s : The system reactive power

Q_j : The value of j -th sampling of Q_s for MI renewing

δ : The phase angle between system voltage and the SVG output voltage.

θ_{ij} : The j -th calculated switching angle by Neural net

$\Delta\theta_i$: The switching angle displace for dc capacitor voltage balancing.

θ_i : The firing angle

2. The operation principles

Refer to Fig. 5-3 and Fig. 5-4, the principle is as follows:

The controller synchronously samples the reactive power Q_s each line cycle, e.g. Q_j is the value of the j -th sample, so the PI controller can get the $(MI)_j$. Then, according to the SHEM, the neural net will give the value of the switching angle θ_{ij}. The reactive power variations during

the line cycle will be compensated by adjusting the phase angle δ - which is continuously sampling. In Fig. 5-3, $\Delta\theta_i$ is the displaced switching angle for dc capacitor voltage balancing.

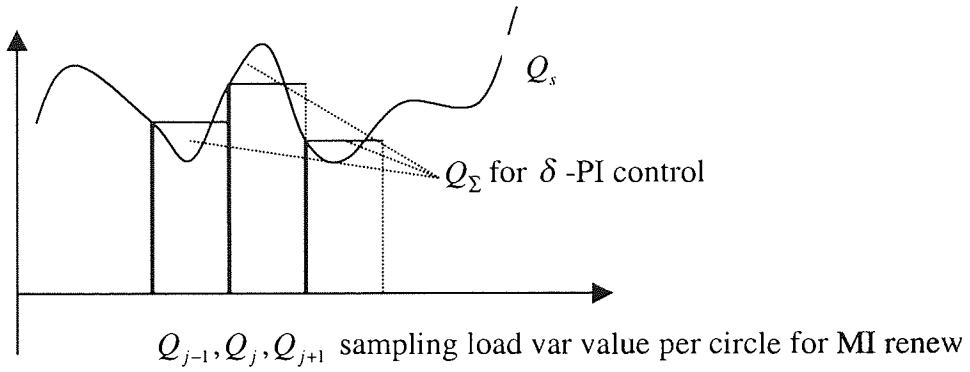

Fig. 5-4, the sampling value illustration of the SVG

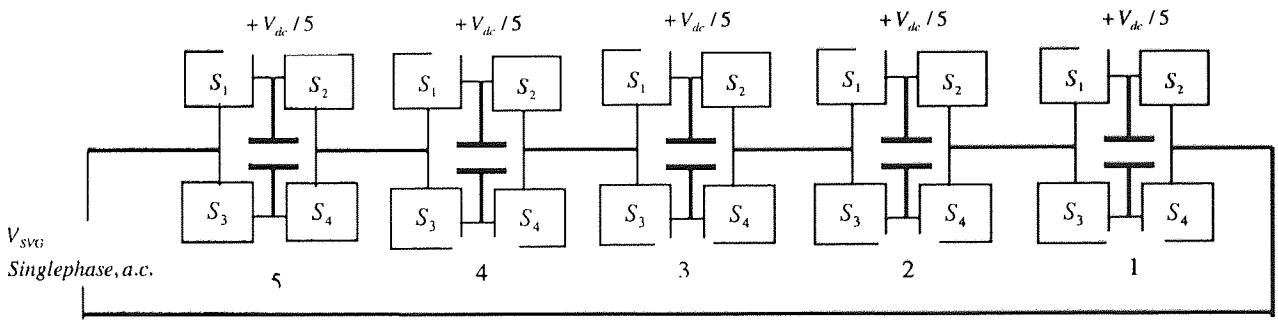

Fig. 5-5, the switching pattern illustration of the SVG converters

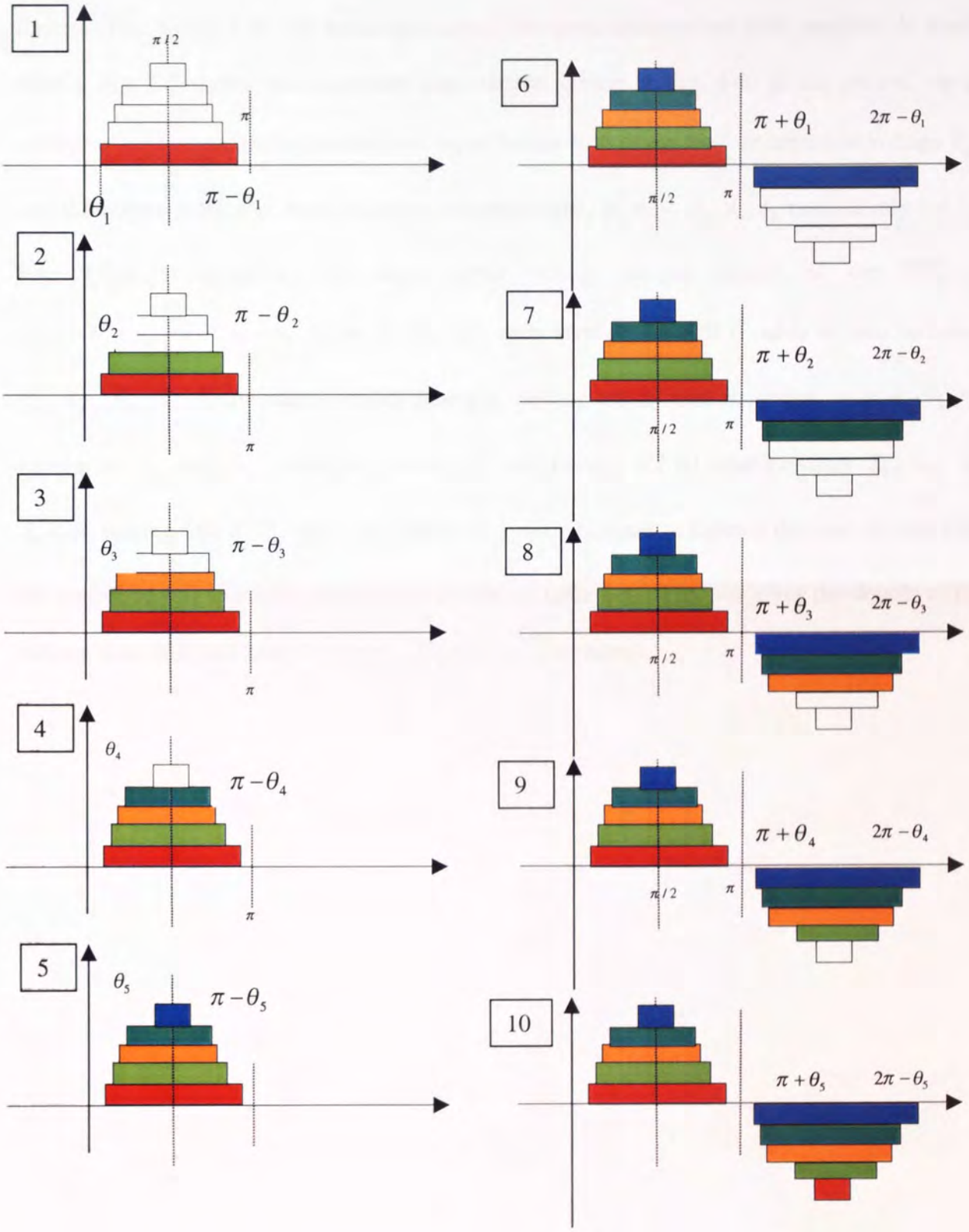

Fig. 5-6, the illustration of SVG inverters step by step firing procedures

3. SVG Switching patterns

Refer to Fig. 4-3 & 4 for the basic structure of the cascaded-inverters with separate dc source (SDC). Fig. 5-5 shows the equivalent logic control circuit of Fig. 4-3. In the system, the dc voltage of each capacitor is the same and equal to one-fifth of the total dc capacitor voltage V_{dc}, and the output voltage of each H-bridge inverters (HBI) is v_1, v_2, v_3, v_4, v_5 respectively for 11-level (5-stage) inverters. The total output voltage (single phase) of the SVG is $v_{SVG} = v_1 + v_2 + v_3 + v_4 + v_5$. Refer to Fig. 5-5, each level of the HBI consists of four switches, S_1, S_2, S_3, S_4. Using stage-1 as an example, turning on S_1 and S_4 yields to $v_1 = +V_{dc}/5$, turning on S_2 and S_3 yields to $v_1 = -V_{dc}/5$ and turning off all four switches S_1, S_2, S_3, S_4 (OR, turning ON S_1 S_2 or S_3 S_4) yields to $v_1 = 0$. In order to balance the load of each HBI, the optimised full switching patterns are shown on table 5-11. Fig. 5-6 gives the details of this scheme (one HBI will keep the same colour in the illustration).

Table 5-11, the switching pattern table

Stages	(v_{svg}) V_{dc}	(v_{svg}) $4V_{dc}/5$	(v_{svg}) $3V_{dc}/5$	(v_{svg}) $2V_{dc}/5$	(v_{svg}) $V_{dc}/5$	(v_{svg}) 0	(v_{svg}) $-V_{dc}/5$	(v_{svg}) $-2V_{dc}/5$	(v_{svg}) $-3V_{dc}/5$	(v_{svg}) $-4V_{dc}/5$	(v_{svg}) $-V_{dc}$
Stage-1											
S_1	On	On	On	On	On	Off	Off	Off	Off	Off	Off
S_2	Off	Off	Off	Off	Off	Off	Off	Off	Off	Off	On
S_3	Off	Off	Off	Off	Off	Off	Off	Off	Off	Off	On
S_4	On	On	On	On	On	Off	Off	Off	Off	Off	Off
Stage-2											
S_1	On	On	On	On	Off	Off	Off	Off	Off	Off	Off
S_2	Off	Off	Off	Off	Off	Off	Off	Off	Off	On	On
S_3	Off	Off	Off	Off	Off	Off	Off	Off	Off	On	On
S_4	On	On	On	On	Off	Off	Off	Off	Off	Off	Off
Stage-3											
S_1	On	On	On	Off	Off	Off	Off	Off	Off	Off	Off
S_2	Off	Off	Off	Off	Off	Off	Off	Off	On	On	On
S_3	Off	Off	Off	Off	Off	Off	Off	Off	On	On	On
S_4	On	On	On	Off	Off	Off	Off	Off	Off	Off	Off
Stage-4											
S_1	On	On	Off	Off	Off	Off	Off	Off	Off	Off	Off
S_2	Off	Off	Off	Off	Off	Off	Off	On	On	On	On
S_3	Off	Off	Off	Off	Off	Off	Off	On	On	On	On
S_4	On	On	Off	Off	Off	Off	Off	Off	Off	Off	Off
Stage-5											
S_1	On	Off	Off	Off	Off	Off	Off	Off	Off	Off	Off
S_2	Off	Off	Off	Off	Off	Off	On	On	On	On	On
S_3	Off	Off	Off	Off	Off	Off	On	On	On	On	On
S_4	On	Off	Off	Off	Off	Off	Off	Off	Off	Off	Off

5.4 CONTROL SYSTEM DESIGN AND MATLAB SIMULATION

5.4.1 An Introduction

Nowadays, MATLAB becomes a very useful tool in control system design. From the transfer function of equation (97), a controller can be designed in order for the SVG to have fast dynamic characteristics. This controller is based on controlling the power angle δ. Fig. 5-3 shows the block diagram of the PI-based controller. The switching scheme is illustrated by Fig. 5 - 4~6 and Table 5-11.

To validate the mathematical model worked out at chapter 4, MATLAB was used to simulate and check the proposed scheme. The data used is from reference [74].

The datum are:

$V_s = 240\sqrt{2}/\sqrt{3} = 196(V)$
$l = 36.8mH$
$C = 22.56mF$ [8]
$R \approx 1\Omega$
$\omega = 314(f = 50Hz)$

5.4.2 MATLAB simulation results of the proposed scheme

The Bode diagram and Step response are shown on Figures 4-13 and 4-14 respectively.

The simulation results of the whole system dynamic response, System sensitivity to plant variations are shown as Fig. 5-7 and 5-8 respectively.

[8] The resistor is not given by the paper, about one percent of active power loss is used to calculate the resistor value.

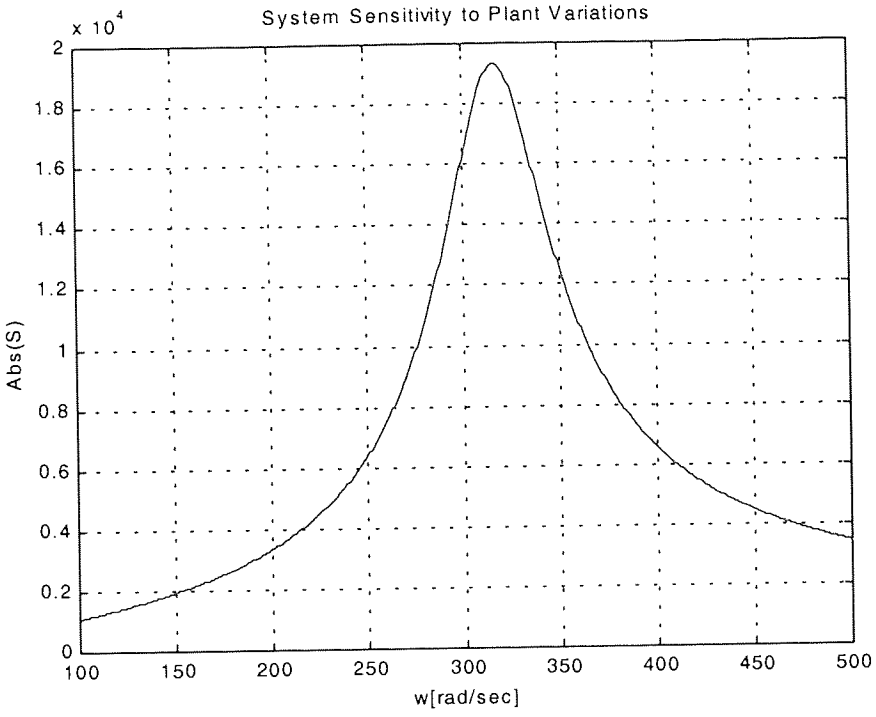

Fig. 5-7, System sensitivity to plant variations [Abs (s) against w]

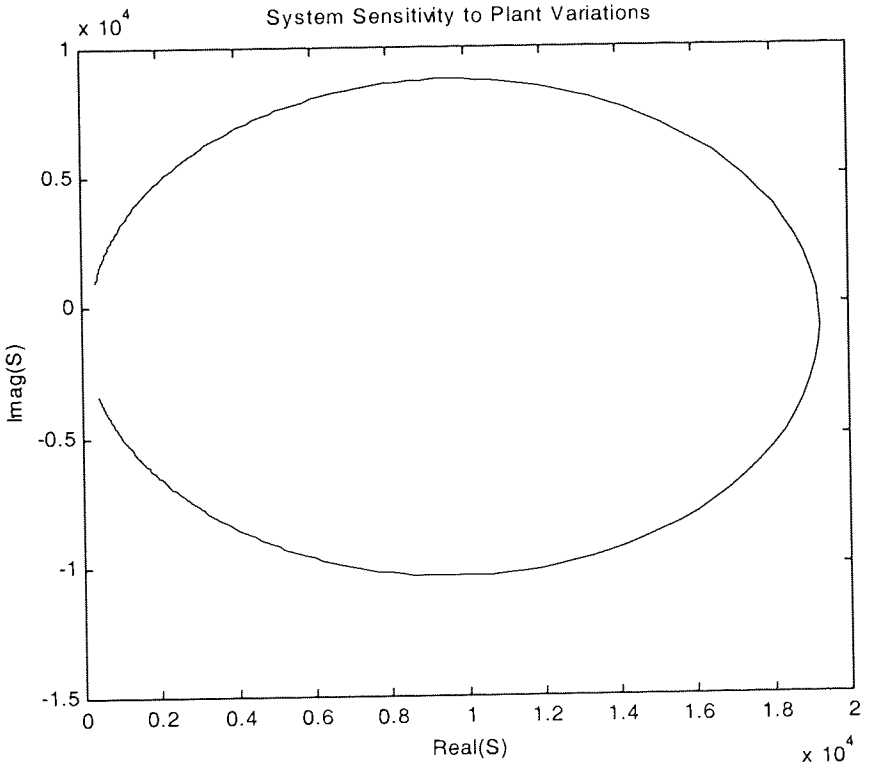

Fig. 5-8, System sensitivity to plant variations [Imag (s) against Real (s)]

5.5 SIMULATION RESULTS AND CONCLUSIONS

Refer to Fig. 5-9, we use the function: $y = \cos(31.4t) + 0.2\sin(628t)$ as the reactive power input (pu), and sample once each line-cycle to renew the MI (the magnitude of the SVG output voltage). Ten samplings are shown on the figure.

In Fig. 5-10, to illustrate, we sample only 5 times in a line cycle (in practice, we can continuous control or sample very fast). You can not tell the δ -shift from the figures as it is too small to distinguish. Fig. 5-10 (b) shows five curves with different δ overlapped together.

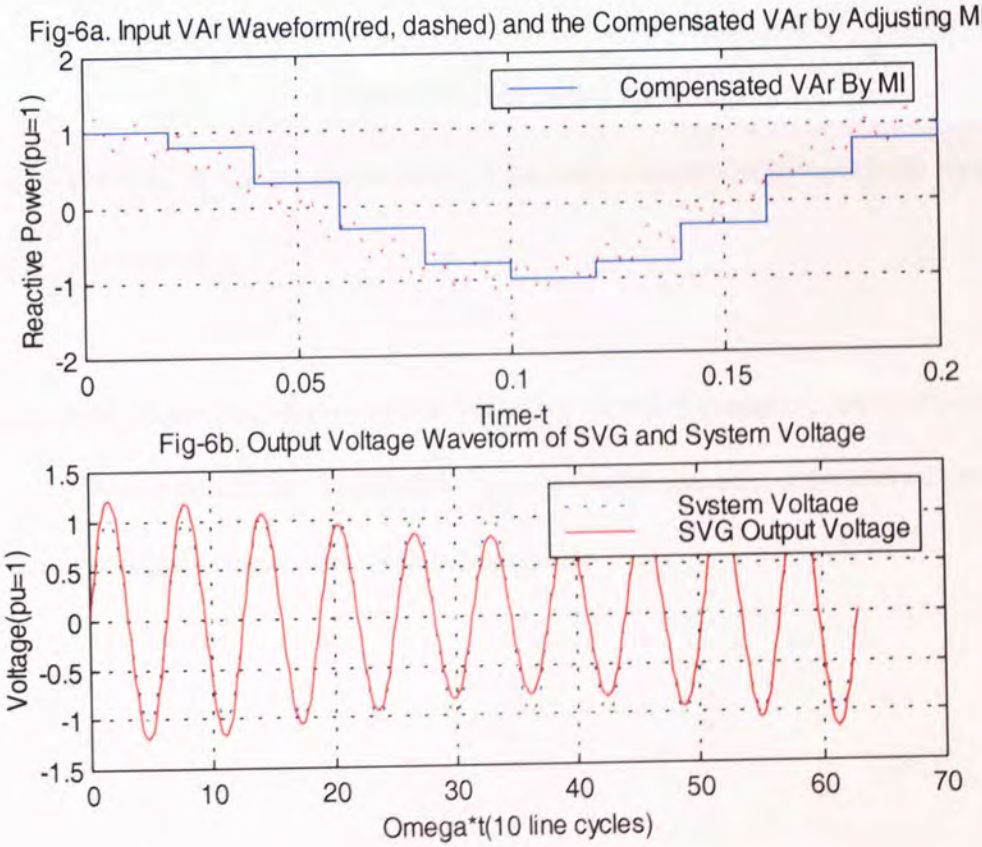

Fig. 5-9, The input VAr waveform and the compensated VAr by renewing the MI each line-circle.

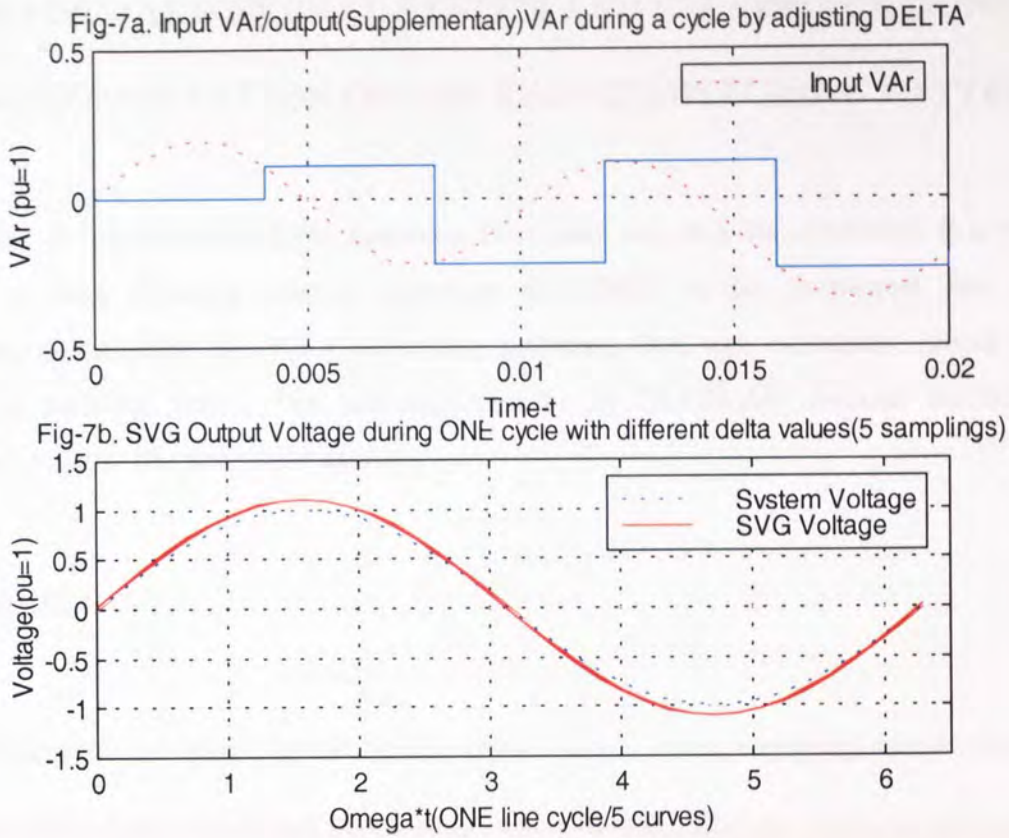

Fig. 5-10, the waveform of the uncompensated VAr and compensation waveform by adjusting the power angle DELTA (δ).

The simulation results show that, the transient model for 11-level cascade converters-based SVG proposed by this research will be applicable for any level cascade converters-based SVG / STATCOM, and the design of the controller is reasonable.

VI. FEED FORWARD NEURAL SYSTEM AND ITS APPLICATIONS FOR ON-LINE COMPUTATION OF THE SVG MI/SWITCHING PATTERNS

ABSTRACT: To shorten the SVG response time and improve its accuracy, this chapter developed a feed forward neural network (FFANN) to be employed for on-line applications, calculating the MI / switching patterns that are currently found by the conventional look-up table. The training results by MATLAB (neural toolbox) are provided to validate the proposed system.

6.1 INTRODUCTION

Neural networks are an attractive solution in several applications requiring massively-parallel computation (e.g., signal and image processing, sensor fusion, robotics, real time control) when no algorithmic approach is known or when it can not be easily formalized, while the desired system operation can be specified through examples [115].

A neural paradigm is composed by a number of functional operators (neurons), which are interconnected by weighted links (synapses) [116]. In any static network, the neuron n_i is modelled by:

$$x_i = f_i(\sigma_i - b_i) = f_i(\sum_{j=1}^{N} w_{i,j}.x_j - b_i) \qquad (115)$$

Where:

x_i is the neuron's output.

$w_{i,j}$ is the interconnection weight from neuron n_j to neuron n_i.

$\sigma_i = \sum_{j=1}^{N} w_{i,j}.x_j$ is the inputs' weighted summation.

b_i is the neuron's threshold (or, bias).

$f_i(.)$ is the nonlinear activation function that generate the neuron's output from the incoming excitation.

During the last decade, extensive research work had been carried out on the application of a neural network. In electrical power systems, it has been used successful for load forecasting [117], security assessment [118], capacitor control [119], alarm processing [120], insulator contour optimisation [121] etc. Today, SVG takes an important role among FACTS apparatus in power system. Usually, PID control, zero dynamic based nonlinear control and fuzzy control are used in the control of an SVG [122-123]. The advantages of using above mentioned controllers are: simple realization, relatively wide operating range and insensitivity to the disturbing of some system parameters. However, the PID controller cannot deal with nonlinear problem and is not adaptable. Although the fuzzy control can be applied for modern power systems that are large, complex, geographically widely distributed and highly nonlinear [124], it cannot "learn" during the control period. Artificial Neural Networks (ANN) have essential non-linear property, strong robustness, parallel calculation and self-learning ability. In this research, we consider only the multi-layered feed-forward artificial neural networks (FFANN) for on-line computation, but the approach can be extended to the any network topology.

6.2 FEED FORWARD NEURAL NETWORKS AND ITS APPLICATION FOR THIS PROJECT

An ANN is a set of processing units or computational elements (nodes) connected with links (arcs) and having connectivity weights representing the strength of the connections. A FFANN, as described in [125], is a hierarchically structured ANN in which nodes are organized into layers, and the directed arcs only link nodes in lower layers to nodes in higher layers. The

direction of an arc represents the direction of the signal flow. Denote node-r in layer-i by n_i^r, and the connectivity weight from n_j^d to n_i^r by w_{ij}^{rd}. Let the number of nodes in layer-i be m_i, and the number of layers with processing units be l. Each node n_i^r, for $i \geq 1$, has a bias or threshold b_{ir}. We treat the node bias as an extra input unit with a constant input of 1 (one) and with connections from it to all nodes in all hidden and output layers. The connectivity weights and node biases are the parameters of the FFANN. A fully connected FFANN with $l = 2$, $m_0 = 1$, $m_1 = 5$, $m_2 = 5$ used in this research is shown in Fig. 6-1.

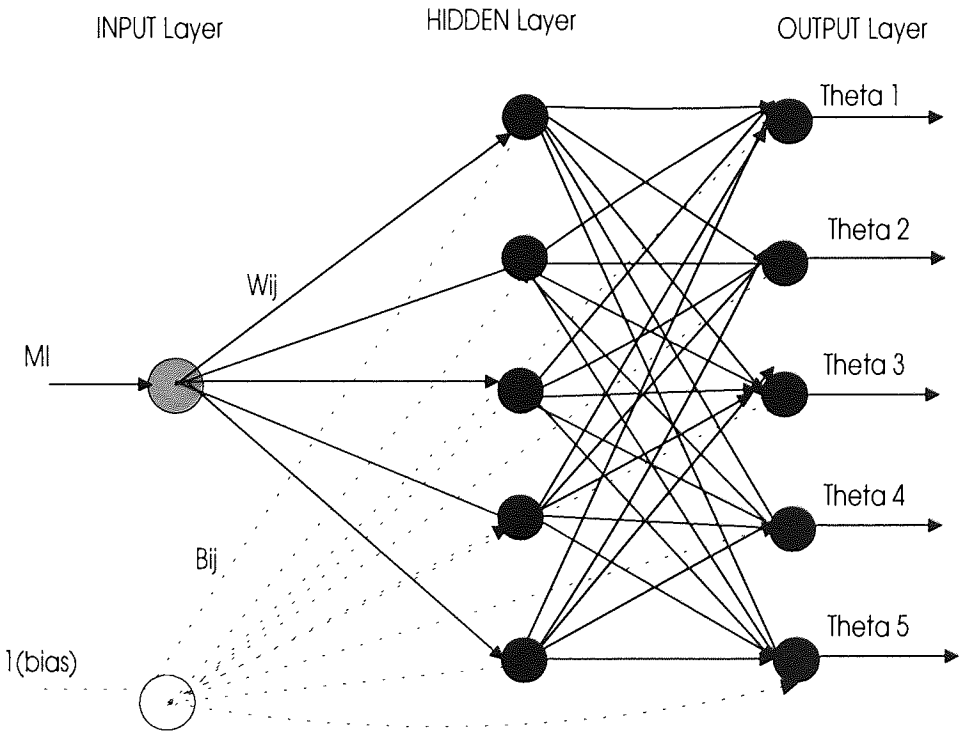

Fig. 6-1, A fully connected FFANN employed in the research

According to above definitions & denotations, and refer to Fig. 6-1, we can derive the network output as shown by equation (116) below, by employing sigmoid function for the hidden layer neurons and linear function for the output layer.

$$Theta\_k = \sum_{i=1}^{5} w_{12}^{ki}(1+\exp(-\frac{1}{\beta}(w_{01}^{0i}MI + b_{1i})))^{-1} + b_{2k} \quad (k = 1,2,3,4,5) \qquad (116)$$

The benefits of using neural computation instead of an off-line calculated look-up table are:

- Less storage room in RAM. The neural method requires a very small number of weights to be stored in the CPU, while an off-line calculated table may need a large number of entries and the possible use of linear interpolation between stored data points.
- Faster response. After training, the neural networks will be consistent in that the same input pattern, and will always produce the same answer, so the calculation speed is very fast.

The FFANN can be trained to accept the desired value of M_i as input and provide the required switching angles θ_k according to the principle of SHEM. By switching the H-bridge inverters at these angles, the undesired harmonics will disappear (or reduced to an acceptable range) in the output voltage. The Net is trained by changing both the weights w_{ij}^{rd} and the biases b_{ir}. To train the set, equations (75) and (76) are solved repeatedly for different values of MI (from 0.5 to 0.75 with equal steps of 0.001). The training method is similar with that used in [112], which uses a sigmoid function for the hidden layer neurons and a linear function for the output layer. The MATLAB (neural tool-box) simulation results are shown in Fig. 6-2.

For real engineering application, in order to improve accuracy, we can set both the error limits and the steps (for training) smaller, but it takes a longer training time.

6.3 SIMULATION RESULTS AND CONCLUSIONS

The MATLAB simulation result is shown in Fig. 6-2, Theta-MI Curves following the SHEM (selected 5^{th} 7^{th} 11^{th} 13^{th} and 15^{th} to be eliminated) in training the FFANN. The error-harmonic voltages are given by table 6-12 after the system has been trained. The full results of the error-harmonic voltages versus various MI are listed in Appendix III.

Table 6-12, The calculated results of the 5^{th}, 7^{th}, 11^{th}, 13^{th}, 15^{th} harmonics peak values(pu) after training the employed FFANN.

MI	$(\sum_{i=1}^{5}\cos 5\theta_i)/5$	$(\sum_{i=1}^{5}\cos 7\theta_i)/7$	$(\sum_{i=1}^{5}\cos 11\theta_i)/11$	$(\sum_{i=1}^{5}\cos 13\theta_i)/13$	$(\sum_{i=1}^{5}\cos 15\theta_i)/15$
0.5010	0.021	-0.00575	0.00862	0.00786	-0.0282
...	...	...	...	...	...
0.5810	-0.0199	-0.0124	0.00892	0.00737	0.00179
...	...	...	...	...	...
0.6605	-0.0162	-0.00606	-0.00432	-0.00581	0.00987
...	...	...	...	...	...
0.7190	-0.0102	0.01	0.00561	-0.0104	-0.0206
...	...	...	...	...	...
0.7600	-0.00424	0.00876	-0.00647	0.00584	-0.0439
...	...	...	...	...	...

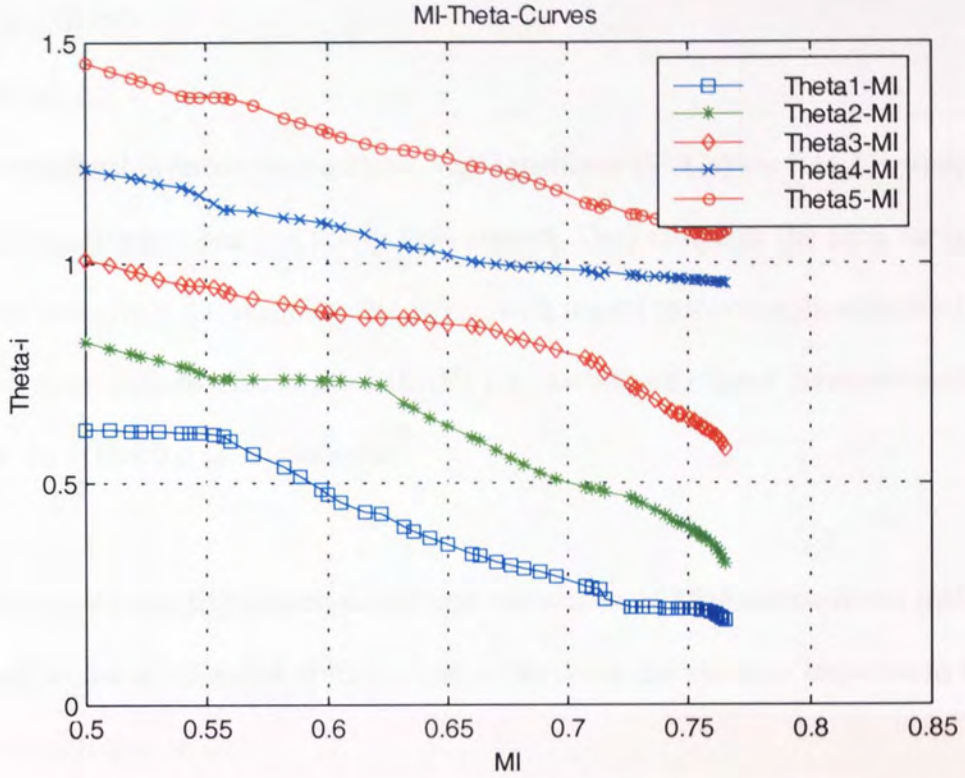

Fig. 6-2, The MI-Theta curves After FFANN trained

VII. FURTHER DISCUSSION

7.1 CONCLUSIONS

7.1.1 General

Cascaded multilevel inverters-based Static Var Generators (SVGs) are FACTS equipment introduced for active and reactive power flow control. They eliminate the need for zigzag transformers and give a fast response. However, with regard to their application for flicker reduction in using Electric Arc Furnace (EAF), the existing multilevel inverter-based SVGs suffer from the following disadvantages:

- To control the reactive power, an off-line calculation of Modulation Index (MI) is required to adjust the SVG output voltage. This slows down the transient response to the changes of reactive power
- Random active power exchange may cause unbalance to the voltage of the d.c. link (HBI) capacitor when the reactive power control is done by adjusting the power angle δ alone.

To resolve these problems, a mathematical model of an 11-level cascaded SVG, was developed. A new control strategy which involving both MI (modulation index) and power angle (δ) is proposed. A selected harmonics elimination method (SHEM) is taken for switching pattern calculations. To shorten the response time and simplify the control system, the feed forward neural networks are used for on-line computation of the switching patterns instead of using look-up tables.

The proposed controller updates the MI and switching patterns once each line-cycle according to the sampled reactive power Q_s. Meanwhile, the remainder reactive power (compensated by the MI) and the reactive power variations during the line-cycle will be continuously compensated by

adjusting the power angles, δ. The scheme senses both variables MI and δ, and takes action through the inverter switching angle, θ_i. As a result, the proposed SVG is expected to give a faster and more accurate response than present designs allow.

In support of the proposal there is a mathematical model for reactive power distribution and a sensitivity matrix for voltage regulation assessment, MATLAB simulation results are provided to validate the proposed schemes. The performance with non-linear time varying loads is analysed and refers to a general review of flicker, of methods for measuring flickers due to arc furnace and means for mitigation.

7.1.2 Research background

This research was begun with the title of "Voltage profile correction of a load bus by static reactive power compensators with quantisation control". Three main areas are involved in the research: voltage profile correction, load characteristics analysis and power electronics based compensators. In order to clarify the power system background for voltage correction, the abnormal voltage conditions and methods for voltage regulation are highlighted in chapter one, and a sensitivity matrix for voltage regulation assessment is included. Based on methods of variational calculus, the Lagrange Equations are developed to resolve the problem of reactive power optimal distribution. At the end of this chapter, combined with the design experience of a 9.2MW synchronous motor using a direct on line (DOL) start up method, it also provides a p.u-impedance method for voltage-dip calculation.

Then, the load feature analysis is given in chapter two. Titled "Special load analysis", it analysed the special loads Electric Arc Furnaces (EAFs), Converters and Railway traction in turn. Analysis were based on theoretical approaches and on results obtained from some on-the-

spot experiments in the real metallurgic industry projects or railway routes in China. The statistical tables and empirical formulae shown, which describe general features of these loads, were concluded from the analysis. From the tables and equations that define operation, the performance of these dynamically changeable loads can be predicted and assessed.

After my First Year Qualification Meeting, my Ph.D. thesis was entitled as "fast response Static VAr Generator for improving the power system performance of an electric arc furnace". At the meeting, I was required to continue my research in following subjects:

1. Characteristics analysis of EAF current variations (chapter two and three).
2. SVG compensation scheme for a real EAF system at pcc (chapter three and four).
3. How to examine flicker and flicker criteria (chapter three).
4. Investigate the devices, methods or the systems to reduce voltage fluctuation at pcc (chapter four).

Following above guidance for my further research, chapter three gives a general review about how to examine/assess voltage flicker and methods followed in measuring flickers due to arc furnace and means for mitigation. It also investigates fast response SVG for arc furnace flicker mitigation. It includes the discussion in the effects of utilities' conditions, compensator response-time and compensator capacity on arc furnace flicker reduction. A comparison between SVC and SVG on the applications of EAF compensation is carried out. Some discussions about the perspective of applying SVG for EAF compensation are also included in this chapter.

Chapter 4 was aimed to investigate the application of cascade multilevel converters-based SVG for EAF compensation. Based on the methods of Vector-Analysis and Switching-Function and combined with the new control strategies by adjusting both MI and the phase angle (δ) between

the system voltage and the SVG output voltage. The mathematical model for transient response of the proposed SVG is developed in this chapter. The details of the new control system are given in chapter 5.

Chapter 6 discusses the FFANN and its application in this research. Conclusions and further discussion are given in Chapter 7.

7.1.3 Contributions in this research

In summary, following work might be valuable in the research:

- First applied FFANN for the MI on-line renew.
- First investigated the cascade multilevel inverters-based SVG for EAF application.
- A new control strategy of the SVG for EAF compensation is proposed, which is by adjusting both MI and power angle (δ).
- A transient mathematics model for the cascade multilevel inverters-based SVG is carried out.

This research also includes:

- A mathematics model for reactive power distribution,
- A sensitivity matrix for voltage regulation assessment,
- The special load analysis, and
- A general review about how to examine / assess voltage flicker and methods followed in measuring flickers due to arc furnace and means for mitigation.

7.2 THE FURTHER WORK.

Began the Ph.D. as an electrical engineer in high voltage engineering, I am new in some subjects like control engineering, power electronics and neural system. So that, my research in these

subjects are still room to improve, and as the time limit, following work can be carried on further:

- Translating the proposed schemes for prototype or practical use.
- The FFANN system might have room for improving
- IF NECESSARY AND/OR POSSIBLE, the quantitive comparison about the benefits of using FFANN on-line renew MI with that of off-line calculated MI look-up table could be performed on the prototype stage.

REFERENCES

1. Liu Sheng, Chi Yu-tien, "Automatic control of voltages and reactive power flows in power systems by means of static var compensator", Journal of Tsing Hua University, vol. 19, no. 3, 1979, pp96-111. China.
2. L. Gyugyi, "Reactive power generation and control by thyristor circuits", IEEE Transaction on Ind. Appl., vol. IA-15, pp521-532, Sep./Oct., 1979.
3. Annabelle van Zyl, "Converter-based solution to power quality problems on radial distribution lines", IEEE Transaction on Ind. Appl., vol. 32, no. 6, pp1323-30, Nov./Dec., 1996.
4. C. Schauder, "STATCOM for compensation of large electric arc furnace installations", IEEE power engineering society, 1999 summer meeting (99 CB36364), IEEE Part vol. 2, pp 1109-12, Edmonton, Alberta, Canada, 18-22 July 1999.
5. C. Schauder, A. Edris, "AEP UPFC project: installation, commissioning and operation of the +/-160 MVAR STATCOM (phase I)", IEEE Transactions on Power delivery, vol. 13, no. 4, pp1530-5, Oct. 1998.
6. L. Gyugyi, "Dynamic compensation of AC transmission lines by solid-state synchronous voltage sources", presented at the IEEE/PES Summer meetings, Vancouver, B. C., Canada, July 1993, paper 434-1.
7. R. J. Nelson, J. Bian, S. L. Williams, "Transmission series power flow control", IEEE Transactions on power delivery, vol. 10, no. 1, pp504-10, Jan. 1995.
8. B.M.Weedy, B.J.Cory, "Electric Power Syatems", John Wiley&Sons Ltd, England, 4th edition, Chap. 5, 1998.
9. Butterworths, "Power Transformer Handbook", Butterworth & Co. (Publishers) Ltd, 1st English edition, Chap. 2, 1987.
10. Charlesa. Gross, "Power System Analysis", 2nd edition 1986.
11. B. M. Weedy, "Voltage stability of radial power links", Proc. IEE, Vol. 115, pp 528-36, April 1968.
12. V. A. Venikov, et al., "Estimation of electric power system steady-state stability in load flow calculation", IEEE Transactions on power applications and systems, Vol. PAS-94, pp1034-41, May/June 1975.
13. R. A. Schlueter, "A voltage stability security assessment method", IEEE Transactions on power systems, vol. 13, no. 4, pp1423-31, Nov. 1998.

14. V. Ajjarapu, B. Lee, "Bibliography on voltage stability", IEEE Transactions on power systems, vol. 13, no. 1, pp115-25, Feb. 1998.
15. D. Thukaram, A. Lomi, "Selection of static VAR compensator location and size for system voltage stability improvement", Electric Power Systems Research, vol. 54 (2000), pp139-150, 2000.
16. Roland.E.Thomas, Albert.J.Rosa, "the Analysis and Design of Linear Circuits", Prentice-Hall Inc., USA, 2nd edition, Chap. 3, 1998.
17. Z. Zhang, "9.2 MW Synchronous Motor DOL start-up Calculation and Design", BOC Project(BOC-TISCO Gases, China) Review Meetings, Guildford, UK, 1996.
18. Harold Cohen, "Mathematics for Scientists & Engineers", Prentice-Hall International Inc., pp400-9, 1992.
19. B.M.Weedy, B.J.Cory; "Electric Power System", John Wiley & Sons Ltd., pp186-7 and pp266-7, 4th Edition, 1998.
20. Noel M.Morris, "Mastering Mathematics for Electrical and Electronic Engineering", The MALMILLAN PRESS LTD., pp213-26, 1994.
21. Allan D. Kraus, "Circuit Analysis", West Publishing Company, pp429-57, 1991.
22. Harold Cohen, "Mathematics for Scientists & Engineers", Prentice-Hall International Inc., pp433-68, 1992.
23. Specialists Research Group, "Harmonics and strategies to restrain their pollution to the power system in Beijing City Network", *Research Report from the Specialist Research Group,* Beijing, China, 1992.
24. E. O'Neill-Carrillo, G. T. Heydt, E. J. Kostelich , S. S. Venkata and A. Sundaram, " Non-linear Deterministic Modelling of Highly Varying Loads", *IEEE Trans. On Power Delivery,* pp.537-542, Vol. 14, No. 2, April 1999.
25. Z. Zhang, "Electric Characteristics of EAF Loads and the Ways to Restrain Their Pollution to Power System", *Design Review,* CERIS, Beijing, China, 1996.
26. Z. Zhang, "A graphic Method Analysing Electric Characteristics of EAF and the Optimum Work-state During Melting State", *Design Review,* CERIS, Beijing, China, 1995.
27. Zuoyi Liao, " The Arc Furnace As A Load On The Network", *Metallurgic Industry (Chinese Quaterly),* pp.27-35(Writing in Chinese), Vol. 3, 1993.
28. Shuqin Sun, "Considerations on the compensation of the reactive current and harmonics", 3rd Int. conf. On harmonics in power systems, Nashville, pp224-231, 1988.
29. Xuehai Lin, "Introductions of voltage fluctuation and flicker standard in power system", *Power Network Technology(A Chinese periodical),* Vol. 1, 1993.

30. *"Electric Design Criteria of Metallurgic Industry of China"*, Ministry of Metallurgic Industry Publishers Ltd., chap. 13, 15,1997.
31. Derek. A. Paice, "Power Electronic Converter Harmonics", the Institute of Electrical and Electronics Engineers Inc., New York, USA, chap.1, 1996.
32. E. Lakervi and E. J. Holmes, "Electricity distribution network design", 2nd ed. Peter Peregrinus Ltd., chap. 12, 1995.
33. David Finney, " Variable frequency AC motor drive systems", Peter Peregrinus Ltd., chap.9, 1988.
34. Ministry of Electric Power Industry of China, "Harmonics and Unbalanced-load caused by the railway traction and their effects to the power system", Beijing China, 1992.
35. DIXON G. F. L., KENDALL P. G., "Supply to arc furnace: measurement and prediction of supply voltage fluctuation", Proc. IEE, 1972, vol. 109, no. 4, pp. 456-65.
36. YANO I. H. M., YUYA M. T. S., "Suppression and measurement of arc furnace flicker with a large static var compensator", IEEE Trans., 1979, PAS-98, no.6, pp. 2276-83.
37. MANCHUR G., "Development of a model for predicting flicker from electric arc furnace", IEEE Trans., 1992, vol. PWRD-7, no. 1, pp. 416-26.
38. BISHOP M. T., DO A. V., "Voltage flicker measurement and analysis system"; IEEE Computer Applications in Power, April 1994, pp.34-38.
39. LAVERS J. D., BIRINGER P. P., "Real time measurement of electric arc furnace disturbances and parameter variations", IEEE Trans., vol. IA-22, no. 4, 1986, pp. 568-77.
40. SRINIVASAN. K., "Digital measurement of voltage flicker", IEEE Trans., 1991, vol. PWRD-6, no. 4, pp. 1593-98.
41. BHARGAVA B., "Arc furnace flicker measurements and control", IEEE Trans., 1993, vol. PWRD-8, no. 1, pp. 400-9.
42. MENDIS, S. R., SHOP M. T., "Investigation of transmission system voltage flicker due to multiple AC and DC furnace operations", IEEE Trans., 1995, vol. PWRD-10, no. 1, pp.483-96.
43. EI-SHARKAWI M. A., etc., "Development and field tasting of an adaptive controller for 15KV systems", IEEE Trans., 1995, vol. PWRD-10, no. 2, pp. 1025-30.
44. CHEN M. T., "Digital algorithms for measurement of voltage flicker", IEE Proc.-Gener. Transm. Distrib., vol. 144, no. 2, Mar. 1997, pp. 175-80.
45. SOLIMAN S.A., EL-HAWARY M.E., "Measurement of voltage flicker magnitude and frequency in a power system for power quality analysis", Electric Machines & Power systems, vol. 27, no. 12, Dec. 1999, pp. 1289-97.

46. KOROSEC A., VORSIC J., "Flickermeter", Elektrotehniski Vestnik, Electrotech. Soc. Slovenia, Slovenia, vol. 64, no. 1, 1997, pp. 26-31.
47. Girgis A.A., Stephens J. W., Makram E. B., "Measurement and prediction of voltage flicker magnitude and frequency", IEEE Transactions on Power Delivery, vol. 10, no. 3, pp 1600-5, July 1995.
48. Halpin S. M., Reuben F. Burch, IV, "An improved simulation approach for analysis of voltage flicker and the evaluation of mitigation strategies", IEEE Transactions on Power Delivery, vol. 12, no. 3, pp 1285-91, July 1997.
49. Y. Y. Hong, L. H. Lee, "Analysis of equivalent 10 Hz voltage flicker in power systems", IEE Proc.-Generation Transmission & Distribution, vol. 146, No. 5, Sep. 1999. Pp447-52
50. Chen-wen Lu, S. J. Huang, C. L. Huang, "Flicker characteristic estimation of an ac electric arc furnace", electric power systems research, vol. 54, pp 121-30, 2000.
51. C. J. Wu, S. S. Yen, "Investigation of 161kV arc furnace on power quality", monthly journal of Taipower's engineering, vol. 575, pp 84-96, July 1996.
52. L. Tang, D. Mueller, "Analysis of dc arc furnace operation and flicker caused by 187 Hz voltage distortion", IEEE Trans. on power delivery, vol.9, no.2, pp1098-107, April 1994.
53. Alper A., Erbil Nalcaci, "Effects of main transformer replacement on the performance of an electric arc furnace system", IEEE Transactions on industry applications, vol.36, no.2, pp649-58, March/April, 2000.
54. Albrecht wolf, Manoharan Thamodharan, "Reactive power reduction in three-phase electric arc furnace", IEEE Transactions on industrial electronics, vol.47, no.4, pp 729-33, Aug. 2000.
55. Constable R., "Tapped series reactors can help optimise arc furnace operation", Elektron, vol. 14, no. 1, pp 85-6, Elektron management partnership, South Africa, Jan., 1997.
56. Sarshar A., Sharp M., "Analysis of harmonic and transient phenomena due to operation of an arc furnace", Iron & steel engineer, vol. 73, no. 4, pp 78-82, Assoc. iron & steel Eng. USA, April, 1996.
57. Schwabe WE, Schwabe GW, "Effect of scrap conditions and charge composition on power delivery and melting in arc furnaces" Elektrowaerme International, Edition B: Industrielle Elektrowaerme, vol. 45, no. 2, pp B92-7, April, 1987, West Germany.
58. Zheng T., Elham B. Makram, "An adaptive arc furnace model", IEEE Transactions on Power Delivery, vol. 15, no. 3, pp 931-39, July 2000.

59. Montanari G. C., D. Zaninelli, "Arc furnace model for the study of flicker compensation in electrical networks", IEEE Transactions on Power Delivery, vol. 9, no. 4, pp 2026-33, Oct. 1994.

60. Le Tang, Sharma kOLLURI, "Voltage flicker prediction for two simultaneously operated ac arc furnaces", IEEE Transactions on Power Delivery, vol. 12, no. 2, pp 985-92, April, 1997.

61. E. O' Neill-Carrillo, G. T. Heydt, S. S. Venkata, "Non-linear deterministic modelling of high varying loads", IEEE Transactions on Power Delivery, vol. 14, no. 2, pp 537-42, April. 1999.

62. M. Z. El-Sadek, M. Dessouky, "A flexible ac transmission system (FACTS) for balancing arc furnace loads", Electric power systems research, vol. 41, pp 211-8, 1997.

63. A. Nabae, M. Yamaguchi, "Suppression of flicker in an arc furnace supply system by an active capacitance-a novel voltage stabiliser in power system", IEEE Transactions on industry applications, vol.31, no.1, pp107-11, Jan./Feb. 1995.

64. Peter Ashmole, " Quality of supply - voltage fluctuations (Power quality tutorial, Part 2)", POWER ENGINEERING JOURNAL, pp 108-114, April 2001.

65. F. Frank, S. Ivner, "TYCAP, power factor correction equipment using thyristor-controlled capacitor for arc furnace", ASEA Journal 46 (1973): 6, pp147-152.

66. S. Etminan, P. H. Kitchin, "Flicker meter results of simulated new and conventional TSC compensators for electric arc furnaces", IEEE Transactions on power systems, vol. 8, no. 3, pp914-19, Aug. 1993.

67. C. Schauder, M. Gernhardt, E. Stacey, "Development of a +/- 100 MVA static condenser for voltage control of transmission systems", IEEE Transactions on power delivery, vol. 10, no. 3, pp1486-96, July 1995.

68. M. D. Cox, A. Mirbod, "A new static var compensator for an arc furnace", IEEE Transactions on power systems, vol. PWRS-1, no. 3, pp110-9, Aug. 1986.

69. Y. Wang, J. Liu, X. Li, "Research on reducting flicker caused by arc furnace with advanced static var generator", Power system technology (in Chinese), vol. 22, no. 9, pp61-4, Sep., 1998.

70. Fang Zheng Peng, Jih-sheng Lai, "A transformerless high-pulse static synchronous compensator based on the 3-level GTO-inverter", IEEE Transactions on power delivery, vol. 13, no. 3, pp883-8, July 1998.

71. C. J. Hatziadoniu, F. E. Chalkiadakis, "Dynamic performance and control of a static var generator using cascade multilevel inverters", IEEE Transactions on industry applications, vol. 33, no. 3, pp748-55, May/June 1997.

72. Menzies R. W., Zhuang Y., "Advanced static compensation using a multilevel GTO thyristor inverter" IEEE Transactions on power delivery, vol. 10, No. 2, April 1995, pp732-38.

73. Peng F. Z., Lai J. S., "A multilevel voltage-source inverter with separate DC source for static var generation", IEEE Transactions on industry applications, vol. 32, No. 5, Sep./Oct. 1996, pp1130-38

74. Peng F. Z., Lai J. S., "Dynamic performance and control of a static var generator using cascade multilevel inverters", IEEE Transactions on industry applications, vol. 33, No.3, May/June 1997, pp748-55.

75. Liang Y., Nwankpa C. O., "A new type of STATCOM based on using cascading voltage source inverters with phase-shifted unipolar SPWM", IEEE Transactions on industry applications, vol. 35, No.5, Sep./Oct., 1999, pp1118-23.

76. Ainsworth J. D., Davies M., "Static var compensator (STATCOM) based on single -phase chain circuit converters", IEE Proc.-Gener. Transm. Distrib., Vol. 145, No.4, July 1998, pp381-6.

77. Patil K. V., Mathur R. M., "Distribution system compensation using a new binary multilevel voltage source inverter" IEEE transactions on power delivery, Vol.14, No.2, April, 1999, pp459-64.

78. CHEN C. M., GUAN J. L., "Attenuation analysis of voltage flicker propagation", Proceedings of 15th symposioum on Electrical power engineering, Taiwan (in Chinese), 1994, pp. 563-69.

79. STADE D., KUZNIETSOV O., "An accurate measurement of voltage flicker using a virtual measuring instrument", PCIM'99, Europe, Official proceedings of 39th international power conversion conference, ZM Commun, GMBH 1999, Nurnberg, Germany, pp. 579-84.

80. NUCCIO S., "A digital instrument for measurement of voltage flicker", IEEE Instrumentation and Measurement Technology Conference. IMTC Proceedings (Cat. No. 97CH36022), IEEE Part vol. 1, 1997, NY, USA, pp. 281-4 vol.1.

81. Fallon C.M., McDermott B.A., "Development and testing of a real-time digital voltage flicker meter", Proceedings of the 1996 IEEE Power engineering society transmission and distribution conference (Cat. No. 96CH35968), IEEE 1996, pp. 31-6, NY, USA.

82. ALCORN R.G., BEATTIE W.C., "Flicker evaluation from a wave-power station", 34th UPEC, Univ. Leicester, Part vol. 1.2, 1999, pp. 395-8 vol. 2. Leicester, UK.

83. Ladakakos P.D., Ioannides M.G., "Assessment of wind turbines impact on the power quality of autonomous weak grids", 8th International conference on harmonics and quality of power

proceedings (Cat. No. 98EX227), IEEE, Part vol. 2, 1998, pp. 900-5 vol. 2., Piscataway, NJ, USA.

84. Li Chao-Hui, Chang Wen-Yao, "Investigation and fabrication of prototype flicker and harmonic monitoring system", Monthly Journal of Taipower's Engineering, vol. 596, April 1998, pp. 45-61, Taiwan Power Co. Power Res. Inst., Taiwan.
85. GIRGIS A.A., MOSS B.D., "Reactive power compensation and voltage flicker control of an arc furnace load", Proceedings of the ICHQP, 7th International conference on harmonics and qualit IEEE Transactions on Power Delivery, vol. 10, no. 3, pp 1600-5, July 1995.
86. Z. Zhang, N. R. Fahmi, Q. M. Zhu, "Special load analysis", UPEC 2000, 35 Universities' Power Engineering Conference, 6-8 Sep. 2000, Belfast, North Ireland, pp 92 at Book of Abstracts.
87. Bogdanoff A., Leiviska K., "Intelligent methods in the electric arc furnace control", Automation in mining, mineral and metal processing 1998. Preprints of the 9th IFAC symposium. Pergamon. 1998, pp. 159-62. Oxford, UK.
88. Mendis SR, Bishop MT, Day TR, "Evaluation of supplementary series reactors to optimise EAF operations" IAS'95 Conference record of the 1995 IEEE industry applications conference (cat. No. 95CH35862). IEEE Part, vol. 2, pp 2154-61, NY, USA, 1995.
89. Robert A, Couvreur M, "Recent experience of connection of big arc furnace with reference to flicker level", Proceedings of the 35th Session international conference on large high voltage electric systems. CIGRE, Part, vol. 2, pp 36-305/1-8, Paris, France, 1995.
90. Montanari GC, Loggini M, Pitti L, "Flicker and distortion compensation in electrical plants supplying arc furnaces", IAS' 94 Conference record of the 1994 Industry applications conference, 29th IAS annual meeting (cat. No. 94 CH34520), IEEE Part, vol.3, pp 2249-55, NY, USA, 1994.
91. Montanari GC, Loggini M, Pitti, L, "The effects of series inductors for flicker reduction in electric power systems supplying arc furnaces", IAS' 93 Conference record of the 1994 Industry applications conference, 28th IAS annual meeting (cat. No. 93 CH3366-2), IEEE Part, vol.2, pp 1496-503, NY, USA, 1993.
92. C. Schauder, "STATCOM for compensation of large electric arc furnace installations", IEEE power engineering society, 1999 summer meeting (99 CB36364), IEEE Part vol. 2, pp 1109-12, Edmonton, Alberta, Canada, 18-22 July 1999.
93. Y. Yoshioka, S. Konishi, "Self-commutated static flicker compensator for arc furnace", APEC' 96. Eleventh annual applied power elctronics conference and exposition. 96CH35871, IEEE Part vol.2, pp891-7, New York, UY, USA, 1996.

94. S. B. Dewan, J. Rajda, "Application of 46 kV, 100MVA smart predictive line controller (SPLC) to ac electric arc furnace", IEEE power engineering society, 1999 winter meeting (99 CB36233), IEEE Part vol. 2, pp 1214-18, Piscataway, NJ, USA, 1999.

95. M. Zouiti, S. Saadate, "Electronic based equipment for flicker mitigation", 8th international conference on harmonics and quality of power. Proceedings (cat. No. 98EX227). IEEE Part vol. 2, pp1182-7, Piscataway, NJ, USA, 1998.

96. L. Gyugi, A. A. Otto, "Static shunt compensation for voltage flicker reduction and power factor correction", 1976 American Power Conference, pp1271-1286.

97. H. Fujita, S. Tominaga, H. Akagi, "Analysis and design of an advanced static VAr compensator using quad-series voltage source inverters", in proceedings of IEEE IAS Annual Meeting, Orlanddo, FL, pp2565-72, 1995.

98. Peng F. Z., Lai J. S., "A ststic generator using a staircase waveform multilevel voltage-source converter", Proceedings PCIM/Power quality, Sep. 1994, pp58-66.

99. Hochgraf C., et, al., "Comparison of multilevel inverter for static var compensation", in Conference Rec. IEEE/IAS annual meeting, 1994, pp921-28.

100. Engineering Recommendations P. 7/2, Fifth Chief Engineer's Conference, July 1970, of the Electricity council, CEGB, England.

101. IEC Publication 868: Flicker-meter, functional and design specification, 1986. .(6)

102. Electric Design Recommendations for Metallurgical Industry, Publishing House of Ministry of metallurgical industry, Chap. 12 (in Chinese), Beijing, China, 1997(56).

103. Peng F. Z., Lai J. S., "A ststic generator using a staircase waveform multilevel voltage-source converter", Proceedings PCIM/Power quality, Sep. 1994, pp58-66.

104. Schauder C., Mehta H., "Vector analysis and control of advanced static VAR compensators", IEE Proceedings-C, Vol. 140, No. 4, July 1993, pp299-306.

105. Shosuke Mori, "Development of a large stattic VAR generator using self-commutated inverters for improving power system stability", IEEE Transactions on power systems, Vol. 8, No. 1, Feb. 1993, pp371-7.

106. J. B. Ekanayake, N. Jenkins, "Mathematical models of a three-level advanced static VAR compensator", IEE Proc.-Gener. Transm. Distrib. Vol. 144, No. 2, Maech 1997, pp201-6.

107. Jiang Qirong, Liu Qiang, "Modelling and control of advanced static VAR generator", Journal of Tsinghua University (Sci. & Tech.), Vol. 37, No. 7, July 1997, pp21-25.

108. NAM S. CHOI, GUK C. CHO and GYU H. CHO., "Modelling and analysis of a multilevel voltage source inverter applied as a static var compensator", INT. J. ELECTRONICS, 1993, VOL. 75, NO. 5, pp1015-1034.

109. Amr M. A. Amin, "A multilevel advanced static VAR compensator with current hysterises control", ISIE, 99 IEEE international symposium on industrial electronics, July 12-16, 1999, pp837-42.

110. Akagi H., Kanazawa Y., Nabae A., "Instantaneous reactive power compensators comprising switching devices without energy storage components", IEEE transactions on industry applications, Vol. IA-20, No.3, May/June, 1984, pp625-30.

111. Peng F. Z., Lai J. S., "Generalized instantaneous reactive power theory for three-phase power systems", IEEE Transactions on instrumentation and measurement, vol. 45, No.1, Feb. 1996, pp293-7.

112. M. Mohaddes, "A neural network controlled optimal PWM STATCOM", IEEE Trans. Power delivery, vol.14, no. 2, April 1999, pp481-8.

113. Chen Y., Mwinyiwiwa B., Wolanski Z., Boon-Teck Ooi, "Regulating and equalizing DC capacitance voltages in multilevel STATCOM", IEEE Transactions on power delivery, Vol. 12, No. 2, April 1997, pp901-7.

114. Hideaki Fujita, Shinji Tominga, Hirofumi Akagi, "Analysis and design of an advanced static var compensator using quad-series voltage-source inverters", IAS '95 conference record of the 1995 IEEE industry applications conference-CAT NO. 95CH35862, New York, 1995, vol. 3, pp2565-2572.

115. Simone Bettola, Vincenzo Piuri, "High performance fault-tolerant digital neural networks", IEEE Transactions on computers, Vol.47, No. 3, March 1998, pp357-63.

116. J. Hertz, A. Krogh, "Introduction to the theory of neural computation", Wesley publication Co., 1991.

117. Y. Y. Hsu, C. C. Yang, "Design of artificial neural networks for short term load forecasting (Part II)", Proc. IEE-C, Vol. 138, 1991, pp414-8.

118. D. J. Sobajic, Y. H. Pao, "artificial neural net based dynamic security assessment for electric power ssytems", IEEE Transactions on PWRS, Vol. 4, 1989, pp220-8.

119. N. I. Santoso, O. T. Tan, "Neural net based real time control of capacitors installed on distribution systems", IEEE Transactions on PWRD, Vol. 5, 1990, pp266-72.

120. E. H. P. Chan, "Application of neural network computing in intelligent alarm processing", Proc. 1989 IEEE-PICA Conference, Seatle, USA, 1989, pp246-51.

121. K. Bhattacharya, S. Chakravorti, P. K. Mukherjee, "Insulator contour optimisation by a neural network", IEEE Transactions on dielectrics and electrical insulation, Vol. 8, No. 2, April 2001, pp157-61.

122. Y. Sun, Z. Yang, Z. Wang, Q. Lu, "Voltage stability improvement using ASVG nonlinear control", Automation of electric power system, Vol. 20, No. 6, June 1996 (in Chinese).

123. S. Chen, Y. Sun, Q. Lu, "Predicting fuzzy control and applications to ASVG", Automation of electric power system, Vol. 21, No. 10, Oct., 1997, pp4-8 (in Chinese).

124. L. O. Mak, Y. X. Ni, C. M. Shen, "STATCOM with fuzzy controller for interconnected power systems", Electric power Systems Research, Vol. 55, 2000, pp87-95.

125. M. Sun, A. Stam, R. E. Steuer, "Interactive multiple objective programming using Tchebycheff programs and artificial neural networks", Computers & Operations Research, Vol. 27, 2000, pp601-20.

BIBLIOGRAPHY

1. G.F. Page, J.B. Gomm and D. Williams, " Application of neural networks to modelling and control ", London, Chapman & Hall, 1993.
2. Carling, Alison, " Introducing neural networks ", Wilmslow, Sigma, 1992.
3. Gallant, Stephen I., " Neural network learning and expert systems ", Cambridge, Mass., MIT Press, c1993.
4. Simpson, Patrick K., " Artificial neural systems, foundations, paradigms, applications and implementations ", Neural networks, research and application, New York, Oxford, Pergamon, 1990.
5. Swingler, Kevin, " Applying neural networks, a practical guide (Accompanying software available at Loans Counter)", London, Academic Press, c1996.
6. Judd, J. Stephen, " Neural network design and the complexity of learning", Cambridge, Mass., MIT Press, 1990.
7. Chester, Michael, " Neural networks, a tutorial, ", Englewood Cliffs, N.J., London, PTR Prentice Hall, c1993.
8. B.M.Weedy, B.J.Cory, "Electric Power Syatems", John Wiley&Sons Ltd, England, 4th edition, Chap. 5, 1998.
9. Butterworths, "Power Transformer Handbook", Butterworth & Co. (Publishers) Ltd, 1st English edition, Chap. 2, 1987.
10. Charlesa. Gross, "Power System Analysis", 2nd edition 1986.
11. W. Thomas Miller, III, Richard S. Sutton and Paul J. Werbos, " Neural networks for control ", Cambridge, Mass, London, MIT Press, c1990.
12. Cichocki, A. " Neural networks for optimzation and signal processing ", Chichester, Wiley, 1993.
13. Peretto, Pierre, " An introduction to the modeling of neural networks ", Cambridge, Cambridge University Press, 1992.
14. Picton, Phil, " Introduction to neural networks ", Basingstoke, Macmillan, 1994.
15. Patrick K. Simpson (editor), " Neural networks theory, technology, and applications ", IEEE technology update series, New York, IEEE, 1995.
16. Roland.E.Thomas, Albert.J.Rosa, "the Analysis and Design of Linear Circuits", Prentice-Hall Inc., USA, 2nd edition, Chap. 3, 1998.
17. Alianna J. Maren, Craig T. Harston, Robert M. Pap., "Handbook of neural computing applications", San Diego, Academic Press, 1990.

18. Harold Cohen, "Mathematics for Scientists & Engineers", Prentice-Hall International Inc., pp400-9, 1992.
19. B.M.Weedy, B.J.Cory; "Electric Power System", John Wiley & Sons Ltd., pp186-7 and pp266-7, 4th Edition, 1998.
20. Noel M.Morris, "Mastering Mathematics for Electrical and Electronic Engineering", The MALMILLAN PRESS LTD., pp213-26, 1994.
21. Allan D. Kraus, "Circuit Analysis", West Publishing Company, pp429-57, 1991.
22. Harold Cohen, "Mathematics for Scientists & Engineers", Prentice-Hall International Inc., pp433-68, 1992.
23. Wasserman, Philip D, "Advanced methods in neural computing", New York, Van Nostrand Reinhold, 1993.
24. R. Beale and T. Jackson, "Neural computing, an introduction", Bristol, Hilger/Institute of Physics, 1990.
25. Igor Aleksander and Helen Morton, "An introduction to neural computing", 2nd ed., London, International Thomson Computer Press, 1995.
26. Tarassenko, Lionel, "A guide to neural computing applications", Arnold, 1998.
27. Pratap, Rudra, "Getting started with MATLAB 5, a quick introduction for scientists and engineers", New York, Oxford University Press, 1999.
28. Higham, D. J., Desmond J., "MATLAB guide", Philadelphia, Society for Industrial and Applied Mathematics, 2000.
29. The Math Works Inc, "MATLAB, high-performance numeric computation and visualization software for UNIX workstations [Version 4.0]", Natick, Mass., The MathWorks, Inc., 1993.
30. The Math Works Inc, "The Student edition of MATLAB for MS-DOS personal computers", Englewood Cliffs, NJ, London, Prentice Hall, 1992.
31. Derek. A. Paice, "Power Electronic Converter Harmonics", the Institute of Electrical and Electronics Engineers Inc., New York, USA, chap.1, 1996.
32. E. Lakervi and E. J. Holmes, "Electricity distribution network design", 2nd ed. Peter Peregrinus Ltd., chap. 12, 1995.
33. David Finney, " Variable frequency AC motor drive systems", Peter Peregrinus Ltd., chap.9, 1988.
34. Ministry of Electric Power Industry of China, "Harmonics and Unbalanced-load caused by the railway traction and their effects to the power system", Beijing China, 1992.
35. Borse, Garold J., " Numerical methods using MATLAB ", P.W.S.-Kent Publishing Co.,U.S., Feb 96: Internat.Thomson Pub.Services.

36. Hanselman, Duane C., " The student edition of MATLAB, version 5, user's guide, [Windows version] ", Upper Saddle River, Prentice Hall, 1997.
37. A. J. Chipperfield and P. J. Fleming, " MATLAB toolboxes and applications for control ", Peter Peregrinus on behalf of The Institution of Electrical Engineers, c1993.
38. King, Joe, " MATLAB for engineers "; Menlo Park, Calif., Harlow, Addison-Wesley, 1998.
39. John Little and Loren Shure, " Signal processing toolbox for use with MATLAB, user's guide ", [new ed.], Natick, Mass., Math Works, 1992.
40. Eva P art-Enander...[et al.], " The MATLAB handbook ", Harlow, Addison-Wesley, 1996.
41. Hahn, Brian D., " Essential MATLAB for scientists and engineers ", London, Arnold, 1997.
42. Shahian, Bahram, " Control system design using Matlab ", Englewood Cliffs, N.J., Prentice Hall, 1993.
43. Duane Hanselman, Bruce Littlefield, " Mastering MATLAB 5, a comprehensive tutorial and reference ", Upper Saddle River, Prentice Hall, 1998.
44. Duane Hanselman and Bruce Littlefield, " The student edition of MATLAB, version 5, user's guide", Upper Saddle River, Prentice Hall, 1997.
45. Adrian Biran, Moshe Breiner, " MATLAB 5 for engineers ", 2nd ed., Harlow, Addison-Wesley Pub. Co., c1999.
46. Darren Redfern, Colin Campbell, " The MATLAB 5 handbook ", Berlin, Springer Verlag, 1998.
47. The MathWorks, " MATLAB, high-performance numeric computation and visualization software [Version 4.0] ", Natick, Mass., The MathWorks, Inc., 1992.
48. Marcus, Marvin, " Matrices and MATLAB, a tutorial ", Englewood Cliffs, New Jersey, Prentice Hall, c1993.
49. John Penny, George Lindfield, " Numerical methods using Matlab ", Upper Saddle River, N.J., Prentice Hall, London, Prentice-Hall International, c2000.
50. Van Loan, Charles F., " Introduction to scientific computing, a matrix-vector approach using MATLAB ", Upper Saddle River, N.J., Prentice Hall, c1997.
51. Friedland, Bernard, "Advanced control system design", Englewood Cliffs, Prentice Hall, 1996.
52. C.J. Chesmond, P.A. Wilson and M.R. le Pla, "Advanced control system technology", London, Edward Arnold, 1991.
53. Csaki, Frigyes, "Modern control theories, nonlinear, optimal and adaptive systems", Budapest, Akedemiai Kiado, 1970.

54. Walter J. Grantham and Thomas L. Vincent, "Modern control systems analysis and design", Wiley, 1993.
55. Bishop, Robert H., "Modern control systems analysis and design using MATLAB", Reading, Mass., Addsison-Wesley, c1993.
56. John J. D'Azzo, Constantine H. Houpis, "Linear control system analysis and design, conventional and modern", 4th ed., London, McGraw-Hill, 1995.
57. Richard C. Dorf, Robert H. Bishop, "Modern control systems", 9th ed., Upper Saddle River, Prentice Hall, c2001.
58. Shinners, Stanley M, "Modern control system theory and design", New York, J. Wiley, c1992.
59. Ogata, Katsuhiko, "Modern control engineering", 2nd ed., Englewood Cliffs, N.J., Prentice Hall, 1990.
60. Hoft, Richard G., "Semiconductor power electronics", New York, Wokingham, Van Nostrand Reinhold, c1986.
61. Lander, Cyril W., "Power electronics", 2nd ed., London, McGraw-Hill, c1987.
62. Williams, B. W., Barry W., "Power electronics, devices, drivers, applications and passive components", 2nd ed., Basingstoke, Macmillan, 1992.
63. Rashid Muhammad H, "Power electronics, circuits, devices, and applications", 2nd ed., Prentice-Hall International, c1993.
64. Derek A. Paice, "Power electronic converter harmonics, multipulse methods for clean power", Piscataway, NJ, IEEE Press, c1996.
65. Weedy, B. M., Birron Mathew, "Electric power systems", 4th ed., New York, Chichester, Wiley, 1998.
66. Bernard Hochart, "Power transformer handbook (edited by Bernard Hochart, first English edition translated from the French by C.E. Davison)", London, Butterworths, 1987.
67. B. M. Bird, K. G. King, D. A. G. Pedder, "An introduction to power electronics", 2nd ed., Chichester, Wiley, 1993.
68. James W. Nilsson, Susan A. Riedel, "Electric circuits", 6th ed., Upper Saddle River NJ, Prentice Hall, 2000.
69. Yorke, R., "Electric circuit theory", Applied electricity and electronics, 2nd ed., Oxford, Pergamon, 1986.
70. David E. Johnson, Johnny R. Johnson, John L. Hilburn, "Electric circuit analysis", Englewood Cliffs, N.J., Prentice Hall, c1989.
71. Sander, K. F., Kenneth Frederick, "Electric circuit analysis, principles and applications", Wokingham, Addison-Wesley, 1992.

72. G.R. Slemon, A. Straughen, "Electric machines", Reading, Mass., London, Addison-Wesley, 1980.

Content of Appendix

1. Z. Zhang, N. R. Fahmi, "Historical Review of the Power System Earthing Methods in China and Ferro-resonance Analysis", CIRED 2003, May 12-15, 2003, Barcelona (Accepted).
2. Z. Zhang, N. R. Fahmi, "Electric Arc Furnace (EAF) Features and its Compensation by Cascaded Multi-level SVG", CIRED 2003, May 12-15, 2003, Barcelona (Accepted).
3. Z. Zhang, N. R. Fahmi, "Modeling and Analysis of A Cascade Multilevel Inverters-based SVG with New Control Strategies for EAF Application", IEE Proceedings-C (Accepted).
4. Z. Zhang, N. R. Fahmi, W. T. Norris, "Flicker analysis and methods for EAF flicker mitigation", Conference IEEE Porto Power Tech'2001, Porto, Portugal, paper-276 (PST1-276 in the program), Sep. 10-13th, 2001.
5. Z. Zhang, N. R. Fahmi, "A sensitivity-matrix for assessing voltage regulation result", UPEC 2001, Swansea, Wales, paper-448 (2A-8 in the program), 12-14 Sep. 2001(accepted).
6. Z. Zhang, N. R. Fahmi, "A recurrent neural networks (RNN)-based control SVG for electric arc furnaces", UPEC 2001, Swansea, Wales, paper-450 (3D-4 in the program), 12-14 Sep. 2001(accepted).
7. Z. Zhang, N. R. Fahmi, Q. M. Zhu, "Special loads analysis" UPEC 2000, Belfast, Northern Ireland, 6-8 Sep. 2000, pp92 at Book of Abstracts.
8. Z. Zhang, N. R. Fahmi, "Reactive power optimal distribution" UPEC 2000, Belfast, Northern Ireland, 6-8 Sep. 2000, pp129 at Book of Abstracts.

Appendixes I EAF & its Typical Power Levels During a Furnace Heat

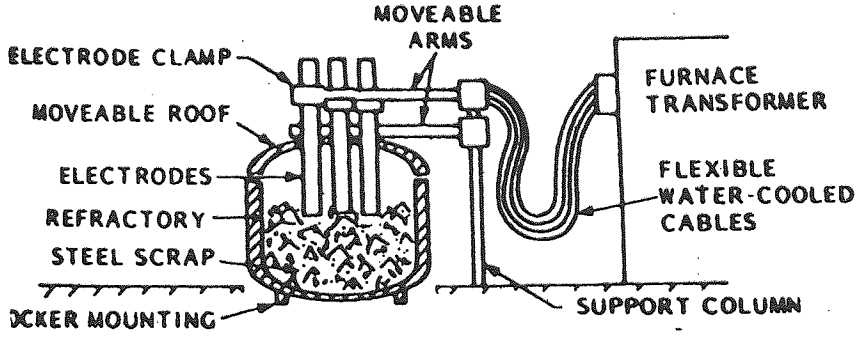

App. I-Fig.-1, Electric Arc Furnace

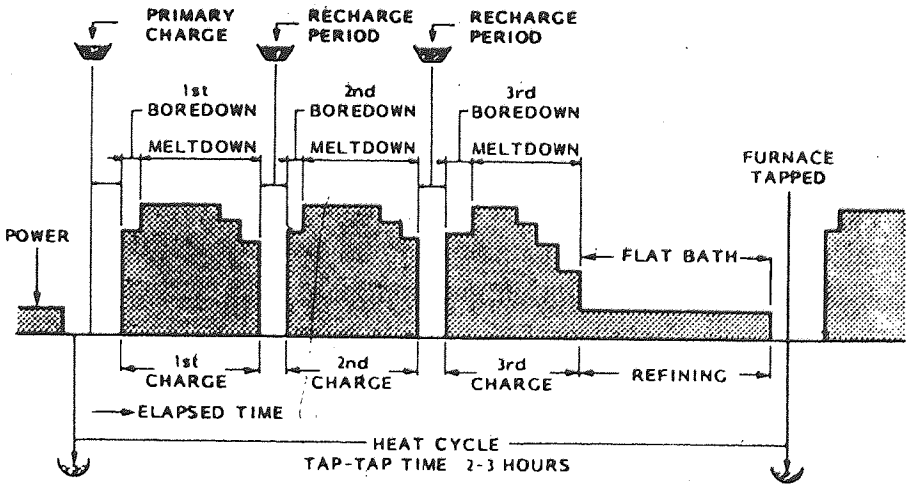

App. I-Fig.-2, Typical Power Levels During a Furnace Heat

Appendixes I Real Measurement of an EAF Voltage/Var Fluctuations and Negative-sequence Current

(Remarks: the EAF is made by ASEA, 1971, 100t, 50.64MVA)

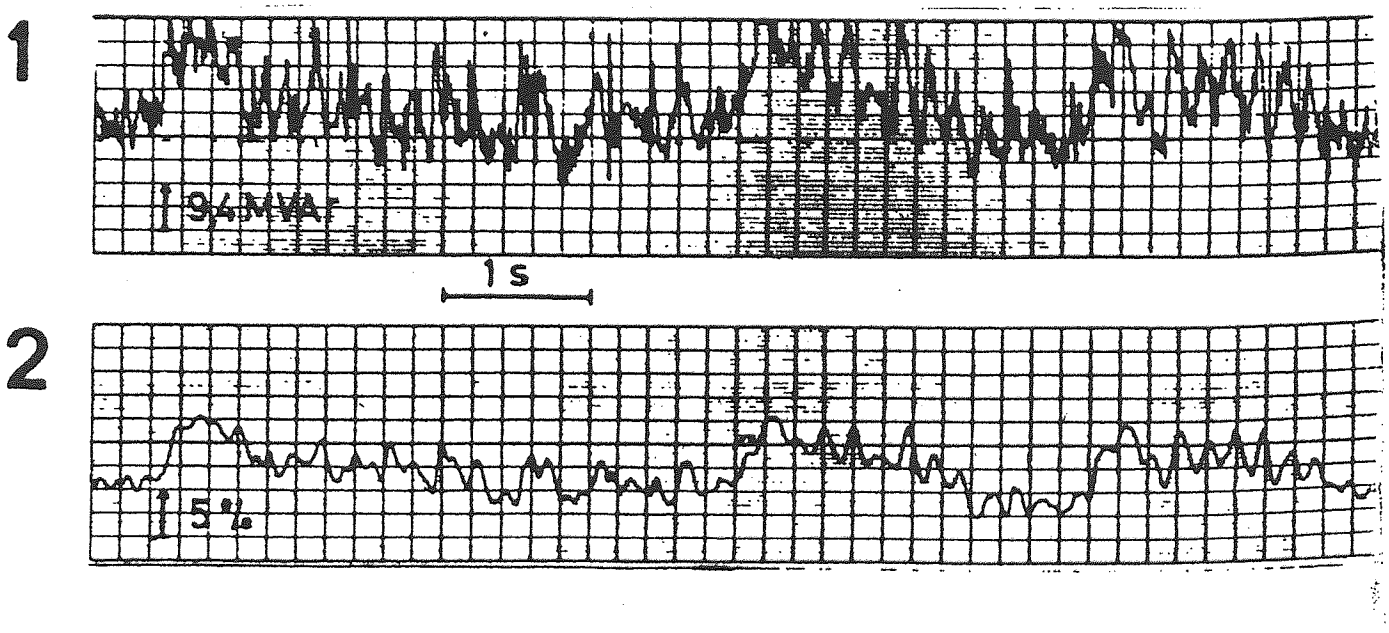

App. I-Fig.-3, Reactive power fluctuations (1) and voltage fluctuations (2) during arc furnace melt-down

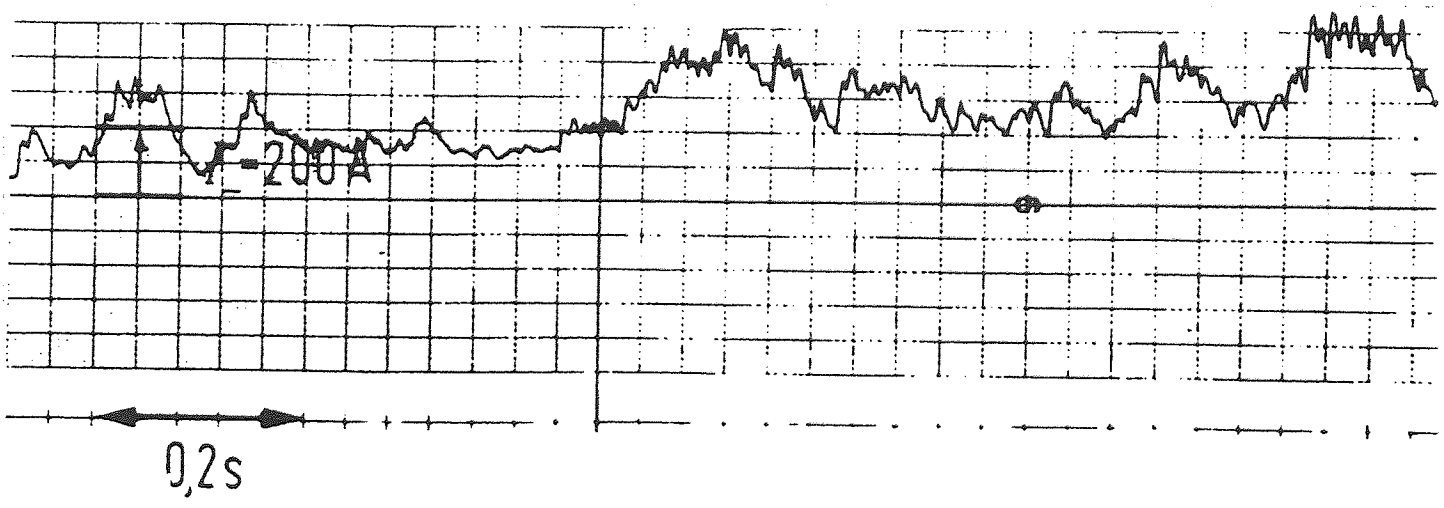

App. I-Fig.- 4, EAF negative-sequence current

Appendixes I Real Measurement of an EAF Reactive Power Loading in 3-phase During operation

(Remarks: the EAF is made by ASEA, 1971, 100t, 50.64MVA)

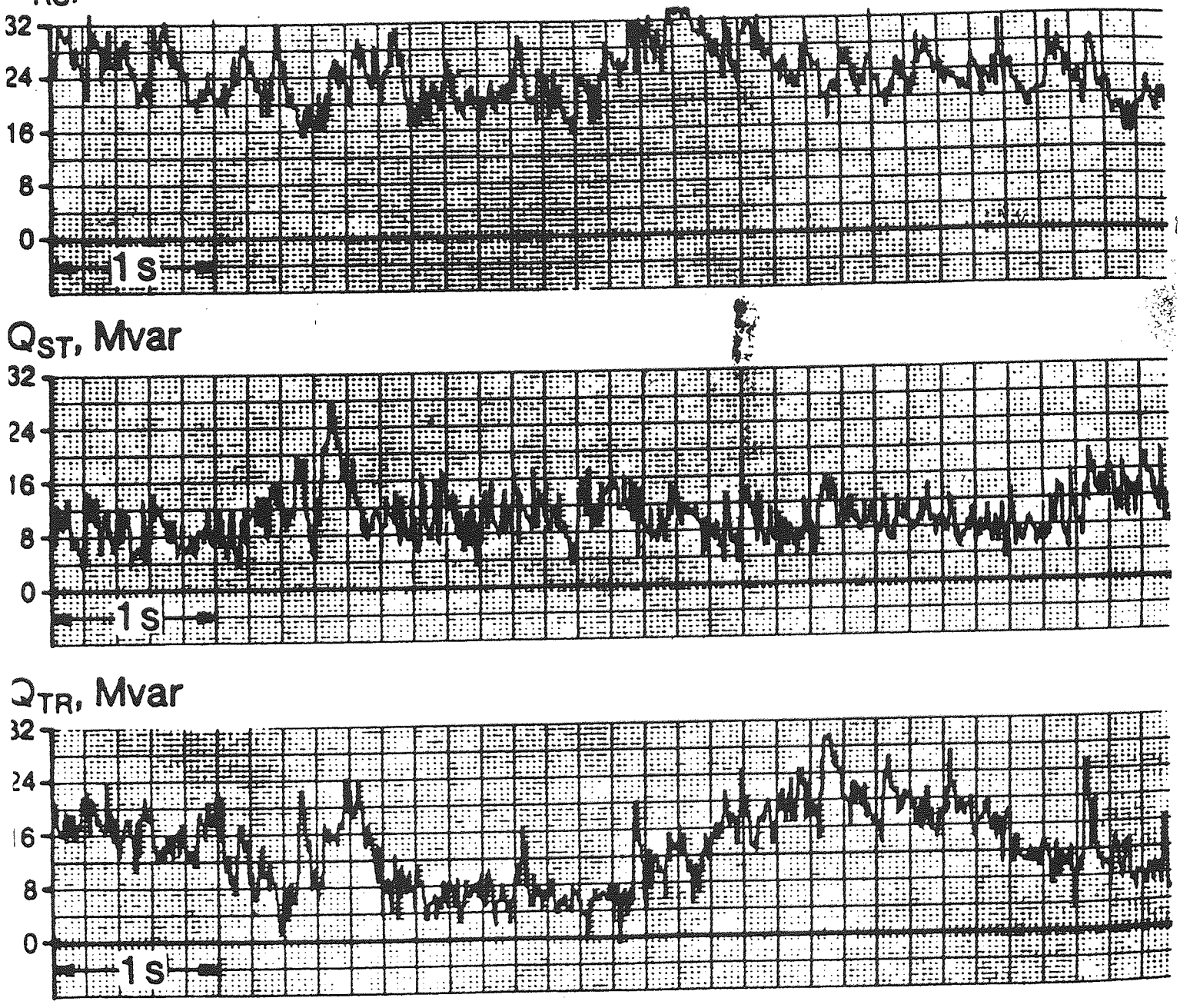

App. I-Fig.-5, Reactive power loading in the three phases during the arc furnace operation.

Appendixes I Static Var Compensator Capacity, Response-time and Flicker Mitigation; Comparison of Reduction Flicker with ASVG and SVC

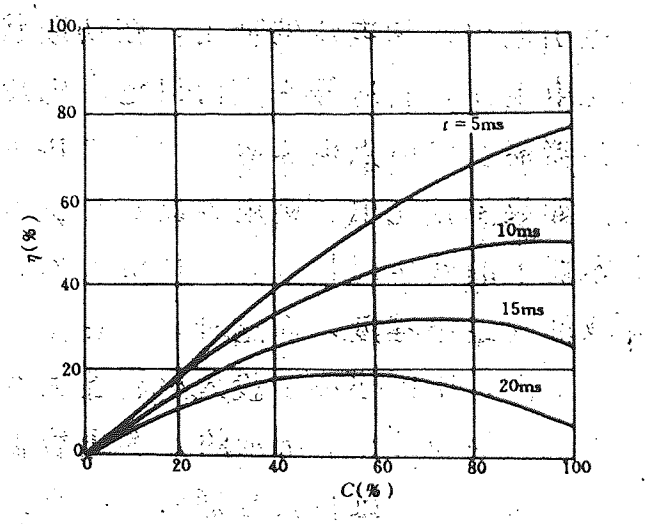

App. I-Fig.-6, Thyristor Controlled Reactor SVC capacity & response-time and flicker mitigation

Where: η is the flicker mitigation ratio, $\eta = \frac{P_{st}(before\_compensation) - P_{st}(after\_)}{P_{st}(before\_compensation)} 100\%$

C is the compensating ratio, $C = \frac{Q_C(SVC - capacity)}{\Delta Q_{max}(EAF - \max - \text{var} - fluctuation)} 100\%$

App. I-Fig.-7, Comparison of reduction flicker with ASVG and SVC
(Wang Yue, Liu Jinping, Li Xiangrong, "Research on reducing flicker caused by arc furnace with advanced static var generator", Power Systam Technology, Beijing, China, Sept. 1998, Vol. 22 No. 9 pp 61-64)

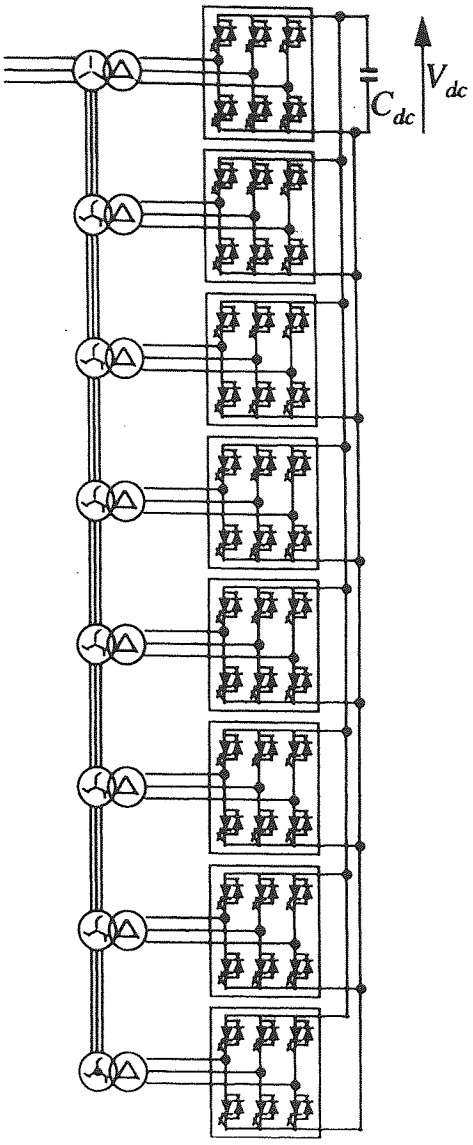

App. II-Fig.-1, Structure of the conventional 48-pulse inverter.

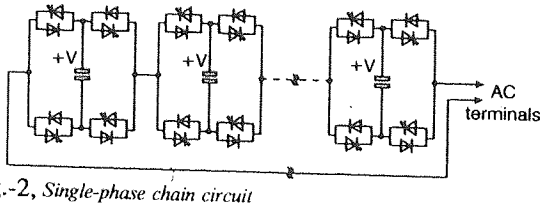

App. II-Fig.-2, *Single-phase chain circuit*

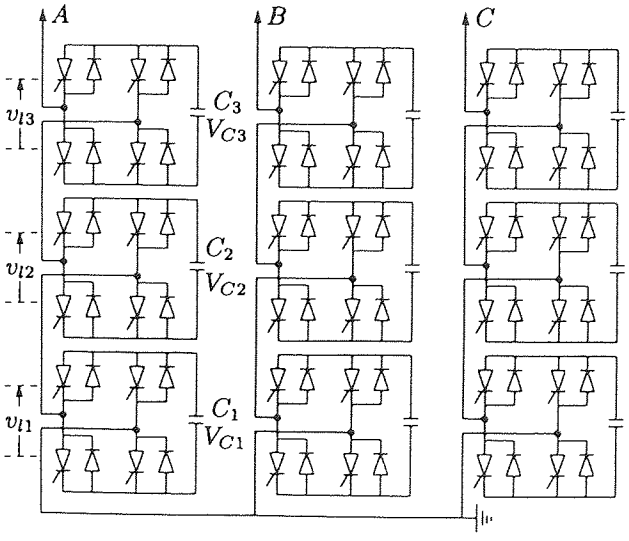

App. II-Fig.-3, Three-phase star connected 3-level binary VSI

App. II-Fig.- 4, illustrates the ac voltage output of each level which is also a conduction period of each capacitor (v_{l1}, v_{l2}, v_{l3}), the resulting ac phase voltage (v_{av}) and the fundamental output voltage (v_a) of the 3-level inverter shown

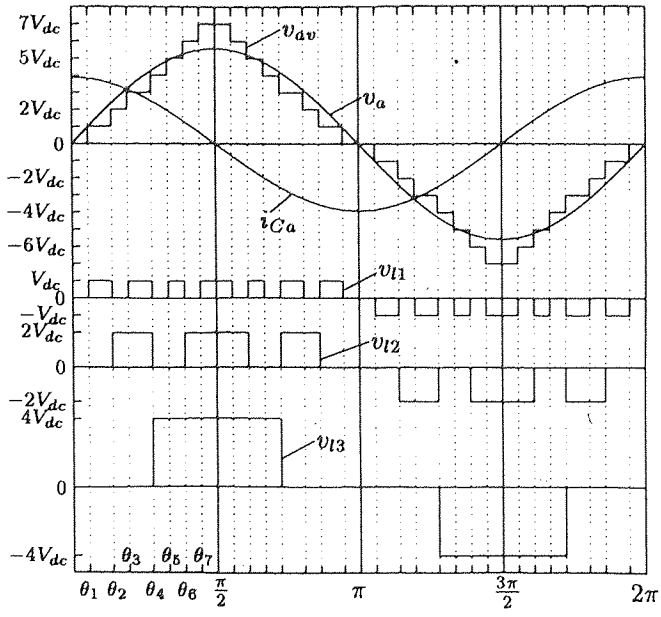

App. II-Fig.- 4, Typical voltages of 3-level binary VSI

Appendices III, The SVG harmonic voltages (errors) after SHEM, according to the trained MI-THETA

(5^{TH}, 7^{TH}, 11^{TH} , 13^{TH} AND 15^{TH} HARMONICS AS FOLLWINGS)

The first line from left to right: THETA1, THETA2, THETA3, THETA4, THETA5 AND MI

The second line from left to right: $\sum_{i=1}^{5}\cos 5\theta_i$, $\sum_{i=1}^{5}\cos 7\theta_i$, $\sum_{i=1}^{5}\cos 11\theta_i$, $\sum_{i=1}^{5}\cos 13\theta_i$, $\sum_{i=1}^{5}\cos 15\theta_i$

FOR EXAMPLE:

θ_1	θ_2	θ_3	θ_4	θ_5	MI
0.6234	0.8166	1.0056	1.2106	1.4500	0.5010
0.0527	-0.0144	-0.0216		0.0197	-0.0706

$\sum_{i=1}^{5}\cos 5\theta_i$, $\sum_{i=1}^{5}\cos 7\theta_i$, $\sum_{i=1}^{5}\cos 11\theta_i$, $\sum_{i=1}^{5}\cos 13\theta_i$, $\sum_{i=1}^{5}\cos 15\theta_i$

0.6234	0.8166	1.0056	1.2106	1.4500	0.5010
0.0527	-0.0144	-0.0216	0.0197	-0.0706	0.5010
0.6232	0.8152	1.0043	1.2096	1.4482	0.5020
0.0516	-0.0147	-0.0220	0.0192	-0.0704	0.5020
0.6230	0.8139	1.0029	1.2086	1.4464	0.5030
0.0504	-0.0150	-0.0223	0.0187	-0.0702	0.5030
0.6228	0.8125	1.0015	1.2075	1.4446	0.5040
0.0492	-0.0153	-0.0226	0.0182	-0.0700	0.5040
0.6226	0.8112	1.0001	1.2064	1.4428	0.5050
0.0480	-0.0156	-0.0228	0.0177	-0.0697	0.5050
0.6224	0.8098	0.9988	1.2054	1.4410	0.5060
0.0468	-0.0159	-0.0230	0.0171	-0.0694	0.5060

0.6222	0.8085	0.9974	1.2044	1.4392	0.5070
0.0456	-0.0162	-0.0232	0.0164	-0.0691	0.5070
0.6220	0.8071	0.9960	1.2033	1.4374	0.5080
0.0444	-0.0165	-0.0233	0.0157	-0.0688	0.5080
0.6218	0.8058	0.9947	1.2022	1.4356	0.5090
0.0432	-0.0168	-0.0234	0.0150	-0.0684	0.5090
0.6216	0.8044	0.9933	1.2012	1.4338	0.5100
0.0419	-0.0171	-0.0234	0.0142	-0.0680	0.5100
0.6214	0.8031	0.9919	1.2002	1.4320	0.5110
0.0407	-0.0174	-0.0234	0.0134	-0.0675	0.5110
0.6216	0.8035	0.9917	1.1999	1.4322	0.5110
0.0405	-0.0165	-0.0238	0.0138	-0.0675	0.5110
0.6214	0.8022	0.9903	1.1989	1.4305	0.5120
0.0392	-0.0167	-0.0238	0.0130	-0.0670	0.5120
0.6212	0.8009	0.9889	1.1978	1.4288	0.5130
0.0379	-0.0169	-0.0237	0.0122	-0.0665	0.5130
0.6210	0.7996	0.9875	1.1967	1.4270	0.5140
0.0366	-0.0171	-0.0236	0.0113	-0.0660	0.5140
0.6208	0.7982	0.9862	1.1957	1.4253	0.5149
0.0352	-0.0173	-0.0235	0.0105	-0.0654	0.5149
0.6206	0.7969	0.9848	1.1946	1.4235	0.5159
0.0339	-0.0175	-0.0233	0.0095	-0.0649	0.5159

0.6204 0.7956 0.9834 1.1935 1.4218 0.5169
0.0325 -0.0178 -0.0231 0.0086 -0.0643 0.5169

0.6202 0.7943 0.9820 1.1924 1.4200 0.5179
0.0311 -0.0180 -0.0228 0.0076 -0.0637 0.5179

0.6200 0.7930 0.9806 1.1914 1.4183 0.5189
0.0297 -0.0181 -0.0225 0.0066 -0.0631 0.5189

0.6198 0.7917 0.9792 1.1903 1.4165 0.5199
0.0283 -0.0183 -0.0222 0.0055 -0.0624 0.5199

0.6196 0.7904 0.9778 1.1892 1.4148 0.5209
0.0269 -0.0185 -0.0218 0.0045 -0.0617 0.5209

0.6194 0.7890 0.9765 1.1882 1.4131 0.5218
0.0255 -0.0188 -0.0213 0.0033 -0.0611 0.5218

0.6192 0.7878 0.9751 1.1872 1.4113 0.5228
0.0242 -0.0190 -0.0209 0.0022 -0.0603 0.5228

0.6190 0.7866 0.9737 1.1862 1.4096 0.5237
0.0228 -0.0192 -0.0205 0.0010 -0.0595 0.5237

0.6188 0.7853 0.9723 1.1852 1.4078 0.5247
0.0214 -0.0194 -0.0200 -0.0001 -0.0587 0.5247

0.6186 0.7841 0.9710 1.1842 1.4061 0.5257
0.0200 -0.0196 -0.0195 -0.0014 -0.0578 0.5257

0.6184 0.7828 0.9696 1.1832 1.4043 0.5266
0.0186 -0.0198 -0.0189 -0.0026 -0.0569 0.5266

0.6182 0.7816 0.9682 1.1822 1.4026 0.5276
0.0172 -0.0200 -0.0183 -0.0039 -0.0560 0.5276

0.6180 0.7803 0.9668 1.1812 1.4008 0.5285
0.0157 -0.0202 -0.0177 -0.0052 -0.0551 0.5285

0.6178 0.7791 0.9654 1.1802 1.3991 0.5295
0.0143 -0.0204 -0.0170 -0.0065 -0.0541 0.5295

0.6176 0.7778 0.9640 1.1792 1.3973 0.5305
0.0128 -0.0206 -0.0163 -0.0079 -0.0532 0.5305

0.6174 0.7766 0.9626 1.1782 1.3956 0.5314
0.0113 -0.0208 -0.0155 -0.0093 -0.0522 0.5314

0.6172 0.7753 0.9612 1.1772 1.3937 0.5324
0.0099 -0.0209 -0.0147 -0.0108 -0.0511 0.5324

0.6171 0.7740 0.9597 1.1762 1.3919 0.5334
0.0083 -0.0211 -0.0139 -0.0124 -0.0501 0.5334

0.6170 0.7727 0.9583 1.1752 1.3901 0.5343
0.0068 -0.0212 -0.0130 -0.0140 -0.0491 0.5343

0.6168 0.7714 0.9569 1.1742 1.3883 0.5353
0.0052 -0.0214 -0.0121 -0.0156 -0.0480 0.5353

0.6166 0.7701 0.9554 1.1732 1.3865 0.5363
0.0036 -0.0215 -0.0111 -0.0173 -0.0470 0.5363

0.6165 0.7688 0.9540 1.1722 1.3847 0.5372
0.0020 -0.0217 -0.0101 -0.0189 -0.0459 0.5372

0.6164 0.7675 0.9526 1.1712 1.3829 0.5382
0.0004 -0.0218 -0.0090 -0.0206 -0.0449 0.5382

0.6162 0.7662 0.9512 1.1702 1.3811 0.5392
-0.0012 -0.0220 -0.0079 -0.0223 -0.0438 0.5392

0.6161 0.7649 0.9497 1.1692 1.3793 0.5401
-0.0028 -0.0221 -0.0068 -0.0241 -0.0428 0.5401

0.6159 0.7636 0.9483 1.1682 1.3775 0.5411
-0.0044 -0.0222 -0.0056 -0.0259 -0.0417 0.5411

0.6158 0.7623 0.9469 1.1672 1.3757 0.5421
-0.0061 -0.0223 -0.0044 -0.0276 -0.0406 0.5421

0.6154 0.7600 0.9469 1.1648 1.3757 0.5429
-0.0085 -0.0223 -0.0016 -0.0270 -0.0450 0.5429

0.6149 0.7577 0.9469 1.1624 1.3757 0.5437
-0.0109 -0.0224 0.0012 -0.0263 -0.0494 0.5437

0.6145 0.7553 0.9469 1.1600 1.3757 0.5445
-0.0134 -0.0225 0.0041 -0.0254 -0.0539 0.5445

0.6140 0.7529 0.9469 1.1576 1.3757 0.5453
-0.0159 -0.0226 0.0068 -0.0244 -0.0585 0.5453

0.6136 0.7506 0.9469 1.1553 1.3757 0.5461
-0.0184 -0.0227 0.0096 -0.0233 -0.0630 0.5461

0.6131 0.7482 0.9469 1.1529 1.3757 0.5469
-0.0209 -0.0228 0.0123 -0.0220 -0.0676 0.5469

0.6127	0.7458	0.9469	1.1505	1.3757	0.5478
-0.0234	-0.0229	0.0149	-0.0206	-0.0722	0.5478
0.6122	0.7434	0.9469	1.1481	1.3757	0.5486
-0.0259	-0.0231	0.0175	-0.0191	-0.0769	0.5486
0.6118	0.7411	0.9469	1.1457	1.3757	0.5494
-0.0283	-0.0232	0.0201	-0.0175	-0.0815	0.5494
0.6113	0.7387	0.9469	1.1433	1.3757	0.5502
-0.0308	-0.0234	0.0226	-0.0157	-0.0861	0.5502
0.6109	0.7363	0.9469	1.1409	1.3757	0.5510
-0.0333	-0.0236	0.0251	-0.0138	-0.0907	0.5510
0.6108	0.7364	0.9460	1.1391	1.3757	0.5515
-0.0352	-0.0215	0.0243	-0.0126	-0.0915	0.5515
0.6108	0.7364	0.9451	1.1373	1.3757	0.5519
-0.0371	-0.0194	0.0234	-0.0115	-0.0923	0.5519
0.6108	0.7364	0.9442	1.1355	1.3757	0.5524
-0.0390	-0.0173	0.0226	-0.0103	-0.0932	0.5524
0.6108	0.7364	0.9433	1.1337	1.3757	0.5529
-0.0409	-0.0152	0.0217	-0.0091	-0.0940	0.5529
0.6108	0.7364	0.9424	1.1320	1.3757	0.5533
-0.0429	-0.0132	0.0207	-0.0079	-0.0948	0.5533
0.6108	0.7364	0.9414	1.1302	1.3757	0.5538
-0.0449	-0.0111	0.0198	-0.0066	-0.0956	0.5538

0.6108 0.7364 0.9405 1.1284 1.3757 0.5543
-0.0468 -0.0091 0.0188 -0.0054 -0.0964 0.5543

0.6108 0.7364 0.9396 1.1266 1.3757 0.5548
-0.0488 -0.0070 0.0178 -0.0042 -0.0971 0.5548

0.6108 0.7364 0.9387 1.1248 1.3757 0.5552
-0.0508 -0.0049 0.0167 -0.0029 -0.0979 0.5552

0.6108 0.7364 0.9378 1.1230 1.3757 0.5557
-0.0528 -0.0029 0.0157 -0.0016 -0.0986 0.5557

0.6108 0.7364 0.9369 1.1212 1.3757 0.5562
-0.0549 -0.0009 0.0146 -0.0004 -0.0993 0.5562

0.6076 0.7363 0.9355 1.1211 1.3749 0.5569
-0.0556 -0.0035 0.0153 0.0017 -0.0965 0.5569

0.6044 0.7362 0.9343 1.1210 1.3741 0.5577
-0.0561 -0.0062 0.0161 0.0038 -0.0937 0.5577

0.6013 0.7361 0.9331 1.1209 1.3734 0.5584
-0.0566 -0.0088 0.0168 0.0059 -0.0908 0.5584

0.5981 0.7360 0.9319 1.1208 1.3726 0.5592
-0.0570 -0.0115 0.0175 0.0080 -0.0877 0.5592

0.5949 0.7358 0.9307 1.1207 1.3718 0.5599
-0.0574 -0.0141 0.0180 0.0101 -0.0845 0.5599

0.5917 0.7357 0.9296 1.1206 1.3710 0.5606
-0.0577 -0.0166 0.0184 0.0121 -0.0811 0.5606

0.5885	0.7356	0.9284	1.1205	1.3702	0.5613
-0.0580	-0.0191	0.0188	0.0141	-0.0777	0.5613
0.5854	0.7355	0.9272	1.1204	1.3695	0.5621
-0.0583	-0.0216	0.0190	0.0160	-0.0741	0.5621
0.5822	0.7354	0.9260	1.1203	1.3687	0.5628
-0.0584	-0.0241	0.0192	0.0179	-0.0704	0.5628
0.5790	0.7353	0.9248	1.1202	1.3679	0.5635
-0.0586	-0.0265	0.0193	0.0197	-0.0666	0.5635
0.5758	0.7352	0.9236	1.1201	1.3671	0.5643
-0.0587	-0.0289	0.0193	0.0214	-0.0627	0.5643
0.5726	0.7352	0.9222	1.1186	1.3638	0.5657
-0.0585	-0.0301	0.0201	0.0221	-0.0570	0.5657
0.5693	0.7352	0.9206	1.1171	1.3605	0.5673
-0.0584	-0.0311	0.0209	0.0226	-0.0510	0.5673
0.5661	0.7352	0.9190	1.1156	1.3573	0.5688
-0.0584	-0.0321	0.0216	0.0230	-0.0450	0.5688
0.5628	0.7352	0.9175	1.1141	1.3540	0.5703
-0.0583	-0.0330	0.0223	0.0232	-0.0389	0.5703
0.5595	0.7352	0.9159	1.1126	1.3507	0.5718
-0.0582	-0.0338	0.0230	0.0234	-0.0327	0.5718
0.5562	0.7351	0.9144	1.1111	1.3474	0.5733
-0.0582	-0.0344	0.0236	0.0233	-0.0265	0.5733

0.5529	0.7351	0.9128	1.1096	1.3441	0.5748
-0.0581	-0.0350	0.0241	0.0232	-0.0202	0.5748
0.5497	0.7351	0.9113	1.1081	1.3409	0.5763
-0.0581	-0.0354	0.0246	0.0229	-0.0138	0.5763
0.5464	0.7351	0.9097	1.1066	1.3376	0.5778
-0.0580	-0.0357	0.0251	0.0226	-0.0075	0.5778
0.5431	0.7351	0.9082	1.1051	1.3343	0.5793
-0.0580	-0.0359	0.0255	0.0220	-0.0011	0.5793
0.5398	0.7351	0.9066	1.1036	1.3310	0.5808
-0.0580	-0.0360	0.0259	0.0214	0.0052	0.5808
0.5366	0.7349	0.9056	1.1027	1.3292	0.5818
-0.0577	-0.0369	0.0256	0.0218	0.0100	0.5818
0.5334	0.7348	0.9046	1.1019	1.3275	0.5828
-0.0572	-0.0377	0.0252	0.0221	0.0148	0.5828
0.5303	0.7347	0.9036	1.1010	1.3257	0.5838
-0.0568	-0.0384	0.0247	0.0224	0.0195	0.5838
0.5271	0.7346	0.9026	1.1001	1.3239	0.5848
-0.0563	-0.0390	0.0241	0.0225	0.0243	0.5848
0.5239	0.7344	0.9016	1.0993	1.3221	0.5857
-0.0558	-0.0395	0.0234	0.0225	0.0291	0.5857
0.5207	0.7343	0.9007	1.0984	1.3204	0.5867
-0.0553	-0.0400	0.0227	0.0224	0.0338	0.5867

0.5175	0.7342	0.8997	1.0975	1.3186	0.5877
-0.0547	-0.0404	0.0219	0.0221	0.0385	0.5877
0.5144	0.7341	0.8987	1.0966	1.3168	0.5887
-0.0542	-0.0407	0.0209	0.0218	0.0431	0.5887
0.5112	0.7340	0.8977	1.0958	1.3151	0.5897
-0.0536	-0.0410	0.0200	0.0213	0.0477	0.5897
0.5080	0.7339	0.8967	1.0949	1.3133	0.5907
-0.0529	-0.0411	0.0189	0.0207	0.0523	0.5907
0.5048	0.7338	0.8957	1.0940	1.3115	0.5916
-0.0523	-0.0412	0.0178	0.0200	0.0567	0.5916
0.5015	0.7335	0.8947	1.0931	1.3097	0.5927
-0.0516	-0.0414	0.0167	0.0191	0.0611	0.5927
0.4983	0.7334	0.8937	1.0923	1.3080	0.5936
-0.0509	-0.0413	0.0154	0.0182	0.0654	0.5936
0.4952	0.7333	0.8927	1.0914	1.3062	0.5946
-0.0502	-0.0412	0.0141	0.0171	0.0696	0.5946
0.4920	0.7332	0.8917	1.0905	1.3044	0.5956
-0.0494	-0.0409	0.0127	0.0159	0.0737	0.5956
0.4888	0.7330	0.8907	1.0897	1.3026	0.5965
-0.0487	-0.0406	0.0112	0.0145	0.0778	0.5965
0.4856	0.7329	0.8898	1.0888	1.3009	0.5975
-0.0479	-0.0402	0.0097	0.0130	0.0817	0.5975

0.4824	0.7328	0.8888	1.0879	1.2991	0.5984
-0.0470	-0.0398	0.0081	0.0114	0.0854	0.5984
0.4793	0.7327	0.8878	1.0870	1.2973	0.5994
-0.0462	-0.0392	0.0064	0.0097	0.0891	0.5994
0.4761	0.7326	0.8868	1.0862	1.2956	0.6004
-0.0453	-0.0386	0.0048	0.0079	0.0926	0.6004
0.4729	0.7325	0.8858	1.0853	1.2938	0.6013
-0.0444	-0.0378	0.0030	0.0059	0.0960	0.6013
0.4697	0.7324	0.8848	1.0844	1.2920	0.6023
-0.0435	-0.0370	0.0012	0.0039	0.0992	0.6023
0.4665	0.7323	0.8838	1.0836	1.2903	0.6032
-0.0426	-0.0361	-0.0006	0.0017	0.1023	0.6032
0.4634	0.7322	0.8828	1.0827	1.2885	0.6042
-0.0417	-0.0352	-0.0024	-0.0006	0.1053	0.6042
0.4602	0.7321	0.8818	1.0818	1.2867	0.6051
-0.0407	-0.0341	-0.0043	-0.0031	0.1080	0.6051
0.4570	0.7319	0.8808	1.0810	1.2849	0.6060
-0.0397	-0.0330	-0.0063	-0.0056	0.1106	0.6060
0.4538	0.7318	0.8799	1.0801	1.2832	0.6070
-0.0387	-0.0318	-0.0082	-0.0082	0.1131	0.6070
0.4506	0.7317	0.8789	1.0792	1.2814	0.6079
-0.0377	-0.0305	-0.0102	-0.0110	0.1153	0.6079

0.4475	0.7316	0.8779	1.0783	1.2796	0.6089
-0.0367	-0.0291	-0.0123	-0.0138	0.1174	0.6089
0.4443	0.7315	0.8769	1.0775	1.2779	0.6098
-0.0357	-0.0276	-0.0143	-0.0168	0.1193	0.6098
0.4411	0.7314	0.8759	1.0766	1.2761	0.6107
-0.0346	-0.0261	-0.0163	-0.0198	0.1210	0.6107
0.4379	0.7313	0.8749	1.0757	1.2743	0.6116
-0.0335	-0.0245	-0.0184	-0.0229	0.1225	0.6116
0.4373	0.7302	0.8748	1.0728	1.2728	0.6126
-0.0358	-0.0220	-0.0185	-0.0217	0.1208	0.6126
0.4366	0.7291	0.8748	1.0700	1.2713	0.6137
-0.0380	-0.0194	-0.0185	-0.0205	0.1193	0.6137
0.4360	0.7281	0.8748	1.0671	1.2697	0.6147
-0.0402	-0.0169	-0.0187	-0.0194	0.1179	0.6147
0.4353	0.7270	0.8747	1.0642	1.2681	0.6157
-0.0425	-0.0144	-0.0189	-0.0182	0.1165	0.6157
0.4346	0.7259	0.8746	1.0614	1.2665	0.6167
-0.0447	-0.0119	-0.0192	-0.0170	0.1152	0.6167
0.4339	0.7248	0.8746	1.0585	1.2650	0.6177
-0.0470	-0.0094	-0.0195	-0.0159	0.1140	0.6177
0.4332	0.7237	0.8746	1.0556	1.2634	0.6187
-0.0494	-0.0069	-0.0200	-0.0147	0.1128	0.6187

0.4326	0.7227	0.8745	1.0527	1.2618	0.6197
-0.0517	-0.0044	-0.0204	-0.0136	0.1118	0.6197
0.4319	0.7216	0.8744	1.0499	1.2603	0.6207
-0.0541	-0.0020	-0.0209	-0.0124	0.1108	0.6207
0.4312	0.7205	0.8744	1.0470	1.2587	0.6217
-0.0566	0.0005	-0.0215	-0.0113	0.1099	0.6217
0.4305	0.7194	0.8744	1.0441	1.2571	0.6227
-0.0590	0.0029	-0.0221	-0.0102	0.1091	0.6227
0.4118	0.6926	0.8743	1.0428	1.2566	0.6281
-0.0543	-0.0182	-0.0148	-0.0164	0.0853	0.6281
0.4096	0.6903	0.8743	1.0416	1.2561	0.6289
-0.0542	-0.0185	-0.0153	-0.0165	0.0833	0.6289
0.4075	0.6880	0.8743	1.0403	1.2555	0.6297
-0.0541	-0.0188	-0.0158	-0.0165	0.0812	0.6297
0.4053	0.6857	0.8743	1.0390	1.2549	0.6305
-0.0539	-0.0190	-0.0163	-0.0166	0.0792	0.6305
0.4031	0.6833	0.8743	1.0377	1.2544	0.6312
-0.0537	-0.0193	-0.0168	-0.0166	0.0771	0.6312
0.4009	0.6810	0.8742	1.0365	1.2538	0.6320
-0.0535	-0.0195	-0.0174	-0.0166	0.0751	0.6320
0.3987	0.6787	0.8742	1.0352	1.2532	0.6328
-0.0533	-0.0197	-0.0179	-0.0166	0.0731	0.6328

0.3966	0.6764	0.8742	1.0339	1.2526	0.6336
-0.0530	-0.0198	-0.0185	-0.0165	0.0710	0.6336
0.3944	0.6741	0.8742	1.0327	1.2521	0.6344
-0.0527	-0.0200	-0.0191	-0.0165	0.0690	0.6344
0.3922	0.6718	0.8742	1.0314	1.2515	0.6352
-0.0524	-0.0201	-0.0197	-0.0164	0.0670	0.6352
0.3900	0.6695	0.8742	1.0301	1.2509	0.6360
-0.0520	-0.0202	-0.0203	-0.0163	0.0651	0.6360
0.3888	0.6673	0.8732	1.0297	1.2504	0.6366
-0.0526	-0.0214	-0.0196	-0.0169	0.0639	0.6366
0.3876	0.6650	0.8722	1.0294	1.2499	0.6373
-0.0533	-0.0228	-0.0187	-0.0174	0.0626	0.6373
0.3865	0.6627	0.8712	1.0290	1.2493	0.6380
-0.0539	-0.0241	-0.0177	-0.0178	0.0615	0.6380
0.3853	0.6604	0.8702	1.0286	1.2487	0.6387
-0.0545	-0.0254	-0.0168	-0.0182	0.0603	0.6387
0.3841	0.6580	0.8692	1.0283	1.2482	0.6394
-0.0550	-0.0268	-0.0159	-0.0186	0.0592	0.6394
0.3829	0.6557	0.8681	1.0279	1.2476	0.6401
-0.0555	-0.0281	-0.0151	-0.0189	0.0581	0.6401
0.3817	0.6534	0.8671	1.0275	1.2470	0.6408
-0.0560	-0.0294	-0.0142	-0.0192	0.0571	0.6408

0.3806	0.6511	0.8661	1.0271	1.2464	0.6415
-0.0565	-0.0307	-0.0134	-0.0195	0.0561	0.6415
0.3794	0.6488	0.8651	1.0268	1.2459	0.6422
-0.0569	-0.0320	-0.0126	-0.0197	0.0551	0.6422
0.3782	0.6465	0.8641	1.0264	1.2453	0.6429
-0.0574	-0.0333	-0.0118	-0.0199	0.0542	0.6429
0.3770	0.6442	0.8631	1.0260	1.2447	0.6436
-0.0577	-0.0346	-0.0110	-0.0200	0.0533	0.6436
0.3747	0.6417	0.8626	1.0247	1.2432	0.6446
-0.0575	-0.0340	-0.0111	-0.0204	0.0517	0.6446
0.3725	0.6392	0.8621	1.0234	1.2417	0.6457
-0.0574	-0.0334	-0.0111	-0.0205	0.0502	0.6457
0.3704	0.6367	0.8616	1.0220	1.2401	0.6468
-0.0573	-0.0327	-0.0112	-0.0206	0.0488	0.6468
0.3682	0.6342	0.8611	1.0206	1.2385	0.6478
-0.0571	-0.0320	-0.0113	-0.0207	0.0473	0.6478
0.3660	0.6316	0.8606	1.0192	1.2369	0.6489
-0.0570	-0.0312	-0.0114	-0.0208	0.0459	0.6489
0.3638	0.6291	0.8600	1.0179	1.2354	0.6500
-0.0568	-0.0304	-0.0116	-0.0208	0.0445	0.6500
0.3616	0.6266	0.8595	1.0165	1.2338	0.6510
-0.0566	-0.0296	-0.0118	-0.0208	0.0431	0.6510

0.3595 0.6241 0.8590 1.0151 1.2322 0.6521
-0.0563 -0.0287 -0.0120 -0.0207 0.0418 0.6521

0.3573 0.6216 0.8585 1.0138 1.2307 0.6531
-0.0561 -0.0278 -0.0123 -0.0206 0.0405 0.6531

0.3551 0.6191 0.8580 1.0124 1.2291 0.6542
-0.0558 -0.0268 -0.0126 -0.0205 0.0393 0.6542

0.3529 0.6166 0.8575 1.0110 1.2275 0.6552
-0.0555 -0.0258 -0.0129 -0.0204 0.0381 0.6552

0.3506 0.6140 0.8570 1.0096 1.2259 0.6563
-0.0551 -0.0247 -0.0133 -0.0202 0.0368 0.6563

0.3484 0.6115 0.8565 1.0083 1.2244 0.6573
-0.0548 -0.0236 -0.0138 -0.0200 0.0357 0.6573

0.3463 0.6090 0.8560 1.0069 1.2228 0.6584
-0.0544 -0.0224 -0.0142 -0.0197 0.0346 0.6584

0.3441 0.6065 0.8555 1.0055 1.2212 0.6594
-0.0540 -0.0213 -0.0147 -0.0195 0.0336 0.6594

0.3419 0.6040 0.8550 1.0041 1.2196 0.6605
-0.0536 -0.0200 -0.0153 -0.0192 0.0326 0.6605

0.3397 0.6014 0.8544 1.0028 1.2181 0.6615
-0.0532 -0.0187 -0.0159 -0.0188 0.0316 0.6615

0.3375 0.5989 0.8539 1.0014 1.2165 0.6625
-0.0528 -0.0174 -0.0165 -0.0185 0.0307 0.6625

0.3354	0.5964	0.8534	1.0000	1.2149	0.6635
-0.0523	-0.0160	-0.0171	-0.0181	0.0299	0.6635
0.3332	0.5939	0.8529	0.9987	1.2134	0.6646
-0.0518	-0.0146	-0.0178	-0.0177	0.0291	0.6646
0.3310	0.5914	0.8524	0.9973	1.2118	0.6656
-0.0514	-0.0132	-0.0186	-0.0173	0.0283	0.6656
0.3288	0.5889	0.8519	0.9959	1.2102	0.6666
-0.0508	-0.0117	-0.0193	-0.0169	0.0276	0.6666
0.3277	0.5863	0.8503	0.9956	1.2096	0.6674
-0.0511	-0.0128	-0.0191	-0.0168	0.0282	0.6674
0.3265	0.5838	0.8488	0.9953	1.2091	0.6681
-0.0512	-0.0138	-0.0192	-0.0168	0.0287	0.6681
0.3254	0.5813	0.8473	0.9949	1.2085	0.6689
-0.0513	-0.0147	-0.0192	-0.0168	0.0292	0.6689
0.3242	0.5788	0.8458	0.9945	1.2079	0.6696
-0.0513	-0.0156	-0.0193	-0.0169	0.0298	0.6696
0.3230	0.5762	0.8442	0.9942	1.2074	0.6704
-0.0514	-0.0165	-0.0194	-0.0169	0.0304	0.6704
0.3218	0.5737	0.8427	0.9938	1.2068	0.6711
-0.0514	-0.0174	-0.0195	-0.0170	0.0311	0.6711
0.3206	0.5712	0.8412	0.9934	1.2062	0.6718
-0.0513	-0.0183	-0.0197	-0.0171	0.0317	0.6718

0.3195	0.5687	0.8397	0.9930	1.2056	0.6726
-0.0512	-0.0191	-0.0199	-0.0172	0.0324	0.6726
0.3183	0.5662	0.8382	0.9927	1.2051	0.6733
-0.0511	-0.0199	-0.0201	-0.0173	0.0331	0.6733
0.3171	0.5637	0.8367	0.9923	1.2045	0.6741
-0.0510	-0.0207	-0.0204	-0.0174	0.0339	0.6741
0.3159	0.5612	0.8352	0.9919	1.2039	0.6748
-0.0508	-0.0215	-0.0207	-0.0176	0.0346	0.6748
0.3148	0.5599	0.8337	0.9915	1.2023	0.6756
-0.0513	-0.0206	-0.0202	-0.0186	0.0337	0.6756
0.3136	0.5574	0.8322	0.9912	1.2008	0.6765
-0.0514	-0.0205	-0.0200	-0.0188	0.0337	0.6765
0.3125	0.5549	0.8307	0.9908	1.1992	0.6774
-0.0514	-0.0203	-0.0198	-0.0189	0.0337	0.6774
0.3113	0.5524	0.8292	0.9904	1.1976	0.6783
-0.0514	-0.0202	-0.0196	-0.0190	0.0336	0.6783
0.3101	0.5498	0.8276	0.9901	1.1960	0.6792
-0.0513	-0.0200	-0.0195	-0.0191	0.0336	0.6792
0.3089	0.5473	0.8261	0.9897	1.1945	0.6801
-0.0513	-0.0197	-0.0194	-0.0192	0.0336	0.6801
0.3077	0.5448	0.8246	0.9893	1.1929	0.6811
-0.0512	-0.0195	-0.0194	-0.0193	0.0335	0.6811

0.3066	0.5423	0.8231	0.9889	1.1913	0.6820
-0.0511	-0.0192	-0.0195	-0.0195	0.0334	0.6820
0.3054	0.5398	0.8216	0.9886	1.1898	0.6829
-0.0510	-0.0188	-0.0196	-0.0196	0.0333	0.6829
0.3042	0.5373	0.8201	0.9882	1.1882	0.6838
-0.0508	-0.0185	-0.0197	-0.0197	0.0331	0.6838
0.3030	0.5348	0.8186	0.9878	1.1866	0.6847
-0.0507	-0.0181	-0.0199	-0.0199	0.0329	0.6847
0.3020	0.5322	0.8170	0.9874	1.1845	0.6857
-0.0509	-0.0174	-0.0199	-0.0198	0.0325	0.6857
0.3008	0.5297	0.8155	0.9871	1.1825	0.6867
-0.0509	-0.0164	-0.0200	-0.0198	0.0318	0.6867
0.2997	0.5272	0.8140	0.9867	1.1804	0.6877
-0.0508	-0.0155	-0.0202	-0.0198	0.0311	0.6877
0.2985	0.5247	0.8125	0.9863	1.1783	0.6886
-0.0508	-0.0145	-0.0204	-0.0198	0.0303	0.6886
0.2973	0.5221	0.8109	0.9860	1.1762	0.6896
-0.0507	-0.0134	-0.0207	-0.0198	0.0295	0.6896
0.2961	0.5196	0.8094	0.9856	1.1742	0.6906
-0.0506	-0.0123	-0.0210	-0.0198	0.0286	0.6906
0.2949	0.5171	0.8079	0.9852	1.1721	0.6916
-0.0505	-0.0112	-0.0214	-0.0198	0.0276	0.6916

0.2938	0.5146	0.8064	0.9848	1.1700	0.6926
-0.0504	-0.0100	-0.0219	-0.0198	0.0266	0.6926
0.2926	0.5121	0.8049	0.9845	1.1680	0.6935
-0.0503	-0.0088	-0.0225	-0.0198	0.0256	0.6935
0.2914	0.5096	0.8034	0.9841	1.1659	0.6945
-0.0501	-0.0075	-0.0231	-0.0198	0.0245	0.6945
0.2902	0.5071	0.8019	0.9837	1.1638	0.6955
-0.0500	-0.0062	-0.0238	-0.0198	0.0233	0.6955
0.2655	0.4900	0.7839	0.9809	1.1345	0.7069
-0.0463	0.0291	-0.0229	-0.0206	-0.0197	0.7069
0.2649	0.4895	0.7824	0.9799	1.1335	0.7075
-0.0481	0.0301	-0.0232	-0.0207	-0.0209	0.7075
0.2644	0.4890	0.7809	0.9788	1.1324	0.7082
-0.0499	0.0311	-0.0235	-0.0208	-0.0222	0.7082
0.2638	0.4885	0.7794	0.9777	1.1313	0.7088
-0.0518	0.0320	-0.0238	-0.0209	-0.0234	0.7088
0.2632	0.4879	0.7778	0.9766	1.1303	0.7095
-0.0536	0.0330	-0.0241	-0.0209	-0.0246	0.7095
0.2626	0.4874	0.7763	0.9756	1.1292	0.7102
-0.0554	0.0339	-0.0244	-0.0210	-0.0259	0.7102
0.2620	0.4869	0.7748	0.9745	1.1281	0.7108
-0.0572	0.0348	-0.0247	-0.0210	-0.0271	0.7108

0.2615 0.4864 0.7733 0.9734 1.1270 0.7115
-0.0590 0.0357 -0.0249 -0.0210 -0.0284 0.7115

0.2609 0.4859 0.7718 0.9724 1.1260 0.7121
-0.0609 0.0366 -0.0252 -0.0210 -0.0296 0.7121

0.2603 0.4854 0.7703 0.9713 1.1249 0.7128
-0.0627 0.0374 -0.0255 -0.0209 -0.0309 0.7128

0.2597 0.4849 0.7688 0.9702 1.1238 0.7135
-0.0645 0.0383 -0.0257 -0.0209 -0.0322 0.7135

0.2590 0.4864 0.7725 0.9755 1.1291 0.7110
-0.0539 0.0342 -0.0213 -0.0241 -0.0306 0.7110

0.2554 0.4853 0.7687 0.9755 1.1291 0.7118
-0.0523 0.0346 -0.0181 -0.0268 -0.0352 0.7118

0.2519 0.4842 0.7649 0.9754 1.1290 0.7127
-0.0508 0.0349 -0.0146 -0.0293 -0.0399 0.7127

0.2483 0.4832 0.7611 0.9753 1.1290 0.7135
-0.0491 0.0352 -0.0109 -0.0314 -0.0445 0.7135

0.2447 0.4822 0.7573 0.9752 1.1289 0.7143
-0.0475 0.0354 -0.0070 -0.0333 -0.0490 0.7143

0.2411 0.4811 0.7534 0.9752 1.1289 0.7151
-0.0458 0.0356 -0.0029 -0.0348 -0.0535 0.7151

0.2375 0.4800 0.7496 0.9751 1.1288 0.7159
-0.0440 0.0358 0.0014 -0.0359 -0.0578 0.7159

0.2340	0.4790	0.7458	0.9750	1.1288	0.7167
-0.0423	0.0359	0.0059	-0.0368	-0.0621	0.7167
0.2304	0.4780	0.7420	0.9750	1.1287	0.7175
-0.0404	0.0360	0.0105	-0.0373	-0.0662	0.7175
0.2268	0.4769	0.7382	0.9749	1.1287	0.7183
-0.0386	0.0360	0.0153	-0.0374	-0.0702	0.7183
0.2232	0.4759	0.7344	0.9748	1.1286	0.7191
-0.0367	0.0360	0.0202	-0.0373	-0.0740	0.7191
0.2200	0.4710	0.7240	0.9691	1.1110	0.7252
-0.0522	0.0492	0.0184	-0.0212	-0.0918	0.7252
0.2198	0.4685	0.7212	0.9689	1.1100	0.7260
-0.0525	0.0476	0.0185	-0.0205	-0.0936	0.7260
0.2197	0.4660	0.7184	0.9686	1.1089	0.7269
-0.0528	0.0460	0.0186	-0.0197	-0.0953	0.7269
0.2195	0.4636	0.7156	0.9683	1.1078	0.7277
-0.0531	0.0444	0.0186	-0.0189	-0.0971	0.7277
0.2193	0.4611	0.7128	0.9680	1.1068	0.7285
-0.0533	0.0429	0.0186	-0.0181	-0.0989	0.7285
0.2191	0.4587	0.7099	0.9678	1.1057	0.7294
-0.0534	0.0413	0.0186	-0.0172	-0.1008	0.7294
0.2189	0.4562	0.7071	0.9675	1.1046	0.7302
-0.0535	0.0398	0.0185	-0.0163	-0.1027	0.7302

0.2188	0.4538	0.7043	0.9672	1.1035	0.7310
-0.0536	0.0384	0.0184	-0.0154	-0.1046	0.7310
0.2186	0.4513	0.7015	0.9670	1.1025	0.7318
-0.0536	0.0369	0.0182	-0.0145	-0.1065	0.7318
0.2184	0.4489	0.6987	0.9667	1.1014	0.7326
-0.0535	0.0355	0.0180	-0.0135	-0.1084	0.7326
0.2182	0.4464	0.6959	0.9664	1.1003	0.7335
-0.0534	0.0341	0.0178	-0.0125	-0.1103	0.7335
0.2180	0.4440	0.6931	0.9662	1.0993	0.7343
-0.0532	0.0328	0.0175	-0.0115	-0.1123	0.7343
0.2179	0.4415	0.6903	0.9659	1.0982	0.7351
-0.0530	0.0314	0.0172	-0.0104	-0.1142	0.7351
0.2177	0.4391	0.6875	0.9656	1.0971	0.7359
-0.0527	0.0301	0.0168	-0.0093	-0.1162	0.7359
0.2175	0.4366	0.6847	0.9654	1.0961	0.7367
-0.0524	0.0289	0.0164	-0.0082	-0.1181	0.7367
0.2173	0.4342	0.6818	0.9651	1.0950	0.7375
-0.0520	0.0277	0.0160	-0.0071	-0.1200	0.7375
0.2171	0.4317	0.6790	0.9648	1.0939	0.7383
-0.0516	0.0265	0.0155	-0.0059	-0.1220	0.7383
0.2170	0.4293	0.6762	0.9645	1.0928	0.7391
-0.0511	0.0253	0.0149	-0.0047	-0.1239	0.7391

0.2168	0.4268	0.6734	0.9643	1.0918	0.7399
-0.0506	0.0242	0.0144	-0.0035	-0.1258	0.7399
0.2166	0.4244	0.6706	0.9640	1.0907	0.7407
-0.0501	0.0232	0.0137	-0.0023	-0.1277	0.7407
0.2164	0.4219	0.6678	0.9637	1.0896	0.7415
-0.0494	0.0221	0.0130	-0.0010	-0.1295	0.7415
0.2163	0.4204	0.6665	0.9634	1.0885	0.7420
-0.0494	0.0224	0.0119	-0.0001	-0.1306	0.7420
0.2162	0.4190	0.6652	0.9632	1.0875	0.7425
-0.0494	0.0227	0.0108	0.0008	-0.1316	0.7425
0.2162	0.4176	0.6639	0.9629	1.0864	0.7431
-0.0494	0.0229	0.0096	0.0018	-0.1327	0.7431
0.2161	0.4161	0.6626	0.9626	1.0853	0.7436
-0.0494	0.0231	0.0085	0.0027	-0.1337	0.7436
0.2160	0.4146	0.6612	0.9624	1.0843	0.7441
-0.0493	0.0234	0.0073	0.0036	-0.1347	0.7441
0.2159	0.4132	0.6599	0.9621	1.0832	0.7446
-0.0493	0.0237	0.0061	0.0045	-0.1357	0.7446
0.2158	0.4117	0.6586	0.9618	1.0821	0.7451
-0.0492	0.0240	0.0050	0.0054	-0.1368	0.7451
0.2158	0.4103	0.6573	0.9615	1.0810	0.7456
-0.0491	0.0243	0.0037	0.0063	-0.1378	0.7456

0.2157	0.4088	0.6560	0.9613	1.0800	0.7461
-0.0491	0.0246	0.0025	0.0072	-0.1388	0.7461
0.2156	0.4074	0.6547	0.9610	1.0789	0.7466
-0.0490	0.0249	0.0013	0.0081	-0.1398	0.7466
0.2155	0.4059	0.6534	0.9607	1.0778	0.7472
-0.0489	0.0252	0.0000	0.0090	-0.1408	0.7472
0.2154	0.4045	0.6521	0.9605	1.0768	0.7477
-0.0488	0.0256	-0.0013	0.0099	-0.1417	0.7477
0.2154	0.4030	0.6508	0.9602	1.0757	0.7482
-0.0486	0.0260	-0.0025	0.0108	-0.1427	0.7482
0.2153	0.4016	0.6495	0.9599	1.0746	0.7487
-0.0485	0.0263	-0.0038	0.0117	-0.1437	0.7487
0.2152	0.4001	0.6481	0.9597	1.0736	0.7492
-0.0484	0.0267	-0.0052	0.0126	-0.1446	0.7492
0.2151	0.3987	0.6468	0.9594	1.0725	0.7497
-0.0482	0.0271	-0.0065	0.0134	-0.1456	0.7497
0.2150	0.3972	0.6455	0.9591	1.0714	0.7502
-0.0481	0.0276	-0.0078	0.0143	-0.1465	0.7502
0.2150	0.3958	0.6442	0.9588	1.0703	0.7507
-0.0479	0.0280	-0.0092	0.0152	-0.1474	0.7507
0.2149	0.3943	0.6429	0.9586	1.0693	0.7512
-0.0477	0.0284	-0.0106	0.0160	-0.1483	0.7512

0.2148 0.3929 0.6416 0.9583 1.0682 0.7517
-0.0475 0.0289 -0.0119 0.0169 -0.1492 0.7517

0.2147 0.3914 0.6403 0.9580 1.0671 0.7522
-0.0474 0.0293 -0.0133 0.0178 -0.1501 0.7522

0.2145 0.3904 0.6393 0.9579 1.0668 0.7525
-0.0466 0.0293 -0.0138 0.0180 -0.1507 0.7525

0.2143 0.3893 0.6383 0.9579 1.0666 0.7528
-0.0458 0.0292 -0.0142 0.0182 -0.1513 0.7528

0.2142 0.3883 0.6373 0.9578 1.0663 0.7530
-0.0450 0.0291 -0.0147 0.0184 -0.1519 0.7530

0.2140 0.3872 0.6363 0.9577 1.0660 0.7533
-0.0442 0.0290 -0.0151 0.0187 -0.1526 0.7533

0.2138 0.3862 0.6353 0.9576 1.0658 0.7536
-0.0434 0.0290 -0.0155 0.0189 -0.1532 0.7536

0.2136 0.3851 0.6342 0.9576 1.0655 0.7538
-0.0425 0.0289 -0.0159 0.0192 -0.1538 0.7538

0.2134 0.3841 0.6332 0.9575 1.0652 0.7541
-0.0417 0.0288 -0.0163 0.0194 -0.1544 0.7541

0.2133 0.3830 0.6322 0.9574 1.0649 0.7544
-0.0409 0.0288 -0.0168 0.0197 -0.1550 0.7544

0.2131 0.3820 0.6312 0.9574 1.0647 0.7546
-0.0400 0.0288 -0.0172 0.0199 -0.1556 0.7546

0.2129	0.3809	0.6302	0.9573	1.0644	0.7549
-0.0392	0.0287	-0.0176	0.0202	-0.1562	0.7549
0.2127	0.3799	0.6292	0.9572	1.0641	0.7551
-0.0383	0.0287	-0.0181	0.0204	-0.1568	0.7551
0.2125	0.3788	0.6282	0.9572	1.0639	0.7554
-0.0375	0.0287	-0.0185	0.0207	-0.1574	0.7554
0.2124	0.3778	0.6272	0.9571	1.0636	0.7557
-0.0366	0.0287	-0.0190	0.0209	-0.1580	0.7557
0.2122	0.3767	0.6262	0.9570	1.0633	0.7559
-0.0357	0.0287	-0.0194	0.0212	-0.1586	0.7559
0.2120	0.3757	0.6252	0.9569	1.0630	0.7562
-0.0349	0.0287	-0.0199	0.0214	-0.1592	0.7562
0.2118	0.3746	0.6241	0.9569	1.0628	0.7565
-0.0340	0.0287	-0.0203	0.0217	-0.1598	0.7565
0.2116	0.3736	0.6231	0.9568	1.0625	0.7567
-0.0331	0.0287	-0.0208	0.0219	-0.1604	0.7567
0.2115	0.3725	0.6221	0.9567	1.0622	0.7570
-0.0322	0.0288	-0.0212	0.0222	-0.1610	0.7570
0.2113	0.3715	0.6211	0.9567	1.0620	0.7572
-0.0313	0.0288	-0.0217	0.0224	-0.1615	0.7572
0.2111	0.3704	0.6201	0.9566	1.0617	0.7575
-0.0304	0.0289	-0.0222	0.0227	-0.1621	0.7575

0.2109	0.3694	0.6191	0.9565	1.0614	0.7578
-0.0295	0.0289	-0.0226	0.0230	-0.1627	0.7578
0.2100	0.3677	0.6178	0.9562	1.0614	0.7581
-0.0273	0.0297	-0.0230	0.0229	-0.1634	0.7581
0.2092	0.3659	0.6165	0.9560	1.0614	0.7585
-0.0251	0.0304	-0.0233	0.0227	-0.1641	0.7585
0.2084	0.3642	0.6152	0.9557	1.0614	0.7588
-0.0229	0.0311	-0.0236	0.0226	-0.1649	0.7588
0.2075	0.3624	0.6139	0.9554	1.0614	0.7592
-0.0206	0.0318	-0.0240	0.0224	-0.1656	0.7592
0.2067	0.3607	0.6125	0.9552	1.0614	0.7595
-0.0183	0.0326	-0.0243	0.0223	-0.1664	0.7595
0.2058	0.3589	0.6112	0.9549	1.0614	0.7599
-0.0161	0.0333	-0.0246	0.0222	-0.1671	0.7599
0.2050	0.3572	0.6099	0.9546	1.0614	0.7602
-0.0138	0.0341	-0.0248	0.0221	-0.1678	0.7602
0.2041	0.3554	0.6086	0.9543	1.0614	0.7606
-0.0115	0.0350	-0.0251	0.0220	-0.1685	0.7606
0.2033	0.3537	0.6073	0.9541	1.0614	0.7609
-0.0092	0.0358	-0.0254	0.0220	-0.1692	0.7609
0.2024	0.3519	0.6060	0.9538	1.0614	0.7613
-0.0069	0.0367	-0.0256	0.0219	-0.1699	0.7613

0.2016	0.3502	0.6047	0.9535	1.0614	0.7616
-0.0046	0.0376	-0.0258	0.0219	-0.1706	0.7616
0.2004	0.3475	0.6024	0.9534	1.0624	0.7620
0.0001	0.0374	-0.0252	0.0210	-0.1717	0.7620
0.1993	0.3447	0.6001	0.9534	1.0635	0.7623
0.0049	0.0374	-0.0244	0.0203	-0.1727	0.7623
0.1981	0.3420	0.5978	0.9533	1.0645	0.7626
0.0097	0.0375	-0.0237	0.0195	-0.1737	0.7626
0.1970	0.3392	0.5955	0.9532	1.0656	0.7629
0.0145	0.0375	-0.0230	0.0188	-0.1746	0.7629
0.1958	0.3365	0.5931	0.9532	1.0666	0.7632
0.0194	0.0377	-0.0222	0.0181	-0.1755	0.7632
0.1947	0.3337	0.5908	0.9531	1.0677	0.7635
0.0243	0.0379	-0.0214	0.0174	-0.1763	0.7635
0.1935	0.3310	0.5885	0.9530	1.0687	0.7639
0.0292	0.0381	-0.0206	0.0167	-0.1770	0.7639
0.1924	0.3282	0.5862	0.9529	1.0698	0.7642
0.0341	0.0384	-0.0198	0.0161	-0.1777	0.7642
0.1912	0.3255	0.5839	0.9529	1.0708	0.7645
0.0391	0.0388	-0.0190	0.0156	-0.1782	0.7645
0.1901	0.3227	0.5816	0.9528	1.0719	0.7648
0.0440	0.0392	-0.0182	0.0151	-0.1787	0.7648

0.1889 0.3200 0.5793 0.9527 1.0729 0.7651
0.0490 0.0397 -0.0173 0.0146 -0.1792 0.7651

0.1889 0.3189 0.5778 0.9526 1.0728 0.7653
0.0503 0.0395 -0.0176 0.0153 -0.1791 0.7653

0.1888 0.3178 0.5763 0.9526 1.0728 0.7656
0.0517 0.0393 -0.0180 0.0158 -0.1790 0.7656

0.1888 0.3168 0.5748 0.9525 1.0727 0.7658
0.0531 0.0391 -0.0183 0.0164 -0.1790 0.7658

0.1887 0.3157 0.5733 0.9524 1.0727 0.7661
0.0546 0.0389 -0.0187 0.0170 -0.1789 0.7661

0.1887 0.3146 0.5718 0.9524 1.0726 0.7663
0.0560 0.0388 -0.0191 0.0176 -0.1788 0.7663

0.1886 0.3135 0.5702 0.9523 1.0726 0.7666
0.0574 0.0386 -0.0194 0.0181 -0.1787 0.7666

0.1886 0.3124 0.5687 0.9522 1.0725 0.7668
0.0589 0.0385 -0.0198 0.0187 -0.1785 0.7668

0.1885 0.3114 0.5672 0.9521 1.0725 0.7671
0.0603 0.0384 -0.0203 0.0192 -0.1783 0.7671

0.1885 0.3103 0.5657 0.9521 1.0724 0.7673
0.0618 0.0383 -0.0207 0.0198 -0.1781 0.7673

0.1884 0.3092 0.5642 0.9520 1.0724 0.7676
0.0633 0.0382 -0.0211 0.0204 -0.1779 0.7676

0.1884	0.3081	0.5627	0.9519	1.0723	0.7678
0.0648	0.0381	-0.0216	0.0209	-0.1777	0.7678

Missing page(s) from the bound copy

REFERENCES

1. Liu Sheng, Chi Yu-tien, "Automatic control of voltages and reactive power flows in power systems by means of static var compensator", Journal of Tsing Hua University, vol. 19, no. 3, 1979, pp96-111. China.
2. L. Gyugyi, "Reactive power generation and control by thyristor circuits", IEEE Transaction on Ind. Appl., vol. IA-15, pp521-532, Sep./Oct., 1979.
3. Annabelle van Zyl, "Converter-based solution to power quality problems on radial distribution lines", IEEE Transaction on Ind. Appl., vol. 32, no. 6, pp1323-30, Nov./Dec., 1996.
4. C. Schauder, "STATCOM for compensation of large electric arc furnace installations", IEEE power engineering society, 1999 summer meeting (99 CB36364), IEEE Part vol. 2, pp 1109-12, Edmonton, Alberta, Canada, 18-22 July 1999.
5. C. Schauder, A. Edris, "AEP UPFC project: installation, commissioning and operation of the +/-160 MVAR STATCOM (phase I)", IEEE Transactions on Power delivery, vol. 13, no. 4, pp1530-5, Oct. 1998.
6. L. Gyugyi, "Dynamic compensation of AC transmission lines by solid-state synchronous voltage sources", presented at the IEEE/PES Summer meetings, Vancouver, B. C., Canada, July 1993, paper 434-1.
7. R. J. Nelson, J. Bian, S. L. Williams, "Transmission series power flow control", IEEE Transactions on power delivery, vol. 10, no. 1, pp504-10, Jan. 1995.
8. B.M.Weedy, B.J.Cory, "Electric Power Syatems", John Wiley&Sons Ltd, England, 4th edition, Chap. 5, 1998.
9. Butterworths, "Power Transformer Handbook", Butterworth & Co. (Publishers) Ltd, 1st English edition, Chap. 2, 1987.
10. Charlesa. Gross, "Power System Analysis", 2nd edition 1986.
11. B. M. Weedy, "Voltage stability of radial power links", Proc. IEE, Vol. 115, pp 528-36, April 1968.
12. V. A. Venikov, et al., "Estimation of electric power system steady-state stability in load flow calculation", IEEE Transactions on power applications and systems, Vol. PAS-94, pp1034-41, May/June 1975.
13. R. A. Schlueter, "A voltage stability security assessment method", IEEE Transactions on power systems, vol. 13, no. 4, pp1423-31, Nov. 1998.

14. V. Ajjarapu, B. Lee, "Bibliography on voltage stability", IEEE Transactions on power systems, vol. 13, no. 1, pp115-25, Feb. 1998.
15. D. Thukaram, A. Lomi, "Selection of static VAR compensator location and size for system voltage stability improvement", Electric Power Systems Research, vol. 54 (2000), pp139-150, 2000.
16. Roland.E.Thomas, Albert.J.Rosa, "the Analysis and Design of Linear Circuits", Prentice-Hall Inc., USA, 2nd edition, Chap. 3, 1998.
17. Z. Zhang, "9.2 MW Synchronous Motor DOL start-up Calculation and Design", BOC Project(BOC-TISCO Gases, China) Review Meetings, Guildford, UK, 1996.
18. Harold Cohen, "Mathematics for Scientists & Engineers", Prentice-Hall International Inc., pp400-9, 1992.
19. B.M.Weedy, B.J.Cory; "Electric Power System", John Wiley & Sons Ltd., pp186-7 and pp266-7, 4th Edition, 1998.
20. Noel M.Morris, "Mastering Mathematics for Electrical and Electronic Engineering", The MALMILLAN PRESS LTD., pp213-26, 1994.
21. Allan D. Kraus, "Circuit Analysis", West Publishing Company, pp429-57, 1991.
22. Harold Cohen, "Mathematics for Scientists & Engineers", Prentice-Hall International Inc., pp433-68, 1992.
23. Specialists Research Group, "Harmonics and strategies to restrain their pollution to the power system in Beijing City Network", *Research Report from the Specialist Research Group,* Beijing, China, 1992.
24. E. O'Neill-Carrillo, G. T. Heydt, E. J. Kostelich , S. S. Venkata and A. Sundaram, " Non-linear Deterministic Modelling of Highly Varying Loads", *IEEE Trans. On Power Delivery,* pp.537-542, Vol. 14, No. 2, April 1999.
25. Z. Zhang, "Electric Characteristics of EAF Loads and the Ways to Restrain Their Pollution to Power System", *Design Review,* CERIS, Beijing, China, 1996.
26. Z. Zhang, "A graphic Method Analysing Electric Characteristics of EAF and the Optimum Work-state During Melting State", *Design Review,* CERIS, Beijing, China, 1995.
27. Zuoyi Liao, " The Arc Furnace As A Load On The Network", *Metallurgic Industry (Chinese Quaterly),* pp.27-35(Writing in Chinese), Vol. 3, 1993.
28. Shuqin Sun, "Considerations on the compensation of the reactive current and harmonics", 3rd Int. conf. On harmonics in power systems, Nashville, pp224-231, 1988.
29. Xuehai Lin, "Introductions of voltage fluctuation and flicker standard in power system", *Power Network Technology(A Chinese periodical),* Vol. 1, 1993.

30. *"Electric Design Criteria of Metallurgic Industry of China"*, Ministry of Metallurgic Industry Publishers Ltd., chap. 13, 15,1997.
31. Derek. A. Paice, "Power Electronic Converter Harmonics", the Institute of Electrical and Electronics Engineers Inc., New York, USA, chap.1, 1996.
32. E. Lakervi and E. J. Holmes, "Electricity distribution network design", 2nd ed. Peter Peregrinus Ltd., chap. 12, 1995.
33. David Finney, " Variable frequency AC motor drive systems", Peter Peregrinus Ltd., chap.9, 1988.
34. Ministry of Electric Power Industry of China, "Harmonics and Unbalanced-load caused by the railway traction and their effects to the power system", Beijing China, 1992.
35. DIXON G. F. L., KENDALL P. G., "Supply to arc furnace: measurement and prediction of supply voltage fluctuation", Proc. IEE, 1972, vol. 109, no. 4, pp. 456-65.
36. YANO I. H. M., YUYA M. T. S., "Suppression and measurement of arc furnace flicker with a large static var compensator", IEEE Trans., 1979, PAS-98, no.6, pp. 2276-83.
37. MANCHUR G., "Development of a model for predicting flicker from electric arc furnace", IEEE Trans., 1992, vol. PWRD-7, no. 1, pp. 416-26.
38. BISHOP M. T., DO A. V., "Voltage flicker measurement and analysis system"; IEEE Computer Applications in Power, April 1994, pp.34-38.
39. LAVERS J. D., BIRINGER P. P., "Real time measurement of electric arc furnace disturbances and parameter variations", IEEE Trans., vol. IA-22, no. 4, 1986, pp. 568-77.
40. SRINIVASAN. K., "Digital measurement of voltage flicker", IEEE Trans., 1991, vol. PWRD-6, no. 4, pp. 1593-98.
41. BHARGAVA B., "Arc furnace flicker measurements and control", IEEE Trans., 1993, vol. PWRD-8, no. 1, pp. 400-9.
42. MENDIS, S. R., SHOP M. T., "Investigation of transmission system voltage flicker due to multiple AC and DC furnace operations", IEEE Trans., 1995, vol. PWRD-10, no. 1, pp.483-96.
43. EI-SHARKAWI M. A., etc., "Development and field tasting of an adaptive controller for 15KV systems", IEEE Trans., 1995, vol. PWRD-10, no. 2, pp. 1025-30.
44. CHEN M. T., "Digital algorithms for measurement of voltage flicker", IEE Proc.-Gener. Transm. Distrib., vol. 144, no. 2, Mar. 1997, pp. 175-80.
45. SOLIMAN S.A., EL-HAWARY M.E., "Measurement of voltage flicker magnitude and frequency in a power system for power quality analysis", Electric Machines & Power systems, vol. 27, no. 12, Dec. 1999, pp. 1289-97.

46. KOROSEC A., VORSIC J., "Flickermeter", Elektrotehniski Vestnik, Electrotech. Soc. Slovenia, Slovenia, vol. 64, no. 1, 1997, pp. 26-31.
47. Girgis A.A., Stephens J. W., Makram E. B., "Measurement and prediction of voltage flicker magnitude and frequency", IEEE Transactions on Power Delivery, vol. 10, no. 3, pp 1600-5, July 1995.
48. Halpin S. M., Reuben F. Burch, IV, "An improved simulation approach for analysis of voltage flicker and the evaluation of mitigation strategies", IEEE Transactions on Power Delivery, vol. 12, no. 3, pp 1285-91, July 1997.
49. Y. Y. Hong, L. H. Lee, "Analysis of equivalent 10 Hz voltage flicker in power systems", IEE Proc.-Generation Transmission & Distribution, vol. 146, No. 5, Sep. 1999. Pp447-52
50. Chen-wen Lu, S. J. Huang, C. L. Huang, "Flicker characteristic estimation of an ac electric arc furnace", electric power systems research, vol. 54, pp 121-30, 2000.
51. C. J. Wu, S. S. Yen, "Investigation of 161kV arc furnace on power quality", monthly journal of Taipower's engineering, vol. 575, pp 84-96, July 1996.
52. L. Tang, D. Mueller, "Analysis of dc arc furnace operation and flicker caused by 187 Hz voltage distortion", IEEE Trans. on power delivery, vol.9, no.2, pp1098-107, April 1994.
53. Alper A., Erbil Nalcaci, "Effects of main transformer replacement on the performance of an electric arc furnace system", IEEE Transactions on industry applications, vol.36, no.2, pp649-58, March/April, 2000.
54. Albrecht wolf, Manoharan Thamodharan, "Reactive power reduction in three-phase electric arc furnace", IEEE Transactions on industrial electronics, vol.47, no.4, pp 729-33, Aug. 2000.
55. Constable R., "Tapped series reactors can help optimise arc furnace operation", Elektron, vol. 14, no. 1, pp 85-6, Elektron management partnership, South Africa, Jan., 1997.
56. Sarshar A., Sharp M., "Analysis of harmonic and transient phenomena due to operation of an arc furnace", Iron & steel engineer, vol. 73, no. 4, pp 78-82, Assoc. iron & steel Eng. USA, April, 1996.
57. Schwabe WE, Schwabe GW, "Effect of scrap conditions and charge composition on power delivery and melting in arc furnaces" Elektrowaerme International, Edition B: Industrielle Elektrowaerme, vol. 45, no. 2, pp B92-7, April, 1987, West Germany.
58. Zheng T., Elham B. Makram, "An adaptive arc furnace model", IEEE Transactions on Power Delivery, vol. 15, no. 3, pp 931-39, July 2000.

59. Montanari G. C., D. Zaninelli, "Arc furnace model for the study of flicker compensation in electrical networks", IEEE Transactions on Power Delivery, vol. 9, no. 4, pp 2026-33, Oct. 1994.

60. Le Tang, Sharma kOLLURI, "Voltage flicker prediction for two simultaneously operated ac arc furnaces", IEEE Transactions on Power Delivery, vol. 12, no. 2, pp 985-92, April, 1997.

61. E. O' Neill-Carrillo, G. T. Heydt, S. S. Venkata, "Non-linear deterministic modelling of high varying loads", IEEE Transactions on Power Delivery, vol. 14, no. 2, pp 537-42, April. 1999.

62. M. Z. El-Sadek, M. Dessouky, "A flexible ac transmission system (FACTS) for balancing arc furnace loads", Electric power systems research, vol. 41, pp 211-8, 1997.

63. A. Nabae, M. Yamaguchi, "Suppression of flicker in an arc furnace supply system by an active capacitance-a novel voltage stabiliser in power system", IEEE Transactions on industry applications, vol.31, no.1, pp107-11, Jan./Feb. 1995.

64. Peter Ashmole, " Quality of supply - voltage fluctuations (Power quality tutorial, Part 2)", POWER ENGINEERING JOURNAL, pp 108-114, April 2001.

65. F. Frank, S. Ivner, "TYCAP, power factor correction equipment using thyristor-controlled capacitor for arc furnace", ASEA Journal 46 (1973): 6, pp147-152.

66. S. Etminan, P. H. Kitchin, "Flicker meter results of simulated new and conventional TSC compensators for electric arc furnaces", IEEE Transactions on power systems, vol. 8, no. 3, pp914-19, Aug. 1993.

67. C. Schauder, M. Gernhardt, E. Stacey, "Development of a +/- 100 MVA static condenser for voltage control of transmission systems", IEEE Transactions on power delivery, vol. 10, no. 3, pp1486-96, July 1995.

68. M. D. Cox, A. Mirbod, "A new static var compensator for an arc furnace", IEEE Transactions on power systems, vol. PWRS-1, no. 3, pp110-9, Aug. 1986.

69. Y. Wang, J. Liu, X. Li, "Research on reducting flicker caused by arc furnace with advanced static var generator", Power system technology (in Chinese), vol. 22, no. 9, pp61-4, Sep., 1998.

70. Fang Zheng Peng, Jih-sheng Lai, "A transformerless high-pulse static synchronous compensator based on the 3-level GTO-inverter", IEEE Transactions on power delivery, vol. 13, no. 3, pp883-8, July 1998.

71. C. J. Hatziadoniu, F. E. Chalkiadakis, "Dynamic performance and control of a static var generator using cascade multilevel inverters", IEEE Transactions on industry applications, vol. 33, no. 3, pp748-55, May/June 1997.

72. Menzies R. W., Zhuang Y., "Advanced static compensation using a multilevel GTO thyristor inverter" IEEE Transactions on power delivery, vol. 10, No. 2, April 1995, pp732-38.
73. Peng F. Z., Lai J. S., "A multilevel voltage-source inverter with separate DC source for static var generation", IEEE Transactions on industry applications, vol. 32, No. 5, Sep./Oct. 1996, pp1130-38
74. Peng F. Z., Lai J. S., "Dynamic performance and control of a static var generator using cascade multilevel inverters", IEEE Transactions on industry applications, vol. 33, No.3, May/June 1997, pp748-55.
75. Liang Y., Nwankpa C. O., "A new type of STATCOM based on using cascading voltage source inverters with phase-shifted unipolar SPWM", IEEE Transactions on industry applications, vol. 35, No.5, Sep./Oct., 1999, pp1118-23.
76. Ainsworth J. D., Davies M., "Static var compensator (STATCOM) based on single -phase chain circuit converters", IEE Proc.-Gener. Transm. Distrib., Vol. 145, No.4, July 1998, pp381-6.
77. Patil K. V., Mathur R. M., "Distribution system compensation using a new binary multilevel voltage source inverter" IEEE transactions on power delivery, Vol.14, No.2, April, 1999, pp459-64.
78. CHEN C. M., GUAN J. L., "Attenuation analysis of voltage flicker propagation", Proceedings of 15th symposioum on Electrical power engineering, Taiwan (in Chinese), 1994, pp. 563-69.
79. STADE D., KUZNIETSOV O., "An accurate measurement of voltage flicker using a virtual measuring instrument", PCIM'99, Europe, Official proceedings of 39th international power conversion conference, ZM Commun, GMBH 1999, Nurnberg, Germany, pp. 579-84.
80. NUCCIO S., "A digital instrument for measurement of voltage flicker", IEEE Instrumentation and Measurement Technology Conference. IMTC Proceedings (Cat. No. 97CH36022), IEEE Part vol. 1, 1997, NY, USA, pp. 281-4 vol.1.
81. Fallon C.M., McDermott B.A., "Development and testing of a real-time digital voltage flicker meter", Proceedings of the 1996 IEEE Power engineering society transmission and distribution conference (Cat. No. 96CH35968), IEEE 1996, pp. 31-6, NY, USA.
82. ALCORN R.G., BEATTIE W.C., "Flicker evaluation from a wave-power station", 34th UPEC, Univ. Leicester, Part vol. 1.2, 1999, pp. 395-8 vol. 2. Leicester, UK.
83. Ladakakos P.D., Ioannides M.G., "Assessment of wind turbines impact on the power quality of autonomous weak grids", 8th International conference on harmonics and quality of power

proceedings (Cat. No. 98EX227), IEEE, Part vol. 2, 1998, pp. 900-5 vol. 2., Piscataway, NJ, USA.

84. Li Chao-Hui, Chang Wen-Yao, "Investigation and fabrication of prototype flicker and harmonic monitoring system", Monthly Journal of Taipower's Engineering, vol. 596, April 1998, pp. 45-61, Taiwan Power Co. Power Res. Inst., Taiwan.
85. GIRGIS A.A., MOSS B.D., "Reactive power compensation and voltage flicker control of an arc furnace load", Proceedings of the ICHQP, 7th International conference on harmonics and qualit IEEE Transactions on Power Delivery, vol. 10, no. 3, pp 1600-5, July 1995.
86. Z. Zhang, N. R. Fahmi, Q. M. Zhu, "Special load analysis", UPEC 2000, 35 Universities' Power Engineering Conference, 6-8 Sep. 2000, Belfast, North Ireland, pp 92 at Book of Abstracts.
87. Bogdanoff A., Leiviska K., "Intelligent methods in the electric arc furnace control", Automation in mining, mineral and metal processing 1998. Preprints of the 9th IFAC symposium. Pergamon. 1998, pp. 159-62. Oxford, UK.
88. Mendis SR, Bishop MT, Day TR, "Evaluation of supplementary series reactors to optimise EAF operations" IAS'95 Conference record of the 1995 IEEE industry applications conference (cat. No. 95CH35862). IEEE Part, vol. 2, pp 2154-61, NY, USA, 1995.
89. Robert A, Couvreur M, "Recent experience of connection of big arc furnace with reference to flicker level", Proceedings of the 35th Session international conference on large high voltage electric systems. CIGRE, Part, vol. 2, pp 36-305/1-8, Paris, France, 1995.
90. Montanari GC, Loggini M, Pitti L, "Flicker and distortion compensation in electrical plants supplying arc furnaces", IAS' 94 Conference record of the 1994 Industry applications conference, 29th IAS annual meeting (cat. No. 94 CH34520), IEEE Part, vol.3, pp 2249-55, NY, USA, 1994.
91. Montanari GC, Loggini M, Pitti, L, "The effects of series inductors for flicker reduction in electric power systems supplying arc furnaces", IAS' 93 Conference record of the 1994 Industry applications conference, 28th IAS annual meeting (cat. No. 93 CH3366-2), IEEE Part, vol.2, pp 1496-503, NY, USA, 1993.
92. C. Schauder, "STATCOM for compensation of large electric arc furnace installations", IEEE power engineering society, 1999 summer meeting (99 CB36364), IEEE Part vol. 2, pp 1109-12, Edmonton, Alberta, Canada, 18-22 July 1999.
93. Y. Yoshioka, S. Konishi, "Self-commutated static flicker compensator for arc furnace", APEC' 96. Eleventh annual applied power elctronics conference and exposition. 96CH35871, IEEE Part vol.2, pp891-7, New York, UY, USA, 1996.

94. S. B. Dewan, J. Rajda, "Application of 46 kV, 100MVA smart predictive line controller (SPLC) to ac electric arc furnace", IEEE power engineering society, 1999 winter meeting (99 CB36233), IEEE Part vol. 2, pp 1214-18, Piscataway, NJ, USA, 1999.

95. M. Zouiti, S. Saadate, "Electronic based equipment for flicker mitigation", 8th international conference on harmonics and quality of power. Proceedings (cat. No. 98EX227). IEEE Part vol. 2, pp1182-7, Piscataway, NJ, USA, 1998.

96. L. Gyugi, A. A. Otto, "Static shunt compensation for voltage flicker reduction and power factor correction", 1976 American Power Conference, pp1271-1286.

97. H. Fujita, S. Tominaga, H. Akagi, "Analysis and design of an advanced static VAr compensator using quad-series voltage source inverters", in proceedings of IEEE IAS Annual Meeting, Orlanddo, FL, pp2565-72, 1995.

98. Peng F. Z., Lai J. S., "A ststic generator using a staircase waveform multilevel voltage-source converter", Proceedings PCIM/Power quality, Sep. 1994, pp58-66.

99. Hochgraf C., et, al., "Comparison of multilevel inverter for static var compensation", in Conference Rec. IEEE/IAS annual meeting, 1994, pp921-28.

100. Engineering Recommendations P. 7/2, Fifth Chief Engineer's Conference, July 1970, of the Electricity council, CEGB, England.

101. IEC Publication 868: Flicker-meter, functional and design specification, 1986. .(6)

102. Electric Design Recommendations for Metallurgical Industry, Publishing House of Ministry of metallurgical industry, Chap. 12 (in Chinese), Beijing, China, 1997(56).

103. Peng F. Z., Lai J. S., "A ststic generator using a staircase waveform multilevel voltage-source converter", Proceedings PCIM/Power quality, Sep. 1994, pp58-66.

104. Schauder C., Mehta H., "Vector analysis and control of advanced static VAR compensators", IEE Proceedings-C, Vol. 140, No. 4, July 1993, pp299-306.

105. Shosuke Mori, "Development of a large stattic VAR generator using self-commutated inverters for improving power system stability", IEEE Transactions on power systems, Vol. 8, No. 1, Feb. 1993, pp371-7.

106. J. B. Ekanayake, N. Jenkins, "Mathematical models of a three-level advanced static VAR compensator", IEE Proc.-Gener. Transm. Distrib. Vol. 144, No. 2, Maech 1997, pp201-6.

107. Jiang Qirong, Liu Qiang, "Modelling and control of advanced static VAR generator", Journal of Tsinghua University (Sci. & Tech.), Vol. 37, No. 7, July 1997, pp21-25.

108. NAM S. CHOI, GUK C. CHO and GYU H. CHO., "Modelling and analysis of a multilevel voltage source inverter applied as a static var compensator", INT. J. ELECTRONICS, 1993, VOL. 75, NO. 5, pp1015-1034.

109. Amr M. A. Amin, "A multilevel advanced static VAR compensator with current hysterises control", ISIE, 99 IEEE international symposium on industrial electronics, July 12-16, 1999, pp837-42.

110. Akagi H., Kanazawa Y., Nabae A., "Instantaneous reactive power compensators comprising switching devices without energy storage components", IEEE transactions on industry applications, Vol. IA-20, No.3, May/June, 1984, pp625-30.

111. Peng F. Z., Lai J. S., "Generalized instantaneous reactive power theory for three-phase power systems", IEEE Transactions on instrumentation and measurement, vol. 45, No.1, Feb. 1996, pp293-7.

112. M. Mohaddes, "A neural network controlled optimal PWM STATCOM", IEEE Trans. Power delivery, vol.14, no. 2, April 1999, pp481-8.

113. Chen Y., Mwinyiwiwa B., Wolanski Z., Boon-Teck Ooi, "Regulating and equalizing DC capacitance voltages in multilevel STATCOM", IEEE Transactions on power delivery, Vol. 12, No. 2, April 1997, pp901-7.

114. Hideaki Fujita, Shinji Tominga, Hirofumi Akagi, "Analysis and design of an advanced static var compensator using quad-series voltage-source inverters", IAS '95 conference record of the 1995 IEEE industry applications conference-CAT NO. 95CH35862, New York, 1995, vol. 3, pp2565-2572.

115. Simone Bettola, Vincenzo Piuri, "High performance fault-tolerant digital neural networks", IEEE Transactions on computers, Vol.47, No. 3, March 1998, pp357-63.

116. J. Hertz, A. Krogh, "Introduction to the theory of neural computation", Wesley publication Co., 1991.

117. Y. Y. Hsu, C. C. Yang, "Design of artificial neural networks for short term load forecasting (Part II)", Proc. IEE-C, Vol. 138, 1991, pp414-8.

118. D. J. Sobajic, Y. H. Pao, "artificial neural net based dynamic security assessment for electric power ssytems", IEEE Transactions on PWRS, Vol. 4, 1989, pp220-8.

119. N. I. Santoso, O. T. Tan, "Neural net based real time control of capacitors installed on distribution systems", IEEE Transactions on PWRD, Vol. 5, 1990, pp266-72.

120. E. H. P. Chan, "Application of neural network computing in intelligent alarm processing", Proc. 1989 IEEE-PICA Conference, Seatle, USA, 1989, pp246-51.

121. K. Bhattacharya, S. Chakravorti, P. K. Mukherjee, "Insulator contour optimisation by a neural network", IEEE Transactions on dielectrics and electrical insulation, Vol. 8, No. 2, April 2001, pp157-61.

122. Y. Sun, Z. Yang, Z. Wang, Q. Lu, "Voltage stability improvement using ASVG nonlinear control", Automation of electric power system, Vol. 20, No. 6, June 1996 (in Chinese).

123. S. Chen, Y. Sun, Q. Lu, "Predicting fuzzy control and applications to ASVG", Automation of electric power system, Vol. 21, No. 10, Oct., 1997, pp4-8 (in Chinese).

124. L. O. Mak, Y. X. Ni, C. M. Shen, "STATCOM with fuzzy controller for interconnected power systems", Electric power Systems Research, Vol. 55, 2000, pp87-95.

125. M. Sun, A. Stam, R. E. Steuer, "Interactive multiple objective programming using Tchebycheff programs and artificial neural networks", Computers & Operations Research, Vol. 27, 2000, pp601-20.

BIBLIOGRAPHY

1. G.F. Page, J.B. Gomm and D. Williams, " Application of neural networks to modelling and control ", London, Chapman & Hall, 1993.
2. Carling, Alison, " Introducing neural networks ", Wilmslow, Sigma, 1992.
3. Gallant, Stephen I., " Neural network learning and expert systems ", Cambridge, Mass., MIT Press, c1993.
4. Simpson, Patrick K., " Artificial neural systems, foundations, paradigms, applications and implementations ", Neural networks, research and application, New York, Oxford, Pergamon, 1990.
5. Swingler, Kevin, " Applying neural networks, a practical guide (Accompanying software available at Loans Counter)", London, Academic Press, c1996.
6. Judd, J. Stephen, " Neural network design and the complexity of learning", Cambridge, Mass., MIT Press, 1990.
7. Chester, Michael, " Neural networks, a tutorial, ", Englewood Cliffs, N.J., London, PTR Prentice Hall, c1993.
8. B.M.Weedy, B.J.Cory, "Electric Power Syatems", John Wiley&Sons Ltd, England, 4th edition, Chap. 5, 1998.
9. Butterworths, "Power Transformer Handbook", Butterworth & Co. (Publishers) Ltd, 1st English edition, Chap. 2, 1987.
10. Charlesa. Gross, "Power System Analysis", 2nd edition 1986.
11. W. Thomas Miller, III, Richard S. Sutton and Paul J. Werbos, " Neural networks for control ", Cambridge, Mass, London, MIT Press, c1990.
12. Cichocki, A. " Neural networks for optimzation and signal processing ", Chichester, Wiley, 1993.
13. Peretto, Pierre, " An introduction to the modeling of neural networks ", Cambridge, Cambridge University Press, 1992.
14. Picton, Phil, " Introduction to neural networks ", Basingstoke, Macmillan, 1994.
15. Patrick K. Simpson (editor), " Neural networks theory, technology, and applications ", IEEE technology update series, New York, IEEE, 1995.
16. Roland.E.Thomas, Albert.J.Rosa, "the Analysis and Design of Linear Circuits", Prentice-Hall Inc., USA, 2nd edition, Chap. 3, 1998.
17. Alianna J. Maren, Craig T. Harston, Robert M. Pap., "Handbook of neural computing applications", San Diego, Academic Press, 1990.

18. Harold Cohen, "Mathematics for Scientists & Engineers", Prentice-Hall International Inc., pp400-9, 1992.
19. B.M.Weedy, B.J.Cory; "Electric Power System", John Wiley & Sons Ltd., pp186-7 and pp266-7, 4th Edition, 1998.
20. Noel M.Morris, "Mastering Mathematics for Electrical and Electronic Engineering", The MALMILLAN PRESS LTD., pp213-26, 1994.
21. Allan D. Kraus, "Circuit Analysis", West Publishing Company, pp429-57, 1991.
22. Harold Cohen, "Mathematics for Scientists & Engineers", Prentice-Hall International Inc., pp433-68, 1992.
23. Wasserman, Philip D, "Advanced methods in neural computing", New York, Van Nostrand Reinhold, 1993.
24. R. Beale and T. Jackson, "Neural computing, an introduction", Bristol, Hilger/Institute of Physics, 1990.
25. Igor Aleksander and Helen Morton, "An introduction to neural computing", 2nd ed., London, International Thomson Computer Press, 1995.
26. Tarassenko, Lionel, "A guide to neural computing applications", Arnold, 1998.
27. Pratap, Rudra, "Getting started with MATLAB 5, a quick introduction for scientists and engineers", New York, Oxford University Press, 1999.
28. Higham, D. J., Desmond J., "MATLAB guide", Philadelphia, Society for Industrial and Applied Mathematics, 2000.
29. The Math Works Inc, "MATLAB, high-performance numeric computation and visualization software for UNIX workstations [Version 4.0]", Natick, Mass., The MathWorks, Inc., 1993.
30. The Math Works Inc, "The Student edition of MATLAB for MS-DOS personal computers", Englewood Cliffs, NJ, London, Prentice Hall, 1992.
31. Derek. A. Paice, "Power Electronic Converter Harmonics", the Institute of Electrical and Electronics Engineers Inc., New York, USA, chap.1, 1996.
32. E. Lakervi and E. J. Holmes, "Electricity distribution network design", 2nd ed. Peter Peregrinus Ltd., chap. 12, 1995.
33. David Finney, " Variable frequency AC motor drive systems", Peter Peregrinus Ltd., chap.9, 1988.
34. Ministry of Electric Power Industry of China, "Harmonics and Unbalanced-load caused by the railway traction and their effects to the power system", Beijing China, 1992.
35. Borse, Garold J., " Numerical methods using MATLAB ", P.W.S.-Kent Publishing Co.,U.S., Feb 96: Internat.Thomson Pub.Services.

36. Hanselman, Duane C., " The student edition of MATLAB, version 5, user's guide, [Windows version] ", Upper Saddle River, Prentice Hall, 1997.
37. A. J. Chipperfield and P. J. Fleming, " MATLAB toolboxes and applications for control ", Peter Peregrinus on behalf of The Institution of Electrical Engineers, c1993.
38. King, Joe, " MATLAB for engineers "; Menlo Park, Calif., Harlow, Addison-Wesley, 1998.
39. John Little and Loren Shure, " Signal processing toolbox for use with MATLAB, user's guide ", [new ed.], Natick, Mass., Math Works, 1992.
40. Eva P art-Enander...[et al.], " The MATLAB handbook ", Harlow, Addison-Wesley, 1996.
41. Hahn, Brian D., " Essential MATLAB for scientists and engineers ", London, Arnold, 1997.
42. Shahian, Bahram, " Control system design using Matlab ", Englewood Cliffs, N.J., Prentice Hall, 1993.
43. Duane Hanselman, Bruce Littlefield, " Mastering MATLAB 5, a comprehensive tutorial and reference ", Upper Saddle River, Prentice Hall, 1998.
44. Duane Hanselman and Bruce Littlefield, " The student edition of MATLAB, version 5, user's guide", Upper Saddle River, Prentice Hall, 1997.
45. Adrian Biran, Moshe Breiner, " MATLAB 5 for engineers ", 2nd ed., Harlow, Addison-Wesley Pub. Co., c1999.
46. Darren Redfern, Colin Campbell, " The MATLAB 5 handbook ", Berlin, Springer Verlag, 1998.
47. The MathWorks, " MATLAB, high-performance numeric computation and visualization software [Version 4.0] ", Natick, Mass., The MathWorks, Inc., 1992.
48. Marcus, Marvin, " Matrices and MATLAB, a tutorial ", Englewood Cliffs, New Jersey, Prentice Hall, c1993.
49. John Penny, George Lindfield, " Numerical methods using Matlab ", Upper Saddle River, N.J., Prentice Hall, London, Prentice-Hall International, c2000.
50. Van Loan, Charles F., " Introduction to scientific computing, a matrix-vector approach using MATLAB ", Upper Saddle River, N.J., Prentice Hall, c1997.
51. Friedland, Bernard, "Advanced control system design", Englewood Cliffs, Prentice Hall, 1996.
52. C.J. Chesmond, P.A. Wilson and M.R. le Pla, "Advanced control system technology", London, Edward Arnold, 1991.
53. Csaki, Frigyes, "Modern control theories, nonlinear, optimal and adaptive systems", Budapest, Akedemiai Kiado, 1970.

54. Walter J. Grantham and Thomas L. Vincent, "Modern control systems analysis and design", Wiley, 1993.
55. Bishop, Robert H., "Modern control systems analysis and design using MATLAB", Reading, Mass., Addsison-Wesley, c1993.
56. John J. D'Azzo, Constantine H. Houpis, "Linear control system analysis and design, conventional and modern", 4th ed., London, McGraw-Hill, 1995.
57. Richard C. Dorf, Robert H. Bishop, "Modern control systems", 9th ed., Upper Saddle River, Prentice Hall, c2001.
58. Shinners, Stanley M, "Modern control system theory and design", New York, J. Wiley, c1992.
59. Ogata, Katsuhiko, "Modern control engineering", 2nd ed., Englewood Cliffs, N.J., Prentice Hall, 1990.
60. Hoft, Richard G., "Semiconductor power electronics", New York, Wokingham, Van Nostrand Reinhold, c1986.
61. Lander, Cyril W., "Power electronics", 2nd ed., London, McGraw-Hill, c1987.
62. Williams, B. W., Barry W., "Power electronics, devices, drivers, applications and passive components", 2nd ed., Basingstoke, Macmillan, 1992.
63. Rashid Muhammad H, "Power electronics, circuits, devices, and applications", 2nd ed., Prentice-Hall International, c1993.
64. Derek A. Paice, "Power electronic converter harmonics, multipulse methods for clean power", Piscataway, NJ, IEEE Press, c1996.
65. Weedy, B. M., Birron Mathew, "Electric power systems", 4th ed., New York, Chichester, Wiley, 1998.
66. Bernard Hochart, "Power transformer handbook (edited by Bernard Hochart, first English edition translated from the French by C.E. Davison)", London, Butterworths, 1987.
67. B. M. Bird, K. G. King, D. A. G. Pedder, "An introduction to power electronics", 2nd ed., Chichester, Wiley, 1993.
68. James W. Nilsson, Susan A. Riedel, "Electric circuits", 6th ed., Upper Saddle River NJ, Prentice Hall, 2000.
69. Yorke, R., "Electric circuit theory", Applied electricity and electronics, 2nd ed., Oxford, Pergamon, 1986.
70. David E. Johnson, Johnny R. Johnson, John L. Hilburn, "Electric circuit analysis", Englewood Cliffs, N.J., Prentice Hall, c1989.
71. Sander, K. F., Kenneth Frederick, "Electric circuit analysis, principles and applications", Wokingham, Addison-Wesley, 1992.

72. G.R. Slemon, A. Straughen, "Electric machines", Reading, Mass., London, Addison-Wesley, 1980.